ACTA UNIVERSITATIS SZEGEDIENSIS

ACTA MINERALOGICA-PETROGRAPHICA

ABSTRACT SERIES

Volume 11 2021

8th "MINERAL SCIENCES IN THE CARPATHIANS"
INTERNATIONAL CONFERENCE
Miskolc, May 13–14, 2021

Published by the Department of Mineralogy, Geochemistry and Petrology, University of Szeged

ACTA MINERALOGICA-PETROGRAPHICA

established in 1923

ABSTRACT SERIES

HU ISSN 0365-8066
HU ISSN 1589-4835

Abbreviated title:
Acta Mineral. Petrogr. Abstr. Ser., Szeged

Editorial Address

H-6722 Szeged, Hungary
2 Egyetem Street
E-mail: asviroda@geo.u-szeged.hu

The Acta Mineralogica-Petrographica Abstract Series is published by the Department of Mineralogy, Geochemistry and Petrology, University of Szeged, Szeged, Hungary

---

On the cover: Kollerite, Pécs-Vasas, Hungary. Width of the picture: 5 mm. Collection and photo: Gábor Koller.

8th MSCC
8th Mineral Sciences in the Carpathians Conference
Miskolc, Hungary, May 13-14, 2021

ABSTRACTS

Edited by
Máté Zs. Leskó

Abstracts revised by
Béla Fehér, Erika Kereskényi, Lívia Leskóné Majoros, Ferenc Mádai and Norbert Zajzon

Organized by
University of Miskolc
Hungarian Geological Society
Herman Ottó Museum

International Scientific Board

Peter Bačík
Comenius University, Bratislava

Ovidiu Gabriel Iancu
University Alexandru Ioan Cuza, Iaşi

Gheorghe Ilinca
University of Bucharest, Bucharest

Victor Kvasnytsya
National Academy of Sciences of Ukraine, Kyiv

Milan Novák
Masaryk University, Brno

Mihály Pósfai
University of Veszprém, Veszprém

Jiří Sejkora
National Museum, Praha

Sándor Szakáll
University of Miskolc, Miskolc

Pavel Uher
Comenius University, Bratislava

Tamás Weiszburg
Eötvös Loránd University, Budapest

Adam Pieczka
AGH University of Science and Technology, Kraków

Local Organising Committee

Norbert Zajzon (*chairman*)

Máté Zs. Leskó (*secretary general*)

Béla Fehér

Ferenc Kristály

Lívia Leskóné Majoros

Ferenc Mádai

HYDROTHERMAL MINERAL ASSEMBLAGE OF THE RARE ELEMENTS ENRICHED ROCK BODIES, BÜKK MOUNTAINS, HUNGARY

BALASSA, Cs., NÉMETH, N. & KRISTÁLY, F.
Institute of Mineralogy and Geology, University of Miskolc, Miskolc, Hungary
E-mail: balassacsillu@gmail.com

The Institute of Mineralogy and Geology at the University of Miskolc conducted a chemical analysis of metavolcanics samples from the southeast Bükk Mountains in 2014 in the frames of the CriticEl project. One of the analysed samples contained unexpected rare earth element (REE) and other rare element (Zr, Nb, Ta, Th, Y) enrichment. These elements belong to the high field strength (HFSE) elements, which are usually stable during the processes of metamorphism and weathering. The enrichment of these elements is rare, mainly connected to carbonatite or alkaline magmatism, although in the Bükk Mts. there is no known magmatic source.

During the new explorations based on the results further occurrences were found in the SE and NE part of the Bükk Mts. (NÉMETH et al., 2016). The enriched rock bodies are Triassic metavolcanics layers (in case of the SE occurrence) and siliciclastic sedimentary layers (in case of both the SE and NE occurrences). All these layers are interbedded to carbonate layers, which do not contain any enrichment. Based on our results the enrichment has a metasomatic origin. We did further investigations to describe the mineral assemblage of the enriched rock bodies. Here we present our new results.

Chemical analyses of the studied samples were carried out by ICP and XRF measurements, while the mineralogical composition was studied with XRD, microprobe analysis and optical microscopy. The XRD method is not appropriate to detect the most interesting, rare element bearing minerals due to their small amount and the overlapping peaks. To identify the micrometre-sized minerals, only the EPMA measurements produced acceptable results. They are usually present as alteration products of earlier grains in mixed aggregates. The most general ones are zircon, REE-phosphates [most probably monazite-(Ce)] and Nb-bearing Ti-oxides. Ca-REE-Ti-Nb-oxide (aeschynite or euxenite) and REE-carbonates (parisite or synchysite) are characteristic for certain sedimentary rock layers only, the first one is from Vesszős Valley (NE Bükk), the second one from Közép-szék-lápa (SE Bükk).

Based on the results of ICP analyses the enrichment of the REEs (except Eu) can reach 5–10 times compared to the upper crust. The presence of the LREEs is more significant, but there is a small increase in the rate of HREE with the increasing total REE content. The REE pattern always shows a strong negative Eu anomaly. The enrichment rate of the Zr usually 2–7 (the maximum is 19), the Nb 12–16, the Th 3–8 (the maximum is 30) times compared to the crust. Usually, the metavolcanics samples have higher rate of enrichment, but a siliciclastic layer from Vesszős Valley (NE Bükk) contains the highest amount of enrichment. In spite the phosphate and Ti-oxide alteration minerals, both P and Ti are depleted during the alteration process.

Regarding the metavolcanics, the most enriched bodies belong to the – often peperitic – basalt of the Central unit of the Bükk Mountains (Szinva Metabasalt Formation). The rock forming minerals are quartz, trioctahedral micas, feldspars and chlorite. With higher rate of the enrichment the samples contain less albite (the rate of the potassic feldspars is higher) and less chlorite. Chlorites are likely to be altered to micas due to the enrichment.

In the enriched siliciclastic sedimentary rocks from the SE part of the mountain (Közép-szék-lápa) quartz and micas are the main components. There are only a few feldspar grains, which are usually albite. In the NE part of the mountains (Vesszős Valley) these rocks almost entirely consist of micas, but there is a smaller enrichment also in marly layers, where calcite and quartz are also present. The analysed carbonate wall rock consists of calcite, dolomite and chlorite (iron-free clinochlore).

The typical accessory minerals of both rock types are iron oxide-hydroxides, titanium oxides, apatite (with REE content) and biotite. Titanite occurs in non-altered rocks only.

According to the small grain size (<10 μm), textural position, sometimes chemical composition of the rare element bearing minerals, the enrichment was caused by a metasomatic process. The fluids reacted with the silicate minerals. The alteration caused the generation of new, rare element bearing minerals and sometimes the incorporation of rare elements into already existing phases. Other minerals, as the alkali feldspars and biotite also could be the product of the alteration. The carbonate layers were not affected by the alteration.

Acknowledgment
Supported by the ÚNKP-20-2-I. New National Excellence Program of the Ministry for Innovation and Technology from the source of the National Research, Development and Innovation Fund.

Reference

NÉMETH, N., BARACZA, M. K., KRISTÁLY, F., MÓRICZ, F., PETHŐ, G. & ZAJZON, N. (2016): Földtani Közlöny, 146: 11–26.

AXINITE FROM METABASALT AT LÉTRÁS-TETŐ, MISKOLC, BÜKK MOUNTAINS, NE HUNGARY

BALASSA, Cs., KRISTÁLY, F., PAPP, R. Z. & NÉMETH, N.
Institute of Mineralogy and Geology, University of Miskolc, Miskolc, Hungary
E-mail: balassacsillu@gmail.com

Axinite-(Fe), a Ca-Al-borosilicate mineral was described from Lillafüred before (SZAKÁLL & FÖLDVÁRI, 1995; OZDÍN & SZAKÁLL, 2014). Here the axinite occurs in hydrothermal quartz-albite-calcite veins penetrating Triassic metabasalts. We introduce a new axinite-(Fe) occurrence discovered at Létrás-tető, near Miskolc, where this mineral occurs as a minor constituent of metabasalt.

The site is characterized by the outcrops of several fragmented metavolcanic bodies originated from various formations of the Bükk parautochthonous successions at a major tectonic boundary zone. The axinite-bearing body is of some 10 metres scale only, embedded in shale matrix. We studied samples from the axinite-bearing rock body, the shale country rock and two neighbouring metavolcanic bodies. The applied methods are electron-microprobe analyses, optical microscopy and X-ray powder diffraction. According to the XRD evaluation, the axinite content of the sample reaches 6 wt%. The major rock forming minerals are potassic feldspars (mainly microcline), albite, and chlorite; minor constituents are titanite, clinopyroxene, actinolite and biotite. The axinite consists of whitish, tabular, some 100 μm or even mm-sized crystals, partly replaced by potassic feldspars (sometimes also with albite; Fig. 1). Around the axinite grains, actinolite laths (not oriented) are very characteristic in the fine-grained, chlorite and potassic feldspar dominated matrix. The albite often forms nests in the matrix. Other accessory minerals are P-Pb-bearing Fe-silicate mixture and in smaller quantities allanitised epidote, a Ce-rich mineral phase and a Pb-V mineral (probably mottramite).

Based on standardless EDX results the axinites are Fe-dominant, but not as close as to the end-member as those analysed by OZDÍN & SZAKÁLL (2014). The average Fe:Mn:Mg ratio is 1:0.35:0.55, but there are some measurement points, where the axinite contains Mn or Mg in equal (or even a little bit higher) quantity than Fe.

In contrast with the already known occurrence, the axinite crystals analysed by us are not formed in hydrothermal veins but were developed as euhedral phenocrysts in supposedly fine-grained matrix, as no pseudomorphs of porphyritic clasts or minerals are observed. The trace element composition indicates basaltic protolith, affected by K-metasomatism. Based on the microprobe data, axinite precedes and is affected by the K-metasomatism as well. Subhedral albite crystals together with actinolite, titanite and chlorite are products of low-grade regional metamorphism. These observations place axinite crystallization to an early, premetamorphic stage, possibly autometasomatism of the volcanic rock

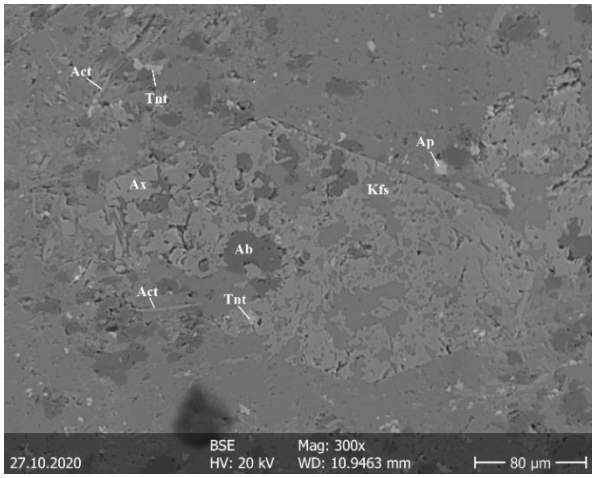

Fig. 1. Axinite (Ax) crystal partly replaced by potassic feldspar (Kfs) and albite (Ab), with characteristic actinolite (Act) laths. The matrix consists mainly of potassic feldspar. BSE image.

References

OZDÍN, D. & SZAKÁLL, S., (2014): In: Fehér, B. (Ed.): Az ásványok vonzásában. Tanulmányok a 60 éves Szakáll Sándor tiszteletére. Herman Ottó Múzeum és Magyar Minerofil Társaság, Miskolc, 203–217.

SZAKÁLL, S. & FÖLDVÁRI, M. (1995): Földtani Közlöny, 125: 433–442.

SPONTANEOUS AND DIRECTED ENVIRONMENTAL MINERAL FORMATION IN WASTEWATER TREATMENT TECHNOLOGY

BENYÓ, J.[1], HARMAN-TÓTH, E. [1,2], MÁRIALIGETI, K.[3], MIREISZ, T.[4] & WEISZBURG, T. G.[1,5]
[1] Department of Mineralogy, Eötvös Loránd University, Budapest, Hungary
[2] Eötvös Museum of Natural History, Eötvös Loránd University, Budapest, Hungary
[3] Department of Microbiology, Eötvös Loránd University, Budapest, Hungary
[4] Budapest Waterworks, Budapest, Hungary
[5] Department of Environmental Sciences, Sapientia Hungarian University of Transylvania, Cluj-Napoca, Romania
E-mail: bejubor@staff.elte.hu

During the activated sludge process combined with biological phosphorus removal, widely used in wastewater treatment plants, dissolved forms of phosphorus are converted into bound polyphosphate by microbes. In a further step of the sludge line, due to the conditions of the anaerobic digestion technology, the polyphosphate bound by the cells is again dissolved in the form of anions. After the digesters, the solubility of the ions in the solution decreases due to temperature decrease in the heat exchangers and pipelines connecting tertiary treatment steps, which can lead to the appearance of mineral precipitates. These crystallizing solids – environmental minerals – may cause technological faults and financially significant expenses to wastewater treatment plants. The reason for this is that the solids precipitating on the walls of the equipment reduce the efficiency of purification, by reducing the internal diameter of or clogging the pipes, finally resulting in the premature wear and tear of the equipment. This places a significant additional burden on the wastewater treatment plant and is clearly a detrimental phenomenon from both the economic and the environmental point of view.

Mineral deposits appearing in the equipment of wastewater treatment plants are a worldwide problem. In addition to Asian countries (LE *et al.*, 2021), this field has been increasingly studied in the last decades in Europe, such as Belgium (SAERENS *et al.*, 2021), Poland (NUMVIYIMANA *et al.*, 2020), and Croatia (BABIĆ-IVANČIĆ *et al.*, 2006), Spain or Germany (RUFÍ-SALÍS *et al.*, 2020) and Austria (MUYS *et al.*, 2021).

The aim of our research at a large wastewater treatment plant in Budapest (Hungary) is to reduce the appearance of these spontaneous mineral precipitates (mainly struvite, $NH_4Mg[PO_4]\cdot 6H_2O^{orthorhombic}$, and vivianite, $Fe_3[PO_4]_2\cdot 8H_2O^{monoclinic}$) by fine-tuning the parameters of the wastewater treatment technology (e.g., pH, temperature, amount of additives). A further aim is to enable the targeted precipitation of struvite in the right quality at a specifically designed technological point by accurately mapping the technological process, as struvite can also be an increasingly important agricultural phosphorus fertilisation product due to its high and lasting phosphate content.

Acknowledgment

This work is supported by the Cooperative Doctoral Program (KDP-2020/999840) granted by The Ministry for Innovation and Technology (ITM) from the source of the National Research, Development and Innovation Fund.

References

BABIĆ-IVANČIĆ, V., KONTREC, J., BREČEVIĆ, L. & KRALJ, D. (2006): Water Research, 40: 3447–3455.

LE, V., VO, D., NGUYEN, N., SHIH, Y., VU, C., LIAO, C. & HUANG, Y. (2021): Journal of Environmental Chemical Engineering, 9: 105019.

MUYS, M., PHUKAN, R., BRADER, G., SAMAD, A., MORETTI, M., HAIDEN, B., PLUCHON, S., ROEST, K., VLAEMINCK, S. E. & SPILLER, M. (2021): Science of the Total Environment, 756: 143726.

NUMVIYIMANA, C., WARCHOŁ, J., IZIZYDOR-CZYK, G., BAŚLADYŃSKA, S. & CHOJNACKA, K. (2020): Journal of the Taiwan Institute of Chemical Engineers, 117: 182–189.

RUFÍ-SALÍS, M., BRUNNHOFER, N., PETIT-BOIX, A., GABARRELL, X., GUISASOLA, A. & VILLALBA, G. (2020): Science of the Total Environment, 737: 139783.

SEARENS, B., GEERTS, S. & WEEMAES, M. (2021): Journal of Environmental Management, 280: 111743.

ENVIRONMENTAL APPLICATION OF CATION-EXCHANGED BENTONITES

BUZETZKY, D., M. NAGY, N. & KÓNYA, J.
Imre Lajos Isotope Laboratory, Department of Physical Chemistry, University of Debrecen, Debrecen, Hungary
E-mail: dorabeata@science.unideb.hu

One of the important goals of the 21st century is to improve the environment. The emission of pollutants can have adverse effects on the environment and public health. Therefore, it is necessary to develop treatment processes that isolate and remove contaminants from their environment. Thus, our aim is to sorb anionic pollutants (phosphate and arsenite ions) and long-lived radioactive isotopes ($^{36}Cl^-$, $^{129}I^-$, $^{99}Tc^-$ isotopes as pertechnetate ions, TcO_4^-) on modified bentonite clay. Since these pollutants are anions, they do not sorb onto natural clays to a significant extent and therefore they can relatively quickly migrate with water in the environment. The modifications create sorbing sites in the clays where anions can also be sorbed or precipitated in the form of weakly soluble salts, thereby reducing migration. The sorption of phosphate (BUZETZKY *et al.*, 2017) and arsenite ions (BUZETZKY *et al.*, 2019a) was studied on bentonites modified with rare earth (REE) ions and Fe(III) ions. The sorption of $^{36}Cl^-$, $^{131}I^-$ isotopes was investigated on Ag-bentonite (BUZETZKY *et al.*, 2020), while the sorption of ^{99m}Tc isotopes as pertechnetate ions (TcO_4^-) was studied on Mn-, Cr-, Sn-bentonites (BUZETZKY *et al.*, 2019b).

The successful cation exchange was confirmed by X-ray fluorescence spectroscopy and X-ray diffraction. Kinetic studies were carried out to determine the rate constants and the activation energy. The equilibrium relationship between the sorbed and the dissolved phosphate and arsenic concentration was described by Langmuir isotherm. The mechanism of phosphate ion sorption is different in the case of REE- and Fe-bentonites.

The sorption of iodide ions on Ag-bentonite is rapid and the equilibrium is reached within a few minutes so the rate constant could not be determined by the batch technique. In the case of iodide ion, the sorption was influenced by iodide carrier solution. Increasing the concentration of the inactive iodide ion reduces the sorption due to the formation of a soluble silver diiodide complex.

The modified bentonites can sorb ^{99m}Tc ions fast and in a high degree. On the basis of the redox potential and the relative sorption values, it can be stated that the Cr-, Sn-modified bentonites showed the most effective sorption, the removal of Tc was 100% after 5 minutes.

These results show that modified clays could play an important role in the treatment of eutrophication processes in the aquatic environment and can be used for removing arsenic ions from water. Moreover, modified bentonites can be suitable for the construction of waste containers as anion sorbents.

References

BUZETZKY, D., NAGY, N. & KÓNYA, J. (2017): Periodica Polytechnica Chemical Engineering, 61(1): 27–32.

BUZETZKY, D., TÓTH, C., NAGY, N. & KÓNYA, J. (2019a): Periodica Polytechnica Chemical Engineering, 63(1): 113–121.

BUZETZKY, D., KOVÁCS, E., NAGY, N. & KÓNYA, J. (2019b): Journal of Radioanalytical and Nuclear Chemistry, 322: 1771–1776.

BUZETZKY, D., NAGY, N. M. & KÓNYA, J. (2020): Journal of Radioanalytical and Nuclear Chemistry, 326: 1795–1804.

CARBONATITES, RARE EARTHS AND THE LESSONS WE LEARN FROM PETROGRAPHY AND TRACE-ELEMENT GEOCHEMISTRY

CHAKHMOURADIAN, A. R.
Department of Geological Sciences, University of Manitoba, Manitoba, Canada
E-mail: anton.chakhmouradian@umanitoba.ca

Synopsis

Carbonatites are carbonate-dominant igneous rocks, which are commonly affected by subsolidus re-equilibration processes. These rocks reach extreme levels of REE enrichment (n × 10^4 mantle values), yet are not known for the same spectacular diversity of REE minerals as undersaturated alkaline rocks, for example. (Only some 40 REE minerals have been reported from carbonatites worldwide, and fewer than 10 are reasonably common.) One of the reasons for this, of course, is the abundance of Ca minerals in these rocks, which provide a perfect alternative host for REE and thus affect the metallogenic aspects of carbonatite evolution. For example, apatite-group minerals can incorporate up to 15 wt.%, calcite up to 2,000 ppm and amphiboles up to 1,000 ppm REE. Despite the importance of carbonatites as a commercial source of REE, the effect of different rock-forming minerals on the trace-element budget of carbonatitic magmas and fluids is poorly understood. Preliminary economic assessments typically report bulk-rock values and disregard this REE dispersal effect. Microbeam trace-element analysis is now increasingly used for this purpose, but a thorough understanding of paragenetic constraints, based on careful petrographic studies, is required to map the distribution of REE among different constituent minerals in a time-resolved fashion. These data can be used in conjunction with the theory of trace-element partitioning to unravel the pathways of carbonatite evolution and to refine the as-yet underdeveloped metallogenic models. Some of the challenges facing researchers in this field include (i) element-partitioning phenomena that do not agree well with the theory, (ii) quasi-equilibrium growth, (iii) experimental oversimplification of natural systems, leading to partitioning data that cannot be feasibly applied to real rocks, and (iv) the effects of subsolidus re-equilibration obscuring primary parageneses and their interrelations.

The role of petrography and trace-element geochemistry in REE deposit research: a case study

The Devonian Aley intrusion in British Columbia (Canada) comprises a wide variety of carbonatites, many of which were produced by subsolidus processes which accompanied deformation and ductile mobilization of these rocks during the Laramide orogeny (CHAKHMOURADIAN *et al*., 2015, 2016). A wide variety of minerals (rock-forming carbonates, mafic silicates and magnetite) were replaced by dolomite. This process was accompanied by the pseudomorphization of phlogopite by chlorite and of pyrochlore by fersmite ($CaNb_2O_6$) and, to a lesser extent, ferrocolumbite ($FeNb_2O_6$). The igneous carbonates and secondary dolomite differ in morphology, isotopic and trace-element composition, indicating that these processes involved re-equilibration of the primary paragenesis with an externally derived fluid. For structural reasons, dolomite has a much lower tolerance for REE than calcite: up to ~700 and 1,600 ppm with median values of 63 and 510 ppm, respectively. In areas of pervasive dolomitization, igneous apatite also shows evidence of chemical re-equilibration, i.e. its peripheral and fractured areas are depleted in REE and characterized by lower $(La/Yb)_{CN}$ ratios (typically, < 5,000 ppm and 75, respectively) than the unaltered material (up to 13,500 ppm and 210, respectively). Primary pyrochlore, containing 7,000–40,000 ppm REE, is replaced by fersmite with comparable levels of REE (3,000–57,000 ppm). However, the latter mineral is notably richer in Y and heavy lanthanides relative to its precursor [median $(La/Yb)_{CN}$ = 2.4 vs. 68, respectively]. Our data show that the process of hydrothermally induced dolomitization resulted in the release of REE and, in particular, the less-compatible light lanthanides into the fluid and their sequestration in the secondary paragenesis (monazite, bastnäsite, parisite, euxenite, xenotime). Our calculations show that dolomitization of a calcite carbonatite intrusion the size of Aley (~7 km^2) would lead to the release of n × 10^5 tons of each La, Ce, Nd and Y. Late-stage mineralization associated with dolomitization is found in intimate association with chlorite, quartz, secondary rhombohedral dolomite, barite, and other minerals filling fractures and voids. One important geochemical characteristic of this late assemblage of minerals is size-driven fractionation between light and heavy REE and relatively low mobility of the latter, which lead to the precipitation of secondary Y-rich minerals with very low $(La/Yb)_{CN}$ (fersmite, euxenite, xenotime) close to their precursor minerals. Notably, similar carbonatite-hosted deposits are known elsewhere, but some of their key petrographic characteristics may have been overlooked or misinterpreted.

Modelling REE behaviour: recognized and emerging challenges

Yttrium-holmium decoupling is a striking example of deviation from trace-element partitioning patterns predicted by theory (e.g., KARATO, 2016). For example, perovskite ($CaTiO_3$) from carbonatites has

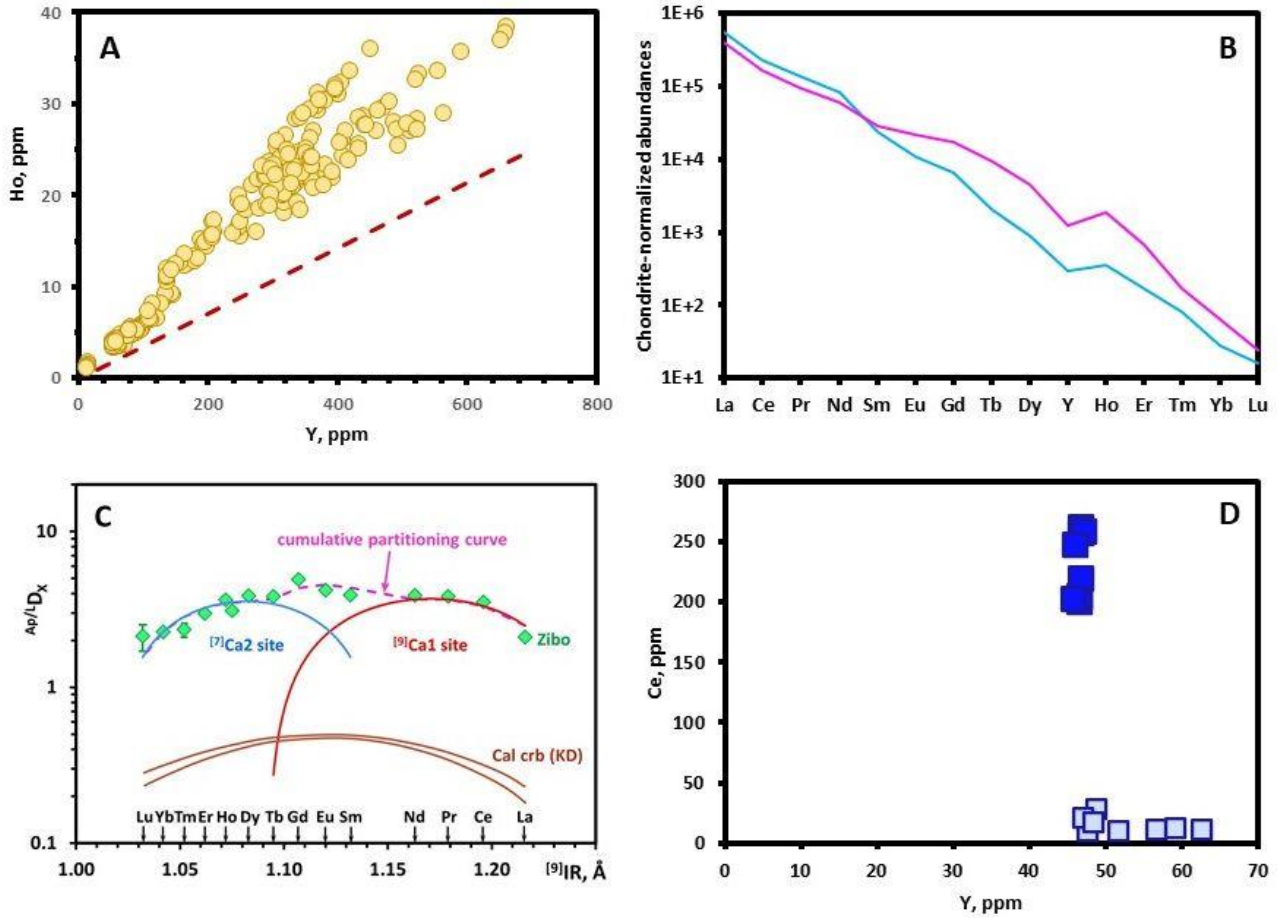

Fig. 1. Selected examples of unusual or poorly understood REE characteristics observed in carbonatites. (A) Y vs. Ho distribution in perovskite (yellow circles, global dataset) showing deviation from the correlation trend expected from ionic radii (dashed red line). (B) Chondrite-normalized REE distributions in prism and pyramid sectors (purple and blue curves, respectively) in carbocernaite from Bear Lodge, Wyoming, USA. (C) Onuma diagram showing variations in REE partition coefficients with ionic radius, calculated for apatite phenocrysts from Zibo, China (green diamonds), compared to the interpolated experimental data of KLEMME & DALPÉ (2003). (D) Y vs. Ce distribution between coarse calcite porphyroclasts (dark blue squares) and fine-grained calcite produced by dynamic recrystallization (pale blue squares).

consistently subchondritic Y/Ho values (15.3 ± 1.9), i.e., higher partition coefficients for Ho in comparison with Y (Fig. 1A). Owing to the lanthanide contraction, Y and Ho have essentially identical ionic radii, and do not readily separate in the geological environment. Yttrium-Ho decoupling has been thought to be restricted to low-T aqueous processes (BAU, 1996), but may clearly play a significant role in magmatic fractionation, as well. This "abnormal" behaviour can be explained by greater strength of Ho bond to its coordinating oxygen atoms. Because of this, the attachment of Ho cations to a growing perovskite nucleus is statistically more likely to occur, even though Y is much more common in its crystallization environment.

Crystallographically controlled REE uptake is poorly understood, but has been demonstrated for a number of minerals. For example, Ca-Sr-rich prism sectors in carbocernaite [$(Na,Ca)(Sr,Ca,REE,Ba)(CO_3)_2$] exhibit a lesser degree of enrichment in light lanthanides relative to heavy lanthanides in comparison with Na-REE-rich pyramid sectors (Fig. 1B). Clearly, REE uptake in this case was affected by the structure of growth surfaces and outpaced the attainment of equilibrium. These effects can be very significant [e.g., the $(La/Yb)_{CN}$ ratio in zoned carbocernaite varies by a factor of three] and should be taken into account in trace-element modelling.

Much experimental work has been published on potential REE hosts in carbonatites. These data are of critical importance to geochemical modelling, but a careful analysis of the literature shows that caution should be exercised to avoid drawing incorrect conclusions from trace-element data acquired for real rocks. For example, the only currently available REE partitioning studies for apatite (HAMMOUDA *et al*., 2010; KLEMME & DALPÉ, 2003) are based on the system $CaCO_3 – Ca_5(PO_4)_3(F,OH)$, which does not take into account the chemical complexity of natural magmas. Further, experimental data are typically fitted

to a simplified partitioning curve that does not agree with the structural data on REE distribution between two topologically distinct Ca sites (FLEET & PAN, 1995, 1997). As a result, the experimental results poorly agree with partition coefficients calculated for real rocks (BRASSINNES *et al*., 2005; CHAKHMOURADIAN *et al*., 2017), which indicate greater compatibility in the middle of the lanthanide series due to overlap between REE partitioning curves representing the two different Ca sites (Fig. 1C).

Petrogenetic models rely on our ability to identify textures indicative of a specific process and to differentiate among visually similar petrographic characteristics produced by different mechanisms. This ability is diminished if the rock has been overprinted by subsolidus processes. For example, many carbonatites show preferred orientation and modal layering, but are these features a manifestation of magma flow or ductile deformation? In comparison to silicate rocks, carbonatites are far more susceptible to textural and chemical re-equilibration, grain abrasion and fragmentation, ductile flow, dissolution and other forms of chemical interaction with fluids even at relatively low pressures and temperatures. Cumulate layers within the intrusion, where REE mineralization is concentrated, have a low calcite (dolomite) content but significantly higher density than the material separating them and thus will behave very differently under stress. Deformation will not only disrupt or obliterate the pre-existing igneous features, but affect REE distribution patterns in the rock and its constituent minerals. For example, dynamic recrystallization in foliated carbonatites facilitates the removal of primary REE minerals included in calcite or dolomite (CHAKHMOURADIAN *et al*., 2016; CHAKHMOURADIAN & DAHLGREN, 2021) and selective mobilization of certain trace elements (Fig. 1D). Clearly, metallogenic modelling or the assessment of mineral potential in these cases will require a thorough understanding of the local tectonic framework and interrelations between the observed geological structures, modal and geochemical variations in the carbonatite

References

BAU, M. (1996): Contributions to Mineralogy and Petrology, 123: 323–333.

BRASSINNES, S., BALAGANSKAYA, E. & DEMAIFFE, D. (2005): Lithos, 85: 76–92.

CHAKHMOURADIAN, A. R. & DAHLGREN, S. (2021): Mineralogy and Petrology, 115: 161–171.

CHAKHMOURADIAN, A. R., REGUIR, E. P., KRESSALL, R. D., CROZIER, J., PISIAK, L., SIDHU, R. & YANG, P. (2015): Ore Geology Reviews, 64: 642–666.

CHAKHMOURADIAN, A. R., REGUIR, E. P. & ZAITSEV, A. N. (2016): Mineralogy and Petrology, 110: 333–360.

CHAKHMOURADIAN, A. R., REGUIR, E. P., ZAITSEV, A. N. COUËSLAN, C., XU, C., KYNICKÝ, J., MUMIN, A. H. & YANG, P. (2017): Lithos, 274–275: 188–213.

FLEET, M. E. & PAN, Y. (1995): American Mineralogist, 80: 329–335.

FLEET, M. E. & PAN, Y. (1997): American Mineralogist, 82: 870–877.

HAMMOUDA, T., CHANTEL, J. & DEVIDAL, J.-L. (2010): Geochimica et Cosmochimica Acta, 74: 7220–7235.

KARATO, S.-I. (2016): American Mineralogist, 110: 2577–2593.

KLEMME, S. & DALPÉ, C. (2003): American Mineralogist, 88: 639–646.

THE NEW $[Ag_2Hg_2]^{4+}$ CLUSTER CATION IN RUDABÁNYAITE, $[Ag_2Hg_2][AsO_4]Cl$ (RUDABÁNYA ORE DEPOSIT, HUNGARY)

EFFENBERGER, H.[1], SZAKÁLL, S.[2], FEHÉR, B.[3], VÁCZI, T.[4,5] & ZAJZON, N.[2]
[1]Institut für Mineralogie und Kristallographie, Universität Wien, Vienna, Austria
[2]Institute of Mineralogy and Geology, University of Miskolc, Miskolc, Hungary
[3]Department of Mineralogy, Herman Ottó Museum, Miskolc, Hungary
[4]Department of Mineralogy, Eötvös Loránd University, Budapest, Hungary
[5]Wigner Research Centre for Physics, Eötvös Loránd Research Network, Budapest, Hungary
E-mail: herta.silvia.effenberger@univie.ac.at

Recently the new mineral rudabányaite, $[Ag_2Hg_2][AsO_4]Cl$, was found in cavities of siliceous sphaerosiderite and limonite rocks at the Rudabánya ore deposit (North-East Hungary). Rudabányaite forms small, mostly xenomorphic crystals up to a diameter of 0.8 mm, crystalline aggregates are usually a few mm across. Cubic symmetry is indicated by optical isotropy, the faces {110} and {100} are rarely observed. The colour is bright yellowish-orange to brownish yellow; however, in natural light it turns slowly to dark brown or dark olive green. EFFENBERGER *et al.* (2019) gave a detailed description of rudabányaite.

Chemical composition: A qualitative energy-dispersive analysis showed that the mineral is rich in Ag, Hg, As, and Cl, minor amounts of S were detected (JEOL JXA-8600 electron microprobe, Institute of Mineralogy and Geology, University of Miskolc, Hungary). No other elements with an atomic number > 10 were detected. Quantitative point analyses gave the experimental formula $[(Ag_{2.06}Hg_{2.05})_{\Sigma=4.11}][(As_{0.97}S_{0.02})_{\Sigma=0.99}O_4]Cl_{1.06}$ based on 4 O atoms per formula unit (CAMECA SX 100 electron microprobe, State Geological Institute of Dionýz Štúr, Bratislava, Slovakia). Considering an Ag:Hg ratio of ~1:1, the idealized formula is $[Ag_2Hg_2][AsO_4]Cl$.

Raman spectroscopy: Micro-Raman spectra were taken on polished samples (HORIBA LabRAM HR UV-vis-NIR confocal microspectrometer). Spectra from areas exhibiting a slight reflectivity contrast observable on optical microscopy images (lighter and darker zones) show a minor but significant variability. Most probably it arise from the different photosensitivities in zones resulting from minor variations of the atomic arrangement (a local disorder of the Ag and Hg atoms is evident). The splitting of all internal modes is consistent with the presence of two symmetrically non-equivalent $[AsO_4]$ tetrahedra in the crystal structure with slightly different As−O bond lengths; from the crystal structure analyses the average bond distances amount 1.718 and 1.694 Å, respectively. The difference correlates with the distinct coordination of the individual O atoms.

X-ray investigation: The crystal-structure investigation was performed using single-crystal X-ray data (four-circle Nonius Kappa diffractometer, CCD detector, 300 µm capillary optics collimator, conventional X-ray tube, monochromated MoK_α radiation). The space group is $F\bar{4}3c$, a = 17.360(3) Å, V = 5231.8 Å^3, Z = 32. In a first step of the structure refinement, two crystallogaphically distinct arsenate tetrahedra and one Cl atom was found. For two further positions a mixed occupation by Hg and Ag atoms is required to balance the scattering power: $M1$ = (Ag,Hg)1 and $M2$ = (Ag,Hg)2. Furthermore, the final difference Fourier summation exhibited large residual densities between -2.31 to +3.75 eÅ^{-3}, the largest maxima are in the surrounding of the M atoms. Three peaks (X1a, X2a and X2b) seen in the electron-density map were considered during structure refinements; the reliability factors were reduced significantly. The centres are < 0.5 Å apart from the sites M1 (X1a) and M2 (X2a, X2b), respectively; consequently, vacancies at these M sites are required (12 atom% at the M1 and 5 atom% at the$M$2 position). For further refinement cycles, the occupation for the sites M1 + X1a and M2 + X2a + X2b was restricted to 1.0. In addition, isotropic displacement parameters for the X sites and anisotropic ones for the other sites as well as the variation of the scattering power Ag:Hg at the M sites were considered. As both M sites show a slight surplus of Ag as compared to Hg atoms, it is expected that the X sites compensate the mismatch to obtain a 1:1 ratio for the total composition expected from the chemical analyses. As conventional X-ray sources do not allow in such cases a refinement of the element ratio at one site, the occupation of the three X sites was arbitrarily set to each 50 atom% Ag and Hg. However, it cannot be proved experimentally by the structure determination due to the minor site-occupation factors of the X sites. The final refinement on F^2 converged at $wR2(F^2)$ = 0.068, $R1(F)$ = 0.031 for all 972 unique data and 53 variable parameters.

The most striking feature of the crystal structure of rudabányaite are two crystallographically different tetravalent 4-center 2-electron bonded cluster cations $[M_4]^{4+}$; M = (Ag, Hg), Ag:Hg ~ 1:1, M−M = 2.62 to 2.75 Å (for a theoretical approach see PYYKKÖ & RUNEBERG, 1993). The point symmetry of the two tetrahedra is 23 and $\bar{4}$, respectively. Numerous attempts were performed to verify an order between Ag and Hg atoms but none of them was successful; any symmetry reduction could not be verified, *super*structure reflections were not detectable. Most probable natural light triggers the displacement of small amounts of the M atoms (~0.5 Å) and cause slow changes of the colour. Raman spectra taken in distinctly coloured areas showed some differences mainly for the band at ~119 cm^{-1}.

[M_4] (M = Ag, Hg) tetrahedra respectively [M_3] (M = Ag, Hg) triangles are extremely rare (see Tab. 1). So far, $[Ag_2Hg_2]^{4+}$ tetrahedra are known from the two synthetic compounds $[Ag_2Hg_2]_3[VO_4]_4$ and $[Ag_2Hg_2]_2[HgO_2][AsO_4]_2$ only (WEIL *et al.*, 2005). The change of the ratio Ag:Hg to 3:1 in the mineral tillmannsite, $[Ag_3Hg][(V,As)O_4]$ (SARP *et al.*, 2003) and in its synthetic vanadate end-member (WEIL *et al.*, 2005) results in a trivalent cation complex. In these tetrahedral cluster cations $[Ag_3Hg]^{3+}$ and $[Ag_2Hg_2]^{4+}$ the atom ratio Ag:Hg is stoichiometric. The atoms Ag and Hg are statistically distributed with a metal—metal bond length of about 2.72 Å. This distance indicates a predominantly covalent bond. For a metallic bond character, the sum of the metal radii of the atoms under consideration would suggest a longer distance than that found in the [M_4] tetrahedra.

The M atoms in all these [M_4] clusters are [6] coordinated by each three M atoms and by three anions; new is the coordination by two O and one Cl atoms in the title mineral whereas in the three other compounds under discussion only O atoms occur in the first coordination sphere of the M atoms. The M—O bond lengths vary on a larger scale obviously because of the distinct coordinations of the O atoms. A clear trend is not observed: The shortest average M—O bond lengths are observed in rudabányaite ($M1$—O = 2.415 Å) and in tillmannsite (natural and synthetic sample 2.417 Å and 2.398 Å, respectively) despite the different tetrahedral cation clusters $[Ag_2Hg_2]^{4+}$ and $[Ag_3Hg]^{3+}$. In $[Ag_2Hg_2]_3[VO_4]_4$ (WEIL, 2005) they are slightly longer: 2.52 to 2.59 Å for the three distinct M atoms. In $[Ag_2Hg_2]_2[HgO_2][AsO_4]_2$ they scatter on a large scale (WEIL 2005). $[Ag_2Hg_2]$ tetrahedra occur also in $[Ag_2Hg_4][XO_4]_2$ (X = P,As) (MASSE *et al.*, 1978; WEIL, 2003). However, the Ag and Hg atoms are ordered; each two $[Ag_2Hg_2]$ tetrahedra share a common Ag—Ag edge forming an $[Ag_2Hg_4]^{6+}$-cluster cation. The shared edge (2.824(4) / 2.8531(11) Å in the phosphate / arsenate compound) is slightly shorter than in native silver but larger than the M—M distance in rudabányaite. The length of the Hg—Hg edges (2.608(2) / 2.6214(5) Å) is comparable to the M–M bond length in rudabányaite, but the Ag—Hg edges again are significantly longer (2.840(3) and 2.941(3) / 2.8388(5) and 2.9404(6) Å). Remarkable is the one-sided coordination of the Cl^{1-} ions in rudabányaite.

Rudabányaite exhibits strong crystal chemical, structural, and topological similarities to tillmannsite, $[Ag_3Hg][(V,As)O_4]$ (space group $I\bar{4}$; SARP *et al.*, 2003, WEIL *et al.*, 2005). Even in both minerals Ag and Hg atoms are disordered, Ag:Hg is stoichiometric. In kuznetsovite ($[Hg_3][AsO_4]Cl$, space group $P2_13$, a = 8.3983(6) Å; SOLOV'EVA *et al.*, 1991, WEIL, 2001), trigonal $[Hg_3]^{4+}$ clusters substitute the larger $[(Hg,Ag)_4]^{4+}$ metal clusters of rudabányaite. The two synthetic compounds exhibiting tetrahedral cationic clusters, *i.e.*, $[Ag_2Hg_2]_3[VO_4]_4$ and $[Ag_2Hg_2]_2[HgO_2][AsO_4]$ (WEIL, 2005), display stoichiometry but disorder of the M atoms. However, in the double-tetrahedron $[Ag_2Hg_4]$ in $[Ag_2Hg_4][XO_4]_2$ (X = P, As) the Ag and Hg atoms are ordered (MASSE et al., 1978; WEIL et al., 2005). New in rudabányaite is the partial displacement of the M atoms.

In rudabányaite the ratio of the $[M1_4]^{4+}$:$[M2_4]^{4+}$ clusters and $[As1O1_4]^{3-}$:$[As2O2_4]^{3-}$ tetrahedra is consistently 1:3. M—O bonds running approximately parallel to <100> link these tetrahedra among each other. Considering the distinct kinds of tetrahedra, they are linked to two different 2D arrangements with the compositions $[M2_4]_2[As1O_4][As2O_4]$ and $[M1_4][M2_4][As2O_4]_2$; they are aligned parallel to {100} (Fig. 1). These layer-like arrangements penetrate each other according to the cubic symmetry. All the $[AsO_4]^{3-}$ tetrahedra are arranged parallel to each other, the As—O bonds point towards <111>; the $[M1_4]^{4+}$ tetrahedra point into the opposite direction $\{\bar{1}\,\bar{1}\,\bar{1}\}$. Thus, polarity of the crystal structure is verified; merohedral twinning was not observed.

The crystal structure of rudabányaite is on high interest from a topological point of view. The barycentres of the $[M_4]^{4+}$ cluster cations and the $[AsO_4]^{3-}$ tetrahedra are arranged in an ideal rock-salt structure type with a' = ½a = 8.680 Å. Considering the grid

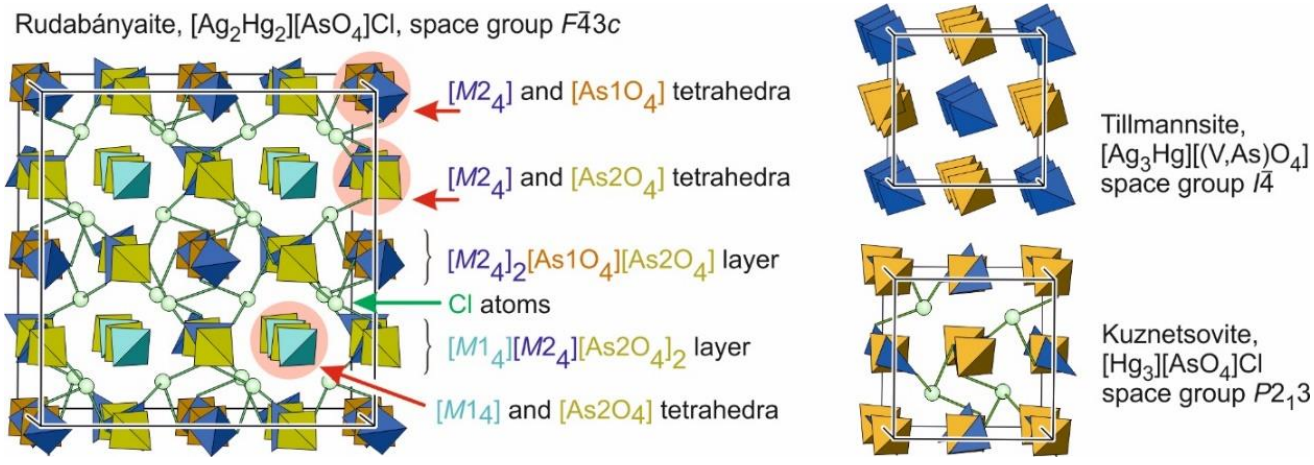

Fig. 1: Topological relations between rudabányaite, tillmannsite, and kuznetsovite.

formed by these two barycentres, *i.e.*, of all the tetrahedral structural units, a cubic primitive (cp) lattice is obtained. The filling of all voids of this lattice results in the well-known CsCl-structure type. Filling only half of the interstitial positions of a cp arrangement suggests a relation to one of the three distinct structure types fluorite (CaF_2) respectively *anti*-fluorite, α-$FeSi_2$, and Hg_2Pt. In rudabányaite the $[M_4]^{4+}$ barycenters of the tetrahedral $[(Ag,Hg)_4]$ clusters and the As^{5+} cations correspond to the position of the F^- ions of the fluorite-structure type whereas the Cl^- ions of the title compound to the positions of the Ca^{2+} ions; consequently the crystal structure of rudabányaite can be derived from the anti-fluorite structure-type. Derivatives of this structure type are well known as the $C1_b$-structure type respectively half-Heusler compounds.

Similarities with the crystal structures of the mineral tillmannsite, $[Ag_3Hg][(V,As)O_4]$, are evident (Fig. 1). Tillmannsite crystallises in the rarely verified tetragonal space group $I\bar{4}$. Two distinct column-like arrangements built solely by $[Ag_3Hg]^{3+}$ cation clusters and $[(V,As)O_4]^{3-}$ tetrahedra are running parallel to [001]; alternatingly arranged $[Ag_3Hg]$ clusters and $[(V,As)O_4]$ tetrahedra are verified only parallel to <100>.

The chemical formula $[Hg_3][AsO_4]Cl$ of kuznetsovite suggests a structural relation to rudabányaite; in fact, the atomic arrangements are identical from a topological point of view. Kuznetsovite crystallizes cubic, space group $P2_13$, the cell parameter *a*(kuznetsovite) is 8.3983(6) Å which is roughly 1/2 *a* (rudabányaite) = 8.680 Å. The difference is caused by the substitution of the trigonal planar $[Hg_3]^{4+}$ clusters by the larger tetrahedral $[(Hg,Ag)_4]^{4+}$ metal clusters. The substitution cause slight rotations respectively shifts of the $[AsO_4]^{3-}$ tetrahedra and Cl^- ions. The atomic arrangement in monoclinic terlinguaite is different: The coplanar $[Hg_3]^{4+}$ triangles are linked by the O atoms to layers running parallel to (100); they are connected by insular Hg^{2+} cations and Cl^- anions to a three-dimensional network. The dominance of acentric crystal structures in this group of compounds should be noted.

References

BRODERSEN, K., GÖBEL, G. & LIEHR, G. (1989): Zeitschrift für Anorganische und Allgemeine Chemie, 575: 145–153.

EFFENBERGER, H., SZAKÁLL, S., FEHÉR, B., VÁCZI, T. & ZAJZON, N. (2019): European Journal of Mineralogy, 31: 537–547.

MASSE, R., GUITEL, J.-C. & DURIF, A. (1978): Journal of Solid State Chemistry, 23: 369–373.

PYYKKÖ, P. & RUNEBERG, N. (1993): Journal of the Chemical Society, Chemical Communications, 1812–1813.

SARP, H., PUSHCHAROVSKY, D. Y., MACLEAN, E. J., TEAT, S. J. & ZUBKOVA, N. V. (2003): European Journal of Mineralogy, 15: 177–180.

SOLOV'EVA, L. P., TSYBULYA, S. V., ZABOLOTNYI, V. A. & PAL'CHIK, N. A. (1991): Kristallografiya, 36: 1292–1294.

WEIL, M. (2001): Zeitschrift für Naturforschung, 56b: 753–758.

WEIL, M. (2003): Zeitschrift für Naturforschung, 58b: 1091–1096.

WEIL, M., TILLMANNS, E. & PUSHCHAROVSKY, D. Y. (2005): Inorganic Chemistry, 44: 1443–145

Table 1: Minerals and synthetic compounds with polyatomic $[(Ag,Hg)_n]$ metal clusters related to rudabányaite.

Mineral name	Chemical composition	Space group symmetry	Reference
rudabányaite	$[Ag_2Hg_2][AsO_4]Cl$	$F\bar{4}3c$	EFFENBERGER *et al.* (2019)
tillmannsite	$[Ag_3Hg][(V,As)O_4]$	$I\bar{4}$	SARP *et al.* (2003), WEIL *et al.* (2005)
	$[Ag_3Hg][VO_4]$	$I\bar{4}$	WEIL *et al.* (2005)
	$[Ag_2Hg_2]_3[VO_4]_4$	$I\bar{4}2d$	WEIL *et al.* (2005)
	$[Ag_2Hg_2]_2[HgO_2][AsO_4]_2$	$P31c$	WEIL *et al.* (2005)
	$[Ag_2Hg_4][AsO_4]_2$	*Pbam*	WEIL (2003)
terlinguaite	$[Ag_2Hg_4][PO_4]_2$	*Pbam*	MASSE *et al.* (1978)
kuznetsovite	$[Hg_3][AsO_4]Cl$	$P2_13$	SOLOV'EVA *et al.* (1991), WEIL (2001)
	$[Hg_3][PO_4]Cl$	$P2_13$	WEIL (2001)
	$[Hg_3]HgO_2Cl_2$	$C2/c$	BRODERSEN *et al.* (1989)

THREE NEW AMMONIUM-IRON-SULFITE PHASES FROM A BURNING DUMP OF THE VASAS ABANDONED OPENCAST COAL MINE, PÉCS, MECSEK MTS., HUNGARY

FEHÉR, B.[1], SAJÓ, I.[2], KÓTAI, L.[3], SZAKÁLL, S.[4], ENDE, M.[5], EFFENBERGER, H.[5], MIHÁLY, J.[3], SZABÓ, D.[6] & KOLLER, G.[7]

[1]Department of Mineralogy, Herman Ottó Museum, Miskolc, Hungary
[2]Szentágothai Research Centre, University of Pécs, Pécs, Hungary
[3]Institute of Materials and Environmental Chemistry, Research Centre for Natural Sciences, Budapest, Hungary
[4]Institute of Mineralogy and Geology, University of Miskolc, Miskolc, Hungary
[5]Institute of Mineralogy and Crystallography, University of Vienna, Vienna, Austria
[6]Department of Mineralogy, Eötvös Loránd University, Budapest, Hungary
[7]Pilisborosjenő, Hungary
E-mail: feherbela@t-online.hu

Introduction

Sulfites are substances used as regulated food additives. However, the sulfite anion [$(SO_3)^{2-}$] is very rarely incorporated into minerals, so far only seven sulfite-bearing minerals are known: scotlandite, hannebachite, gravegliaite, orschallite, hielscherite, albertiniite and fleisstalite.

In October 2009, one of the authors (GK) collected red, brown, and yellow efflorescences on one of the burning waste dumps of the Vasas open-pit coal mine, near Pécs, Mecsek Mts., Hungary. In this material, three unknown ammonium-iron-sulfite (AIS) phases can be detected: AIS-1 is a trigonal $(NH_4)_9Fe^{3+}(SO_3)_6$, AIS-2 is a trigonal $(NH_4)_2Fe^{2+}(SO_3)_2$ and AIS-3 is an orthorhombic $(NH_4)_2Fe^{3+}(SO_3)_2(OH) \bullet H_2O$. AIS-1 and AIS-2 are metastable phases that break down in a few weeks and a few years, respectively. However, AIS-3 is a stable phase, which was approved as a new mineral species under the name kollerite by the Commission on New Minerals, Nomenclature and Classification of the International Mineralogical Association (IMA CNMNC) with IMA no. 2018-131. Synthetic analogues of the three AIS phases were studied by ERÄMETSÄ & VALKONEN (1972).

Short description of the AIS phases

AIS-1 forms red, hexagonal, stubby columnar to thick tabular crystals up to 0.2 mm in length. Its crystals are quite simple, only a hexagonal prism and a basal pinacoid can be observed. Its X-ray powder diffraction pattern is identical to ICDD 00-070-1539 card. The structure of synthetic analogue of AIS-1 was described by LARSSON & NIINISTÖ (1973). AIS-1 is very hygroscopic, it dissolves even in humid air and then flows off.

AIS-2 appears as brown tabular to rhombohedral crystals up to 0.1 mm in diameter. The crystals, which are the combinations of a rhombohedron and the basal pinacoid, often form columnar intergrowths. XRPD pattern of AIS-2 corresponds to ICDD 00-007-0427 card. The structure of synthetic AIS-2 was solved by single-crystal X-ray diffraction: space group $R\bar{3}m$, a = 5.3879(8) Å, c = 19.980(4) Å, V = 502.3 Å^3.

Sprays of AIS-3 (kollerite) up to 1.5 mm are composed of yellow, long-prismatic or lath-like crystals up to 0.7 mm, elongated along [001] and usually flattened on {100} with crystal forms {100}, {110} and {001}. The mineral is translucent with pale yellow streak and vitreous lustre. Its Mohs hardness is about 2. Density, measured on synthetic material, is 2.07(2) g/cm^3. Kollerite is brittle, cleavage is not observed. Its fracture is uneven. The mineral dissolves easily in water. XRPD pattern of AIS-3 corresponds to ICDD 00-030-0059 card. The structure of natural kollerite was solved by single-crystal X-ray diffraction: space group *Cmcm*, a = 17.803(7) Å, b = 7.395(4) Å, c = 7.096(3) Å, V = 934.2(7) Å^3, Z = 4. Thermal properties of synthetic AIS-3 were described by KOCSIS *et al*. (2018).

Occurrence, origin, associated minerals

Coalbeds of Liassic age occur in the Jurassic sedimentary formations in the Mecsek Mts. They have been mined since the 18th century. AIS phases were found only once on a burning dump of the Vasas abandoned opencast coal mine, near Pécs. AIS phases were deposited on the surface of the debris, not deeper than 10 cm. They formed by the interaction of organic matter and the decomposition products of iron sulfides. They are rare intermediate products of oxidation between iron sulfides and sulfates. Probably the formation of sulfites was facilitated by the locally suppressed oxidation of spontaneous slow combustion. There are numerous secondary ammonium minerals (sulfates, chlorides) in near-surface position, especially in the open pits. The accompanied minerals of AIS phases are anhydrite, gypsum, hannebachite, clairite, mohrite and ammoniomagnesiovoltaite.

References

ERÄMETSÄ, O. & VALKONEN, J. (1972): Suomen Kemistilehti, 45(3): 91–94.

KOCSIS, T., MAGYARI, J., SAJÓ, I. E., PASINSZKI, T., HOMONNAY, Z., SZILÁGYI, I. M., FARKAS, A., MAY, Z., EFFENBERGER, H., SZAKÁLL, S., PAWAR, R. P. & KÓTAI, L. (2018): Journal of Thermal Analysis and Calorimetry, 132: 493–502.

LARSSON, L. O. & NIINISTÖ, L. (1973): Acta Chemica Scandinavica, 27: 859–867

THE FIRST FIVE YEARS OF THE "MINERAL/FOSSIL OF THE YEAR" PROGRAMME IN HUNGARY – JOINT FORCES IN MUSEUM SCIENCE EDUCATION

FELKER-KÓTHAY, K.
Eötvös Museum of Natural History, Eötvös Loránd University, Budapest, Hungary
E-mail: kothay.klara@ttk.elte.hu

Why Mineral/Fossil of the Year?

The geological education, in general, is very limited in the public education in Hungary. Mineralogy is a stepchild due to the 1948 termination of the subject **natural history** in public education. Zoology and botany, two of the three main fields of the earlier natural history survived and are taught in details within the subject of biology. Mineralogical issues were partly arranged to physical geography, as well as to chemistry and physics, but none of these teachers, during their training, are properly prepared to deal with this task. Hence, mineralogical knowledge of the Hungarian population is very incomplete: the importance of natural resources and the environmental impact of solid technological materials are not recognised. That situation is a good substrate even for orienting to esotericism.

Museums, but later also universities and academic research institutions had been active through separate actions in the last decades in filling up the gap, raising interest in the public for geology. The Hungarian Geological Society (HGS) found a way in 2016 to unite these individual forces by starting the popular science education programme **Mineral of the Year** and **Fossil of the Year**. The aim of the country-wide programme is to mobilize a critical mass of experts, teachers, collectors, etc. for working together, to bring people closer to geological ideas and applications by using the two best known "faces" of geology: minerals and fossils.

Tools of the programme

The last five years have been regarded as a success story, and the programme became a well-defined brand by now (Fig. 1). The preparation of the coming programme year starts in May–June, when a professional board nominates three-three candidates. End of August–mid October is the public voting period, when, based on 6–7000 votes, the winner mineral and fossil are selected by the broadest public. Voting is both online and onsite, the latter realized at outreach programmes in museums, schools, mineral fairs, but even among teacher candidates in universities. The winner of the (next) year is publicized at the largest outreach programme of the HGS, the **Fair of Earth Sciences** in November. The winners so far: garnet (2016), quartz (2017), fluorite (2018), galena (2019), tourmaline (2020); resp. *Nummulites* (2016), cave bear (2017), *Ammonites* (2018), *Komlosaurus* (2019), megalodon (2020).

Throughout the actual calendar year, from January till November multiple tools are used to reach the goal. **Popular articles** are published in magazines and small posts are put on the online platforms (homepage, Facebook…) to introduce the winners. **Outreach programmes** present the winners via touch-on experiences using real pieces of the minerals and fossils, interesting and interactive games, tests, etc. These programmes are effective for reaching different age-groups (children, parents, grandparents) simultaneously, as they often have the same, minimum level background.

Every year, the 3–14 age group is invited to participate in a **drawing competition**. The best drawings, accompanied by a topic-related **photo exhibition** migrate cross the country and are on show in museums.

Talks and **presentations** in different settings, mainly in open programmes of museums and universities, and **demonstrations in schools** are also important tools of the programme. Museums join in growing numbers these activities and often present **small exhibitions** of the winner according to their capacity.

Fig. 1. Posters of the first 5 years of the Mineral of the Year and Fossil of the Year programmes

SECTOR ZONED LUMINESCENT GYPSUM CRYSTALS FROM GÁNT, HUNGARY

HEGYESI, E. B.[1] TOPA, B. A.[1,2] & WEISZBURG, T. G.[1]
[1]Department of Mineralogy, Eötvös Loránd University, Budapest, Hungary
[2]Department of Mineralogy and Petrology, Hungarian Natural History Museum, Budapest, Hungary
E-mail: eszterbernadett@gmail.com

Gypsum crystals can be found at an abandoned bauxite mine in Gánt, Hungary which show photoluminescence under short and long wave UV light (254 nm and 365 nm, respectively). UV excitation reveals sector zoning in the crystals (IWASE, 1936). Luminescent sector zoning in gypsum crystals is quite common, just in Hungary we found them at four other localities (Dévaványa, Herend, Pilisborosjenő and Törökbálint), and it occurs in many other countries including Belgium, Canada, China, Germany, Poland, Romania and Turkey (IWASE, 1936; LENGYEL, 1943; TAGA *et al.*, 2011). In spite of its common occurrence, the cause of luminescence in gypsum is not fully understood yet. TAGA *et al.*, (2011) proposed organic molecular inclusions to be potential source of luminescence, besides the common fluorescence phenomena caused by trace element substitution. In trace amounts, organic molecular inclusions in the luminescent sectors can also effect unusual luminescence. Optical spectra published by Nurieva (1999; cited by GOROBETS & ROGOJINE, 2002) indicated the presence of organic matter as flourophore in gypsum, too. In this research we examine the morphology, inclusions and luminescent properties of gypsum crystals from Gánt, Hungary, and we make an attempt to find out the cause of their luminescence.

Euhedral single crystals, crystal groups and swallow-tail twins were common in the locality.

The morphology of the crystals was cleared by determining the position of the crystallographic *c* axis using the optical properties in polarizing microscope. For indexing we used the β = 127.46° (BOEYENS & ICHHARAM, 2002) setting. Three crystal forms build up the crystals: the {010} pinacoid, the {011} prism and the {120} prism. The luminescent sectors are formed along the {011} prism. Two types of elongation arose: one by the **c**, another by the **a** axes, causing an apparent alternative position of sector zoning (Fig. 1).

Solid inclusions were characterised in gypsum by different light microscopy techniques and Raman spectrometry. The 10–100 μm inclusions represented pyrite and dolomite. None of the inclusion was connected to the luminescence.

Luminescence was examined macroscopically, microscopically and also by optical spectroscopy. The crystals show light blue fluorescence combined with 15 second long phosphorescence in 254 nm UV excitation. The samples were examined under transmitted light microscope equipped with UV excitation source and filter set.

Experiments were conducted also to observe the changes of luminescent properties as an effect of changing temperature. Gypsum specimens were heated from 250 °C up to 600 °C in 50 °C/10 minutes steps. XRD patterns revealed the presence of bassanite, anhydrite and subordinate gypsum at 300 °C, while anhydrite was the only phase at 600 °C. In a cooling experiment down to –17 °C, phosphorescence lasted longer by 1 second as compared to the room temperature reference counterpart, registered by video camera.

Most of these results indicate organic matter as luminophore in the Gánt gypsum crystals.

This work was completed in the ELTE Institutional Excellence Program (TKP2020-IKA-05) financed by the Hungarian Ministry of Human Capacities.

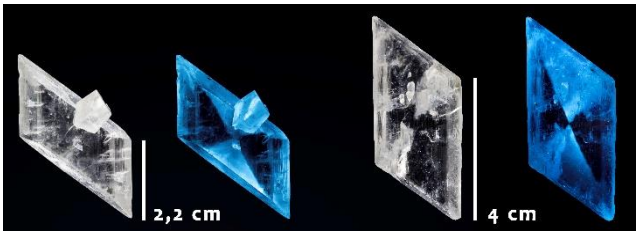

Fig. 1. Gypsum crystals of different elongation directions from Gánt, Hungary (visible light and 254 nm UV light).

References

BOEYENS, J. C. A. & ICHHARAM, V. V. H. (2002): Zeitschrift für Kristallographie, 217: 9–10.

GOROBETS, B. S. & ROGOJINE, A. A. (2002): Luminescent Spectra of Minerals: Reference Book. RPC VIMS Press, Moscow.

IWASE, E. (1936): Bulletin of the Chemical Society of Japan, 11: 475–479.

LENGYEL, E. (1943): Földtani Közlöny, 73: 285–295.

TAGA, M., KONO, T. & YAMASHITA, M. (2011): Journal of Mineralogical and Petrological Sciences, 106: 169–174.

NEW MINERALS OF THE SKARN DEPOSIT OF THE RECSK ORE COMPLEX, MÁTRA MTS., HUNGARY

HENCZ, M.[1], BIRÓ, M.[1], ARADI, L.[2] & B. KISS, G.[1]
[1]Department of Mineralogy, Eötvös Loránd University, Budapest, Hungary
[2]Department of Petrology and Geochemistry, Eötvös Loránd University, Budapest, Hungary
E-mail: henczmate1@gmail.com

The NE Hungarian Paleogene Recsk Ore Complex is well known for its porphyry copper and epithermal Cu-Au mineralisations, but polymetallic skarn and carbonate replacement (CR) ores can also be found, although limited information is available about them. The skarn ore is located around the porphyry intrusion, hosted by Oligocene and Mesozoic carbonate and siliciclastic sedimentary rocks (BAKSA, 1983; HAAS *et al.*, 2013).

The polymetallic skarn ores of Recsk contain mainly andradite garnet, diopside, tremolite, epidote, zoisite, anhydrite, calcite with pyrite, chalcopyrite, galena, sphalerite and minor fahlore as well as various sulphosalts. However, a few new minerals have been identified from the Rm-77 drillcore at 470.0 m. This rock consists of yellowish-grey wall-rock along with massive, macroscopically homogenous black material and a few millimetres thick galena veins. X-ray powder diffraction analysis, Raman microspectroscopy and SEM-EDS were used to identify the minerals of this rock. The presence of brucite, alabandite, monticellite, tochilinite/valleriite along with sphalerite galena, magnetite, serpentine and hydrous garnet were confirmed with all the above mentioned methods, while the presence of perovskite is also possible based on SEM-EDS observations. Perovskite has not been described from the area while alabandite, monticellite, valleriite, and tochilinite are new minerals in Hungary (SZAKÁLL & FEHÉR, 2020).

These minerals, with the exception of alabandite, have been reported in Mg-skarns from the Slovakian Vysoká-Zlatno Cu-Au skarn deposit (UHER *et al.*, 2011). Brucite and monticellite are known in the Mg-skarn of the Yerington District, Nevada, where brucite appears as pseudomorph after periclase (HARRIS & EINAUDI, 1982). The periclase alteration by brucite was also observed from the Recsk skarn deposit by CSILLAG (1975), which was described as a kind of replacement of an unstable Mg-skarn.

Tochilinite, along with brucite and antigorite or lizardite can form with Mg-rich hydration of pentlandite and pyrrhotite (VAN DE VUSSE & POWELL, 1983). The presence of pyrrhotite in the Zn-Cu skarns (FÖLDESSY & SZEBÉNYI, 2008) enables the formation of tochilinite, while valleriite may replace chalcopyrite (COOK & CIOBANU, 2001).

Alabandite most often can be found in epithermal veins associated with rhodochrosite and rhodonite (RAMDOHR, 1980) and in low-temperature hydrothermal deposits, usually accompanied by sphalerite, galena and chalcopyrite. It has also been described from the Western Carpathians in metamorphic deposits and polymetallic veins (KANTOR & KRIŠTÍN, 1973).

The newly identified minerals in the drillcore are unmentioned as of today in any of the studies from Recsk. This skarn specimen might represent a unique mineral assemblage formed during fluid-rich retrograde metasomatism. Our new findings inspire a more detailed research to understand metasomatic skarn processes associated with the porphyry stock at Recsk.

This work was completed in the ELTE Institutional Excellence Program (TKP2020-IKA-05) financed by the Hungarian Ministry of Human Capacities. The study is supported by the ENeRAG project that has received funding from the European Union's Horizon 2020 research and innovation programme under grant agreement No. 810980.

This work was completed in the ELTE Institutional Excellence Program (TKP2020-IKA-05) financed by the Hungarian Ministry of Human Capacities.

References

BAKSA, CS. (1983): Acta Mineralogica-Petrographica, 26/1: 87–97.

COOK, N. J. & CIOBANU, C. L. (2001): Mineralogical Magazine, 65: 351–372.

CSILLAG, J. (1975): Földtani Közlöny, 105: 646–671.

FÖLDESSY, J. & SZEBÉNYI, G. (2008): Publications of the University of Miskolc, Series A, Mining, 73: 7–20.

HAAS, J., PELIKÁN, P., GÖRÖG, Á., JÓZSA, S. & OZSVÁRT, P. (2013): Geological Magazine, 150: 18–49.

HARRIS, N. B. & EINAUDI, M. T. (1982): Economic Geology, 77: 877–898.

KANTOR, J. & KRIŠTÍN, J. (1973): Geologica Carpathica, 24: 247–253.

RAMDOHR, P. (1980): The ore minerals and their intergrowths. Pergamon Press, Oxford.

SZAKÁLL, S. & FEHÉR, B. (2020): In: Fehér, B. (Ed.): 40 éves a Herman Ottó Múzeum Ásványtára. Herman Ottó Múzeum, Miskolc, 19–43.

UHER, P., KODĚRA, P. & VACULOVIČ, T. (2011): Mineralia Slovaca, 43: 247–254.

VAN DE VUSSE, R. & POWELL, R. (1983): Mineralogical Magazine, 47: 501–505.

NON-CONVENTIONAL FLUORIDE SPECIATION IN PHOSPHOGYPSUM: A WAY TO BETTER ASSESS ITS ENVIRONMENTAL BEHAVIOUR

HMISSI, N.[1]*, PRASETYO, D. G.[1], HARMAN-TÓTH, E.[1,2] & WEISZBURG, T. G.[1,3]
[1] Department of Mineralogy, Eötvös Loránd University, Budapest, Hungary
[2] Eötvös Museum of Natural History, Eötvös Loránd University, Budapest, Hungary
[3] Department of Environmental Sciences, Faculty of Science and Arts, Sapientia Hungarian University of Transylvania, Cluj-Napoca, Romania
E-mail: naoureshmissi@gmail.com

Due to recent climate goals (limiting global warming to 1.5 °C, a target of the Paris Agreement), the phasing out of coal power plants is expected at a growing rate. This in turn will generate a growing demand for gypsum in the construction industry, up to now satisfactorily met by the flue gas desulfurization (FGD) gypsum of coal power plants. Thus, another alternative should be found, and a prospective alternative could be phosphogypsum. Phosphogypsum (PG) is a byproduct of the fertilizer industry, produced at a yearly rate of 200–250 million tons. It is generated by attacking natural phosphate rock (PR, mostly of sedimentary phosphorite origin) with sulphuric acid (H_2SO_4) to obtain phosphoric acid (H_3PO_4). PG is a heterogeneous aggregated mixture. Gypsum is the major component, but it is reported to contain also quartz, bassanite, brushite, the partly soluble malladrite (Na_2SiF_6), fluorite (CaF_2), apatite, some organic matter (OM), acid residuals and clay mineral(s) as well.

The direct use of PG is limited by the presence of some radioactive elements, fluorine, potentially toxic metals and phosphorus. Leaching tests revealed that the most problematic elements in PG are F and P, classifying it as hazardous waste (ZMEMLA *et al*., 2020). In this study of a mainland-deposited Tunisian PG we intend to quantitatively specify to which phases is fluorine linked. Previous leaching tests showed that the water-leachable fluoride content is 500–1000 ppm while the total F-content of PG is on the 5 000–10 000 ppm order of magnitude (ZMEMLA *et al*., 2020), i.e., approximately 10% of the total fluoride content is water-soluble. Main F-bearing phases are thought to be malladrite and fluorite, but both clay mineral(s) (CM, with F replacing OH groups) and OM can host some F.

A standard leaching test (e.g., EN 12457) is concerned about the created solution only, but does not follow what happens with the solid phases upon leaching. PG is an unbalanced mixture, with acid residuals, chemically destroyed OM and silicates (incl. CM) that could have important adsorptive properties. In a 24-hour leaching test with 1:10 solid:water ratio even new phases form, including ettringite [$Ca_6Al_2(SO_4)_3(OH)_{12} \cdot 26H_2O$ – may host F replacing OH-group] in larger quantity in the fine fraction (<32 μm) and fluellite [$Al_2(PO_4)F_2(OH) \cdot 7H_2O$], a positive F-host, in smaller quantity (in the 63−125 μm fraction). The pH during the leaching test moved from the starting 3.27 over a minimum, 2.79 at 3.66 hours to 2.84 after 24 hours.

In this study we are concentrating with physical methods (sieving and filtering, hand picking), as much as possible, the different possible fluoride-hosts: OM, CM (represented by diffuse 15 Å reflection at the XPD patterns) and the newly formed phases to see how much they carry from the original fluoride content of the studied phosphogypsum. For the determination of the fluoride content in solids we applied the method developed for silicate rocks (INGRAM, 1970).

Our results confirmed the earlier findings of ZMEMLA *et al*. (2020) regarding the total and water leachable fluoride content of the bulk sample. OM, concentrated by hand-picking of dark grains from both the dry-sieved and leached sample show enrichment of fluoride: the dry sieved, organic-rich dark grains contain 25 000–26 000 ppm fluoride, whereas the black grains collected from the leached sample (>250 μm) have 21 000 ppm fluoride, suggesting that OM may release 20% of its fluoride content during the 24-hour leaching. It is to be noted, however, that the total OM content of these subsamples has not been measured, and they still contain gypsum as the main phase, so stronger conclusions need further analyses. CM-rich subsample yielded 11 600 ppm fluoride content, while ettringite- and fluorite-bearing fine fraction, still having gypsum as the main phase, 28 300 ppm.

A standard leaching test may not tell what happens in the environment, e.g., PG at mainland deposition in Tunisia will not meet large amounts of water; PG deposited directly to sea, at a slightly alkaline, much buffered pH can behave quite differently from what we experience in distilled water. We shall pay attention to design leaching tests that model better what happens in the environment or during the potential reutilisation of an industrial waste.

This work was completed in the ELTE Institutional Excellence Program (TKP2020-IKA-05) financed by the Hungarian Ministry of Human Capacities.

References

INGRAM, B. L. (1970): Analytical Chemistry, 42: 1825−1827.

ZMEMLA, R., SDIRI, A., NAIFAR, I., BENJDIDIA, M. & BOUBAKER, E. (2020): Environmental Engineering Research, 25(3): 345−355.

POLYTYPISM OF CRONSTEDTITE FROM THE NAGYBÖRZSÖNY ORE DEPOSIT, NORTHERN HUNGARY

HYBLER, J.[1], DOLNÍČEK, Z.[2], SEJKORA, J.[2] & ŠTEVKO, M.[2,3]
[1]Institute of Physics, Czech Academy of Sciences, Praha, Czech Republic
[2]Department of Mineralogy and Petrology, National Museum, Praha, Czech Republic
[3]Earth Science Institute, Slovak Academy of Sciences, Bratislava, Slovakia
E-mail: hybler@fzu.cz

Introduction

Nagybörzsöny is a well-known Au-Ag-Pb-Zn ore deposit in northern Hungary, exploited since the Middle ages. It is located in the Börzsöny Mountains, the part of the Neogene Intra-Carpathian Volcanic Arc. Volcanic activity occurred in Middle Badenian during two periods (Lower and Upper units), of the age of 15.2±0.8 My and 14.2±0.9 My, respectively. The Lower Unit was affected by hydrothermal processes in its central area and the deposit was formed during this event (KORPÁS & LANG, 1993). More than 120 minerals were described from this locality (*e. g*. PANTÓ & MIKÓ, 1964; SZAKÁLL *et al*., 2012). The rare mineral cronstedtite was identified in a piece of the ore material collected in 2000 from the dump of the Alsó-Rózsa adit, about 5 km ENE from the village of Nagybörzsöny (GPS coordinates: 47.9408644°N, 18.8943714°E).

Cronstedtite, $(Fe^{2+}_{3-x}\ Fe^{3+}_{x})(Si_{2-x}Fe^{3+}_{x})O_5(OH)_4$, where $0 < x < 0.85$ is a trioctahedral 1:1 layered silicate of the serpentine-kaoline group. It forms many polytypes by stacking equivalent structure building layers composed of octahedral and tetrahedral sheets, with trigonal protocell $a = 5.50$, $c = 7.10$ Å, layer group $P(3)1m$. Polytypes are subdivided into four OD (Ordered-disordered) subfamilies (Bailey's group A, B, C, D), representing the four possible stacking rules of layers. For the accurate determination of polytypes, the single-crystal diffraction techniques are needed – precession photographs, reciprocal space (RS) sections generated from the data collected by the single-crystal diffractometer with an area detector, and/or electron diffraction tomography (EDT) (HYBLER *et al*., 2016, 2017, 2018, 2020).

Experimental

Single crystals of cronstedtite were selected from the sample, glued on the glass fiber, and put on the four-circle (double-wavelength) X-ray diffractometer Gemini A Ultra (Rigaku Oxford Diffraction, Wroclaw, Poland) equipped with the CCD area detector Atlas in the Institute of Physics, Czech Academy of Sciences. The Mo$K\alpha$ radiation, with graphite monochromator, λ = 0.71070 Å, Mo-enhance fiber optics collimator were used throughout all experiments.

The RS sections $(2h\bar{h}l_{\mathrm{hex}})$*, (hhl_{hex})*, $(\bar{h}2hl_{\mathrm{hex}})$*, $(h0l_{\mathrm{hex}})$*, $(0kl_{\mathrm{hex}})$*, and $(\bar{h}hl_{\mathrm{hex}})$* were created by the diffractometer software and used to determine the OD subfamilies and particular polytypes. The chemical composition of some specimens was thereafter determined by electron probe microanalysis (EPMA) (HYBLER *et al*., 2020).

Results

With one exception, all crystals studied belong entirely to the subfamily A. The rare polytype 1*M*, a = 5.51, b = 9.54, c = 7.33 Å, β = 104.5º, space group *Cm* is relatively abundant in the occurrence. Another polytype 3*T*, a = 5.51, c = 21.32 Å, space group $P3_1$ was found, too. Both polytypes occur separately or in the mixed, mostly 1*M* dominant crystals. Some 1*M* polytype crystals are twinned by order 3 reticular merohedry with a 120º rotation along the $\mathbf{c}_{\mathrm{hex}}$ axis as the twin operation. A rare 1*M*+3*T* mixed crystal with 1*M* part twinned contains also a small amount of the subfamily C. A possible presence of the most common 1*T* polytype of this subfamily cannot be confirmed because of overlapping of characteristic reflections with these of 3*T*. Several completely disordered crystals produce diffuse streaks instead of discrete characteristic reflections on the RS sections. EPMA reveals Fe, Si, traces of Mg, Al, S and Cl. The 1*M* polytype is known from Eisleben, Germany (HYBLER, 2014), and from the synthetic run product (PIGNATELLI *et al*., 2013).

References

HYBLER, J. (2014): Acta Crystallographica, B70: 963–972.

HYBLER, J., SEJKORA, J. & VENCLÍK, V. (2016): European Journal of Mineralogy, 28: 765–775.

HYBLER, J., ŠTEVKO, M. & SEJKORA, J. (2017): European Journal of Mineralogy, 29: 91–99.

HYBLER, J., KLEMENTOVÁ, M., JAROŠOVÁ, M., PIGNATELLI, I., MOSSER-RUCK, R. & ĎUROVIČ, S. (2018): Clays and Clay Minerals, 66: 379–402.

HYBLER, J., DOLNÍČEK, Z., SEJKORA, J. & ŠTEVKO, M. (2020): Clays and Clay Minerals, 68: 632–645.

KORPÁS, L. & LANG, B. (1993): Ore Geology Reviews, 8(6): 477–501.

PANTÓ, G. & MIKÓ, I. (1964): Annals of Hungarian Geological Institute, 50(1): 1–153.

PIGNATELLI, I., MUGNAIOLI, E., HYBLER, J., MOSSER-RUCK, R., CATLINEAU, M. & MICHAU, N. (2013): Clays and Clay Minerals, 61: 277–289.

SZAKÁLL, S., ZAJZON, N. & KRISTÁLY, F. (2012): Acta Mineralogica-Petrographica, Abstract Series, 7: 134.

ASBESTOS IN THE NATURAL ENVIRONMENT – EUROPEAN OCCURRENCES AND THE LACK OF LEGISLATION

HYSKAJ, A.[1]*, HARMAN-TÓTH, E.[1,2] & WEISZBURG, T. G.[1,3]
[1] Department of Mineralogy, Eötvös Loránd University, Budapest, Hungary
[2] Eötvös Museum of Natural History, Eötvös Loránd University, Budapest, Hungary
[3] Department of Environmental Sciences, Faculty of Science and Arts, Sapientia Hungarian University of Transylvania, Cluj-Napoca, Romania
E-mail: ambrahyskaj@caesar.elte.hu

Naturally occurring asbestos in Europe

Asbestos fibers, recently referred to as naturally occurring asbestos (NOA), are found in the environment as a result of certain geological processes. Asbestos fibers pose a human health risk in any moment if they become respirable or less frequently ingestible from contaminated waters. NOA fibers in Europe are part of ophiolitic environments in mafic and ultramafic rocks that previously underwent metamorphic and tectonic stages. Occurring together with the regulated asbestos (chrysotile, the amphiboles riebeckite, actinolite, anthophyllite, grunerite and tremolite) there are other minerals showing asbestiform habit that in one case also pose human health risk (e.g., balangeroite), whereas at other cases these are harmless (e.g., brucite, pyroaurite, HYSKAJ et al., 2020). However, the presence of these latter may lead to the overestimation of the amount of and risk related to the given asbestos occurrence.

For this reason, the mapping and detailed mineralogical characterisation of natural asbestos occurrences is necessary to create a database, make advice on safe land use, help urban planning and public awareness. Various fibrous phases such as brucite (nemalite), pyroaurite-2*H* or even the elongated mineral particulates (EMP) are often mixed with or accompanying clearly hazardous phases (regulated asbestos). In such cases, it is important to perform a detailed local phase and chemical analysis in order to properly estimate the asbestos hazard at the natural occurrence. Only a macroscopic evaluation would lead us to an overestimation of the asbestos fibers present in the host rock. At the moment there are few actions taken on the national level (France - CAGNARD & LAHONDÈRE, 2020; Italy - BARALE *et al*., 2020) to map and show the likelihood of NOA based on previous geological information.

Legislation and guidance

Asbestos minerals are all declared as Type 1 carcinogen agents regardless of the asbestos mineral species (IARC, 2012). In Europe it is prohibited to mine, process and use asbestos, the only accepted activities related to asbestos is the removal of asbestos-bearing materials from buildings. In working environments, there is an exposure limit set at 0.1 fibres/cm^3 in 8-hour time-weighted average (TWA) (2009/148/EC). The focus of these regulations is to protect workers or possible exposure from the industrially used asbestos (the true, highly fibrous variety of chrysotile and the amphiboles used). In nature, all transitions from cleavage fragments to real fibers are possible to occur. The natural asbestos occurrences are not included or regulated in any of the directives.

So far, many studies on NOA have followed the recommendations of the World Health Organization (WHO, 1997) on fiber identification and counting criteria but also on analytical methodology. Being a carcinogenic agent, having no safe threshold of exposure and occurring naturally in several countries in Europe, a European Union-level collaboration of experts is needed to set up criteria for identifying risky localities, creating a risk assessment framework and the legislative background for NOA treatment and management, with special emphasis laid on the society-related aspects like safe landuse.

This work was completed in the ELTE Institutional Excellence Program (TKP2020-IKA-05) financed by the Hungarian Ministry of Human Capacities.

References

BARALE, L., PIANA, F., TALLONE, S., COMPAGNONI, R., AVATANEO, C., BOTTA, S., MARCELLI, I., IRACE, A., MOSCA, P., COSSIO, R. & TURCI, F. (2020): Environmental & Engineering Geoscience, 26: 107–112.

CAGNARD, F. & LAHONDÈRE, D. (2020): Environmental & Engineering Geoscience, 26: 53–59.

HYSKAJ, A., HARMAN-TÓTH, E., TOPA, B. A., ARADI, L. E., DEDA, A. & WEISZBURG, T. G. (2020): ProScience, 7: 55–63.

IARC Monographs on the Evaluation of Carcinogenic Risks to Humans (2012): 100/C, 499 pp.

WHO (1997): Determination of airborne fibre number concentrations, a recommended method, by phase-contrast optical microscopy (a membrane-filter method). ISBN 92 4 154496 1, 53 pp.

2009/148/EC: Directive 2009/148/EC of the European Parliament and of the Council of 30 November 2009 on the protection of workers from the risks related to exposure to asbestos at work. Official Journal of the European Union, L 330 (16.12.2009): 28–36

NEW DATA ON CHEMICAL COMPOSITION OF LUZONITE-FAMATINITE SERIES MINERALS IN PRECIOUS AND BASE METAL DEPOSIT ZLATÁ BAŇA (SLOVAKIA)

JELEŇ, S.[1,2], KURYLO, S.[2] & WEIS, K.[1]
[1]Department of Geography and Geology, Matej Bel University, Banská Bystrica, Slovak Republic
[2]Earth Science Institute, Slovak Academy of Sciences, Banská Bystrica, Slovak Republic
E-mail: stanislav.jelen@umb.sk

Geology and mineralogy of the precious and base metal mineralization

The epithermal precious and base metal mineralization of low-sulphidation type at the Zlatá Baňa deposit is located in the Central Zone of the Zlatá Baňa Stratovolcano (Slanské Vrchy Mts., Eastern Slovakia). It occurs in various altered effusive, extrusive and intrusive bodies mainly of pyroxene andesite and diorite porphyries. The central part of the volcanic structure hosts to miscellaneous mineralization types with dominant presence of Pb-Zn(-Au-Ag) type of ores, however, the marginal parts are characterised by Sb(-Au) and Hg type of ores only.

Main ore minerals of the vein mineralization are pyrite, sphalerite and galena, accompanied by chalcopyrite, marcasite, arsenopyrite, Pb-Sb sulphosalts, stibnite, berthierite and cinnabar. The gangue consists of variety of carbonates, minor amount of quartz and barite is very rare. The precious metal mineralization in the deposit is superimposed on the base metal ores and is concentrated in the near-surface parts of veins. The average Au and Ag content in the deposit (in the area of calculated reserves) is 1.42 g/t and 39.74 g/t, respectively. The precious metal mineral association is represented by gold, electrum, silver, Au and Ag tellurides (petzite, hessite), acanthite, polybasite, miargyrite and numerous rare and less rare Ag-Pb-Sb sulphosalts. Reserve of the deposit are 1,623 kt of ore with 1.17% Pb, 2.78% Zn, and 0.1% Cu (KOVALENKER *et al*., 1988, 2000; BAKOŠ *et al*., 2017).

Chemical composition of the luzonite-famatinite series minerals

During a detailed investigation of vein filling ores in Gemerka adit were found a continuous series of solid solutions of Cu_3SbS_4 – Cu_3AsS_4 (luzonite-famatinite) series minerals, unusual for their optical properties and chemical composition. They form separate isometric and irregular grains intergrowing with Ag- and Hg-tetrahedrite, thin veins in chalcopyrite, also thin reaction rims (thickness up to 10 μm) on the border of the pyrite grains. Colour in reflected light is pale brownish pink. The variable chemical composition also documents of the investigated phases (13 WDS analyses; representative analyses are presented in Table 1). Antimony content ranges from 0.26 to 26.63 wt.%, As from 0.46 to 18.4 wt.% and Fe from 0.74 to 2.05 wt.%. Content of other elements is low (Ag up to 0.28; Pb up to 0.19 wt.%). SUGAKI *et al*. (1978) concluded, that the complete solid solution between luzonite and famatinite exists at low temperature. Relationships of above mentioned minerals in aggregates indicate that the minerals of the famatinite-luzonite series were formed at the end of the ore-forming process after the polymetallic mineralization.

Acknowledgment: This contribution was supported by Research Agency of the Ministry of Education, Science, Research and Sport of Slovak Republic (No. VEGA 1/0326/18) and by project KEGA 041UMB-4/2019.

References

BAKOŠ, F. et al. (2017): Gold in Slovakia. Lúč Press, Bratislava.

KOVALENKER, V. A., JELEŇ, S., GENKIN, A. D., ĎUĎA, R., KOTUL'ÁK, P., MALOV, V. S. & SANDOMIRSKAJA, S. M. (1988): Mineralia Slovaca, 20: 481–498.

KOVALENKER, V. A., JELEŇ, S., HÁBER, M., ĎUĎA, R. & PROKOFIEV, V. YU. (2000): Mineralia Slovaca, 32: 249–250.

SUGAKI, A., SHIMA, H. & KITAKAZE, A. (1978): Journal of Mineralogy, Petrology and Economic Geology, 73: 63–77.

Table 1. Chemical composition of the famatinite-luzonite series minerals from Zlatá Baňa in wt.%.

Sample	Sb	Ag	Cu	As	Fe	S	Total	Sb/(Sb+As)
1. ZB-6A 3	26.56	0.05	44.20	0.84	0.74	29.22	101.58	0.97
2. ZB-6A 2	20.26	0.13	45.10	5.07	0.83	29.41	100.83	0.80
3. ZB-6A 6	9.56	0.15	47.10	11.56	1.27	32.76	102.40	0.45
4. ZB-6A 29	0.73	0.10	48.70	17.79	1.40	33.30	102.01	0.04

Empirical formulae: **1.** $(Cu_{3.01}Fe_{0.06})_{\Sigma 3.07}(Sb_{0.94}As_{0.05})_{\Sigma 0.99}S_{3.94}$; **2.** $(Cu_{3.03}Fe_{0.06}Ag_{0.01})_{\Sigma 3.10}(Sb_{0.71}As_{0.29})_{\Sigma 1.00}S_{3.91}$,
3. $(Cu_{2.94}Fe_{0.09}Ag_{0.01})_{\Sigma 3.04}(Sb_{0.31}As_{0.61})_{\Sigma 0.92}S_{4.05}$; **4.** $(Cu_{2.95}Fe_{0.10}Ag_{0.01})_{\Sigma 3.06}(Sb_{0.02}As_{0.92})_{\Sigma 0.94}S_{4.00}$

AN EARLY 18TH CENTURY SCIENTIFIC NETWORK BETWEEN ENGLAND AND TRANSYLVANIA – MINERALS, FOSSILS, AND BOOKS OF SÁMUEL KÖLESÉRI, JR.

KÁZMÉR, M.
Eötvös Loránd University, Budapest, Hungary
E-mail: mkazmer@gmail.com

Fourteen copperplates in the first palaeobotany handbook, the *Herbarium Diluvianum* (1723) of the Swiss medical doctor Johann Jacob Scheuchzer, bear dedications to his most prestigious friends (Fig. 1). They range from the Archbishop of Canterbury and Isaac Newton to learned men residing in the Low Countries, France, Germany, Switzerland, Italy, Hungary, and Turkey. Five of the dedicatees and the author himself were extremely successful members of the medical profession. Their correspondence, published books, mineral and fossil specimens, and catalogues of their personal libraries and collections have been studied in order to map a network of scientific exchange in Early Modern Europe. Three medical doctors: the Englishman John Woodward of London, the Swiss Johann Jacob Scheuchzer of Zürich, and the Hungarian Samuel Köleséri of Transylvania shared interests in collecting and preserving minerals and fossils, and in using them to support their scientific ideas. They regularly supplied each other with newly found specimens, communicating about their characters and origins. Each of them published monographic works in their respective fields of interest, using mineral and fossil specimens received from their partners in the scientists' network to provide substantial evidence for the Flood, a novel and progressive idea of the age.

Sámuel Köleséri, Jr., (1663–1732) owned the largest private library in Hungary and Transylvania. Additionally, he collected minerals and fossils, of which almost nothing remained. His scientific correspondence and specimens preserved in the surviving collections of John Woodward, a British medical doctor, and Johann Jakob Scheuchzer, a Swiss medicus and in their catalogues, and remarks in the travelogue of Edmund Chishull preserves sufficient information to outline the contents of his mineral and fossil collection, the way of collecting, and the use of the specimens.

Fig. 1. A plate from Scheuchzer's Herbarium Diluvianum (1728) depicting a fossil *Isis* coral, a Tertiary leaf imprint and a block with manganese dendrite incrustation. Dedication of the plate is to *Ill. D.o Samueli Kölesero de Keres-eer. Secretario Guberniali Caesareo-Regio Principatus Transylvaniae.* [To the respected Samuel Köleséri of Keres-eer, secretary of the imperial-royal government of the Transylvanian Principality].

Reference

KÁZMÉR, M. (1998): Journal of the History of Collections, 10: 159–168. http://kazmer.web.elte.hu/pubs/Kazmer_1998_Woodwardian_Coll_JHisColl.pdf

ARCHAEOMETRICAL RESULTS OF A K-METASOMATISED VOLCANITE POLISHED STONE TOOL FROM SZERENCS-TAKTAFÖLDVÁR, HUNGARY

KERESKÉNYI, E.[1], SZAKMÁNY, Gy.[2], KRISTÁLY, F.[3], KASZTOVSZKY, Zs.[4] & FEHÉR, B.[1]
[1]Herman Ottó Museum, Miskolc, Hungary
[2]Department of Petrology and Geochemistry, Eötvös Loránd University, Budapest, Hungary
[3]Institute of Mineralogy and Geology, University of Miskolc, Miskolc, Hungary
[4]Centre for Energy Research, Budapest, Hungary
E-mail: kereskenyierika@yahoo.com

Archaeological background and macroscopic description

An archaeometric study was carried out on a late Neolithic Tisza culture related, 74.44.5 inventory numbered polished stone tool originated from Szerencs-Taktaföldvár archaeological site. The colour of the flat polished stone implement is black with red patches on its surface, which can be seen by naked eye. The weight of the tool is strikingly heavy. The magnetic susceptibility of the implement is extremely high 76.57 $\times 10^{-3}$ SI.

Results

The bulk chemistry was performed by non-destructive PGAA. The alkali content of the polished stone tool is exceedingly high (10.19 wt.%), the Al_2O_3-content is also high (21.70 wt.%), while the CaO content is very low (0.56 wt.%) and the SiO_2 content is 50.70 wt.%. Based on the high alkali content it can be possible that the rock was affected by alkali metasomatism.

Studying the BSE image of the stone implement, the duality of the texture is striking. One half of the polished section is inequigranular and porphyritic with potassium feldspar megacrysts, while the other half of the section is fine-grained. The size of the potassium feldspars is over 1 mm. Its composition varies: the Ba content increases from core to rim (0.03 to 0.10 apfu), but this trend does not appear in each crystal, so the rock contains Ba-rich and Ba-free potassium feldspars, either. The other observed minerals in the implement are oligoclase, relict enstatite, REE-rich epidote, biotite, clinochlore in large amount, dravitic tourmaline, magnetite and ulvöspinel in even distribution.

XRD analyses confirmed the presence of sanidine, feldspar, enstatite, ulvöspinel and magnetite.

In the Carpathian Basin and its surroundings, similar rocks with SiO_2 content cc. 50 wt.%, affected by alkali metasomatism, are known as potassic-trachyte from Mátra Mountains, Telkibánya, both in Hungary and Baia Mare, Romania (KUBOVICS, 1966). However, they can be excluded as source areas, because of the much higher iron content of the stone tool. In the Veporicum and the Gemericum (Slovakia) alkali metasomatism took place, but more acidic rocks, mainly granite were affected by the process (ŠIMURKOVÁ *et al*., 2016). Hyalophane-bearing, magnetite-rich rocks were described from the Slovak Ore Mountains, near Tisovec (HURAI & HURAIOVÁ, 2011), furthermore dravite-bearing rock is mentioned from this area, too (BAČÍK *et al*., 2015). Knowing the fact that the polished stone implement belongs to the Tisza culture, it is imaginable that the raw material came from southern areas (e.g., Balkan region or Romania) to the Szerencs-Taktaföldvár archaeological site. It is since the Tisza culture spread over a wide area, covering the Danube-Tisza interfluve and Tiszántúl areas, either (KREITER *et al*., 2017). Furthermore, the Tisza culture also appeared in the Banat region (Romania), and showing many analogies with the Vinča culture, which spread in North Serbia (RACKY, 1992).

Despite of the numerous unique signatures, the exact provenance field cannot be determined, and remote source areas cannot be excluded either.

References

BAČÍK, P., ERTL, A., ŠTEVKO, M., GIESTER, G. & SEČKÁR, P. (2015): The Canadian Mineralogist, 53: 221–234.

HURAI, V., & HURAIOVÁ, M. (2011): Neues Jahrbuch für Mineralogie – Abhandlungen, 188: 119–134.

KREITER, A., KALICZ, N., KOVÁCS, K., SIKLÓSI, ZS., VIKTORIK, O. (2017): Journal of Archaeological Science: Reports, 16: 589–603.

KUBOVICS, I. (1966): Földtani Közlöny, 96: 13–26.

RACKY, P. (1992): Balcanica, 23: 147–165.

ŠIMURKOVÁ, M., IVAN, P. & GARGULÁK, M. (2016): Acta Geologica Slovaca, 8/1: 87–98.

UNWANTED SOLID DEPOSITION ACCOMPANYING BIOGAS COMBUSTION IN BIOGAS-TO-ENERGY PLANTS IN HUNGARY

KHAIDI, A.[1], HARMAN-TÓTH, E.[1,2], GÖNCZI, I.[3], MIREISZ, T.[4], KŐVÁRI, T.[4] & WEISZBURG, T. G. [1,5]
[1]Department of Mineralogy, Eötvös Loránd University, Budapest, Hungary
[2]Eötvös Museum of Natural History, Eötvös Loránd University, Budapest, Hungary
[3]NRG Group, Kecskemét, Hungary
[4]Budapest Waterworks Ltd., Budapest, Hungary
[5]Department of Environmental Sciences, Sapientia Hungarian University of Transylvania, Cluj-Napoca, Romania
E-mail: ameershabreen@gmail.com

Hungarian energy systems are supported by a mix of primary energy sources including fossil fuels (coal, oil, natural gas), nuclear power and renewables (biomass, solar, wind, biogas, hydro, geothermal). According to the Hungarian Energy and Public Utility Regulatory Authority (ALFÖLDI *et al*., 2019), Hungary has high energy import dependency, which was twice as much as the total primary energy production (458 PJ) in the year 2019, and most of the energy consumption (60%) was dominated by hydrocarbons (natural gas and oil products). The share of renewables within the electricity consumption in 2019 is only 9.72%. Not just in Hungary, but all around the world the renewable sources cannot yet fully replace the fossil fuels. With no doubt renewable energy would be the future of energy systems in fighting the climate change and its adverse effects to our environment, the question is just how the renewables can support current energy systems?

We are working with one of the renewables, biogas that is produced as a result of waste management, namely urban waste landfill (UWL) and wastewater treatment (WWTP). Biogas is produced through anaerobic digestion of organic-rich waste, it fuels cogeneration technology (Combined Heat and Power Systems, CHPs) to produce both heat and electricity (ISA *et al*., 2018). The electricity and heat produced is used to support the operation of the plants and the excess can be sold to the local grid. In this way, the energy produced promotes the self-sustainability of waste industry.

The main technological challenge in the biogas-to-energy industry is the solid deposition on the gas engine reaching thickness over the mm range, deteriorating engine working conditions and increasing maintenance needs. Moreover, the deposits formed in different parts of engine can get into the lubricating oil, decreasing its lifespan and increasing the oil consumption of the system. Ideally, in the combustion process CH_4 content of the biogas is converted to CO_2 and water, however, in reality, trace contaminants like H_2S and siloxanes are also involved in the oxidation process. High-temperature and constantly changing pressure conditions of the internal-combustion engines, with special flow dynamics lead to the formation of both glassy (short-range-order only; SRO) and crystalline phases.

We sampled solid engine deposits from biogas-to-energy facilities at two UWL and three WWTP sites, including the largest facilities serving the capital, Budapest, of 1.7 million population. The deposits formed multilayer crust on the piston crown and cylinder head surfaces. Physically, the crusts at the UWL are harder, resistant, and hard to remove from the surface compared to WWTP. The deposits varied in colour from whitish, greyish to brownish, some burnt parts are black. Some of the exhaust valves from the UWL are broken indicating advanced state engine failure, too.

In the UWL combustion chambers deposition of crystalline phases (anhydrite – $Ca[SO_4]$; cristobalite & quartz – SiO_2 polymorphs) beside the dominant Ca-silicate glass could be observed. The combustion chambers at the WWTP only suffered from calcium sulfate deposition, anhydrite. These findings suggest that either siloxanes are properly removed or are present in much smaller amounts at WWTP. Inside the heat exchanger compartment at WWTP the exhaust gas deposited formed large amounts of hydronium-jarosite $(H_3O)Fe_3(SO_4)_2(OH)_6$[trig]. It shows that H_2S, converted to SO_3 during combustion, is not fully deposited as anhydrite and some escaping with the exhaust gas leads to the corrosion of Fe-bearing parts of the engines.

To develop a strategical approach in green technology development, it is important to have a proper characterization of forming deposits during biogas combustion and to understand their formation conditions and transport inside the engine, from initial input biogas and final output exhaust gas.

This work was completed in the ELTE Institutional Excellence Program (TKP2020-IKA-05) financed by the Hungarian Ministry of Human Capacities.

References

ALFÖLDI, G. et al. (eds., 2019): Data of the Hungarian Electricity System 2019. MEKH-MAVIR ZRt. Budapest. http://www.mekh.hu/a-magyar-villamosenergia-rendszer-2019-evi-adatai

ISA, N. M., TAN, C. W. & YATIM, A. H. M. (2018): Renewable and Sustainable Energy Reviews, 81: 2236–2263.

MAGMATIC EVOLUTION OF HUNGARIAN DURBACHITE-TYPE VARISCAN GRANITOID BASED ON U-Pb ZIRCON GEOCHRONOLOGY

KIS, A.[1,2], WEISZBURG, T. G.[1], DUNKL, I.[3], VÁCZI, T.[4] & BUDA, Gy.[1]
[1] Department of Mineralogy, Eötvös Loránd University, Budapest, Hungary
[2] Department of Mineralogy and Petrology, Hungarian Natural History Museum, Budapest, Hungary
[3] Department of Sedimentology and Environmental Geology, Geoscience Center, GU, Göttingen, Germany
[4] Department of Applied and Nonlinear Optics, Institute for Solid State Physics and Optics, Wigner Research Centre for Physics, Eötvös Loránd Research Network, Budapest, Hungary
E-mail: annamari.kis@gmail.com

We analysed two hundred sixty three well-determined, carefully pre-selected (KIS *et al.*, 2019), non-metamict spots in ninety eight zircon crystals with different morphological characteristics (short, normal, long prismatic) from all rock types (felsic, hybrid, mafic) in the Mórágy pluton, Hungary using laser ablation inductively coupled plasma mass spectrometry (LA-ICP-MS).

The routinely used LA-ICP-MS can result in reliable age constraints only if the system is not overprinted by multiple geological processes that affect the isotope system of zircons. To overcome the ambiguities our zircon U-Pb age data were evaluated first using simple statistical models, then a zircon internal (primary and secondary) texture related complex approach was applied. That latter method demonstrated that the U-Pb age in our overprinted system show correlation with the local structural state of the zoned zircon crystals (Fig. 1).

Individual zircon internal texture and structural state based evaluation made possible to select the least overprinted age components of the system and identify five steps **(phases A–E)** in the evolution of the studied intrusive.

In **phase A** two magmas, a granitoid felsic and a lamprophyre-derived mafic were generated separately. In **phase B**, the thermodynamic conditions favoured the long and short prismatic type zircon growth morphology over the normal prismatic type. By cooling of the system crystallization of rock forming minerals was initiated in **phase C**. This is the first point when we can try to assign time and temperature to the system (~800–850 °C; ~355 ± 3–4 Ma). For zircon crystal morphology the normal prismatic type gains dominance over the short and long types. Already at this phase, or at the beginning of **phase D** at the latest, mingling of the two magmas went on. Zircon crystallizes continuously in normal prismatic shape. Phase D may overarch the ~ 348–338 Ma period and the 800–700 °C temperature range. **Phase E** is the eutectic crystallization of the rest magmas. The rims of these long and normal prismatic zircons are embedding Na-free K-feldspar, albite and quartz, indicating a ~650 °C closing temperature, besides show the ~334 ± 4 Ma closing age.

The post-crystallization history, denoted here technically as **phase F**, is even more complicated than the previous five phases: more, possibly separated impacting events (F1, F2, F3) can be distinguished. In **event F1** lead loss of worse structural state zircon zones results younger concordant ages. In **event F2** the secondary texture type (convolute zonation) fully overprints the zircon primary internal texture (growth zonation). These convolute zones are of good structural state and give well defined concordant zircon U-Pb ages (~300 Ma). **Event F3** resulted in overprints causing slightly discordant ages. **Event F3** could be attributed to a proven magmatic event of the area in the Cretaceous.

This work was completed in the ELTE Institutional Excellence Program (TKP2020-IKA-05) financed by the Hungarian Ministry of Human Capacities.

Reference

KIS, A., WEISZBURG, T. G. & BUDA, GY. (2019): Földtani Közlöny, 149: 93–104.

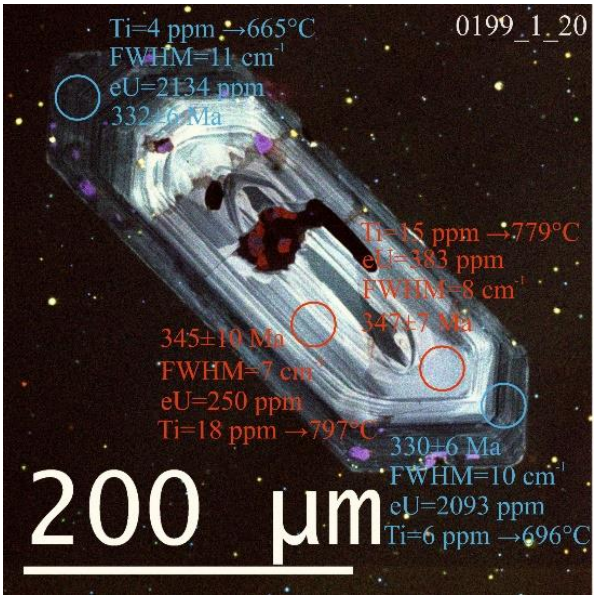

Fig. 1. Zircon crystal (grain #0199_1_20) with a large antecrystic / xenocrystic core and growth zoning texture. Notation: Circles show the U-Pb dated areas. Same colour means same internal texture part. Concordant age with error (Ma), effective U = eU(ppm) = U(ppm) + 2.4*Th(ppm), $\nu_3(SiO_4)$ FWHM (cm^{-1}), Ti-in-zircon thermometry data (5080/(6.01-log(Ti in ppm))-273) are indicated to each area analysed.

STRUCTURE CHANGES OF LANTHANIDE (LN)-BENTONITES

KOVÁCS, E. M., KÓNYA, J. & M. NAGY, N.
Imre Lajos Isotope Laboratory, Department of Physical Chemistry, University of Debrecen, Debrecen, Hungary
E-mail: kovacs.eszter.maria@science.unideb.hu

In this work, the structure of lanthanide-bentonites was analyzed for nuclear waste treatment, and environmental protection purposed by several analytical methods. The main mineral of the bentonite is montmorillonite, which has a permanent negative charge. The negative charge is neutralized by cations attracted to the interlayer space where cation exchange takes place and sometimes modifies the properties of the bentonite. The natural interlayer cations may be exchanged by Lns. The importance of lanthanide ions is that they are model interactions between soil and transuranium ions, furthermore, lanthanide cations are produced during the fission of ^{235}U in nuclear power plants.

Ln-exchanged bentonites were prepared from Ca-bentonite by ion exchange procedure from Ln-perchlorate solution. To prove the successful modification, scanning electron microscopy, energy-dispersive X-ray analysis (SEM-EDX) was used showing distribution of Ln's and other components of bentonite. The natural bentonite and the lanthanide exchanged bentonites were characterized by X-ray diffraction (XRD), which revealed the same mineral composition, and the increase of the basal spacing of montmorillonite. The amount of Ca^{2+}, Fe^{3+}, and Ln^{3+} on the bentonite were determined by X-ray-fluorescence spectrometry (XRF). In most Ln-bentonites, the quantity of the exchanged Ln ions was about 80–90% of the cation exchange capacity (CEC) of the bentonite. For some lanthanide bentonite (Y^{3+}, La^{3+}, Ce^{3+}, and Gd^{3+}), the sorbed quantity of lanthanide ions was higher that the cation exchange capacity. Moreover, the iron(III) content of lanthanide bentonite was less than that of the original Ca-bentonite (KOVÁCS *et al.*, 2017).

The observation is that lanthanide ions can somehow supersede iron from the octahedral positions of crystal lattice. We assume that the departure of positively charged iron ions from the lattice increases the negative layer charge and the cation exchange capacity. This can motivate the enhance sorption of lanthanides.

To prove our previous statement, we examined how the pH and the concentration influences the bentonite structure without and with Lns. Ca-H, Ca-Y and Ca-La cation exchange were carried out. The results revealed that the pH had high influence during the Ca-H cation exchange procedure. The more acidic solution, the more calcium was exchanged. In this case, iron loss was not observed. In the case of Ca-Y, La cation exchange procedure, the pH has low influence, meanwhile the concentration has higher influence to high amount of iron loss during divalent-trivalent cation exchange. Thus, the high amount of trivalent lanthanides cause the structural iron release (KOVÁCS *et al.*, 2019).

Furthermore, the concentration of lanthanide, calcium and iron ions undergoes a three-step change during the kinetic study of lanthanide ion sorption. We assumed that beside the bivalent-trivalent cation exchange, diffusion of the iron ion from the octahedral layer would be started from the first moment, due to the high concentration of the lanthanide ions. It also depends on the temperature, but the pH has only a slight influence on the three-step process.

A strong evidence detected by X-ray photoelectron spectroscopy (XPS) measurement that the bentonite is capable of such a big structural change in the presence of lanthanide ions. The increase of the negative layer charge of the Ln-bentonites can be confirmed by XPS since the positive or negative correlations between the Si 2s (2p), Al 2p and O 1s photoelectron binding energies refer to the silicate structure (SEYAMA & SOMA, 1984, 1985, 1988). The value of the photoelectron binding energies decreases with the increase in the negative layer charge of the silicate. Due to the over-sorption of the lanthanide ions and the decrease in iron content, the decrease of the binding energies is measured which is supported our statement.

References

KOVÁCS, E., BARADÁCS, E., KÓNYA, P., KOVÁCS-PÁLFFY, P., HARANGI, SZ., KUZMANN, E., KÓNYA, J. & M. NAGY, N. (2017): Colloids and Surfaces A: Physicochemical and Engineering Aspects, 522: 287–294.

KOVÁCS, E., KÓNYA, J. & M. NAGY, N. (2019): Journal of Radioanalytical and Nuclear Chemistry, 322: 1747–1754.

SEYAMA, H. & SOMA, M. (1984): Journal of the Chemical Society, Faraday Transactions 1, 80: 237–248.

SEYAMA, H. & SOMA, M. (1985): Journal of the Chemical Society, Faraday Transactions 1, 81: 485–495.

SEYAMA, H. & SOMA, M. (1988): Research Report from the National Institute for Environmental studies, Japan, No. 111.

DIFFERENTIATION OF MICA STRUCTURES AND POLYTYPES BY DECONVOLUTION OF X-RAY POWDER DIFFRACTION PATTERNS

KRISTÁLY, F.
Institute of Mineralogy and Geology, University of Miskolc, Miskolc, Hungary
E-mail: askkf@uni-miskolc.hu

Mica group and related minerals are important rock-forming phases bearing information of petrogenesis and petrological evolution of numerous rock formations. Beyond metamorphic crystallization, processes of hydration and alteration and sedimentary transformations can be recognized by the detailed evaluation of X-ray diffraction patterns of complex rock powders. While talc-pyrophyllite, true micas and brittle micas can be routinely identified, there are quite a number of problems in interpreting species and solid solutions of the flexible and interlayer cation deficient micas – the most important from petrogenetic point of view. The commonly accepted view persists, according to which muscovite(s), biotite(s), illite(s) and related minerals may not be distinguished by XRPD. However, recent observations on large and various sample types show that even highly detailed differentiation is possible even on bulk rock analysis. The application of supporting methods like electron-beam microanalysis, rock chemistry and vibration spectroscopic methods must be applied.

Samples of clays, clastic and volcanic sedimentary rocks, shales and phyllites, schists, cataclastic and different magmatic, hydrothermal materials were investigated. Results serving as the base of this research are XRPD patterns recorded on Bruker D8 Advance (Vantec1 position sensitive detector) and Discover (LynxEye XE-T position sensitive detector) diffractometers with Cu-$K\alpha_{(1,2)}$ radiation and 40 kV with 40 mA generator settings. Step size, counting time and instrument geometry were chosen both with similar and different settings, to enhance possibilities of developing technical solutions. Observations and calculations were tested on high purity monomineralic samples and their mixtures.

As expected, several important peaks and angular regions can be delimited, which serve as the basis of recognizing and distinction between several mica phases present in one mixed sample: 4.5–4.2 Å, 3.4–3.2 Å, 2.6–2.3 Å and other special peaks for polytypes, but also (00*l*) and (060) peaks are important. Beyond *d*-values of (00*l*) peaks the shape and asymmetry are important parameters, however the information related to different structures can be extracted only through whole powder pattern deconvolution. The process also requires instrumental parametrisation either by Fundamental Parameters Approach, or by empirical profile convolution definition. Rietveld refinement is an optimal approach for such tasks, and it has the advantage that samples with complicated mineralogy can also be solved. It also handles the preferred orientation and anisotropic size distribution effects on peak intensity and shape distortions. On the other hand, it offers the possibility to select those few mica-related entries from ICDD PDF database which can be trusted for Search/Match identification – always validated by deconvolution-based solutions.

Presence and ratio of muscovite and biotite series can be fixed by solving the fit of the 10 Å, 5 Å and ~2.5 Å peaks, while in the case of biotite-dominated mica fraction Mg vs. Fe^{2+} dominancy may be approximated on the (060) peak. Effects of interlayer cation substitution are detectable on the (00*l*) peaks position, while cation deficiency can be tracked and approximated by occupancy related intensity refinement. Moreover, the presence and ratio of octahedral substitutions can be clarified. This way, transitions towards illite-group phases and glauconites can be observed and quantified, taking into account space group and lattice parameter constraints. While celadonites and paragonites are easily recognized, the Li-bearing phases poses more problems and less results do their scarcity and problems of chemical analysis. For polytype identification, after consulting the relevant literature it was also possible to select suitable ICDD PDF data entries and define starting structural models for deconvolution.

Crystallite size and strain effects are handled in the necessary manner that even nanocrystalline broadening does not obstruct the above possibilities. The measurement conditions were tested on grain size fractions of different samples obtained by sieving and sedimentation but also on nanocrystalline powders produced by milling. After testing the solution possibilities on high purity phases and their mixtures, investigations of multiphase known mixtures and rock specimens were also conducted. Results show that the presence of more than 2 mica types can be recognized even at ~2–3 wt% total mica fraction with ~0.5 wt% of detection limit, while for a mica fraction of > 10 wt% the presence of several types is recognized. Supporting results from additional analytical techniques is usually required to validate the solutions but improving diffractometer and software solutions provide significant potential for detailed mica characterization. Moreover, testing the effect of X-ray optics from improved towards lower angular resolution possibilities might facilitate mica differentiation in various application fields.

Acknowledgement
Supported by the Bolyai János research scholarship program (BO/00920/19/10) of the Hungarian Academy of Sciences.

MICRO-PIXE INVESTIGATION OF THE TRACE ELEMENTS IN THE MINERALS OF THE RÓZSABÁNYA HYDROTHERMAL ORE DEPOSIT (BÖRZSÖNY MTS., NORTH HUNGARY)

LÁSZLÓ, T.[1], KERTÉSZ, Zs.[2], MÉSZÁROSNÉ TURI, J.[3] & DOBOSI, G.[1]
[1]Department of Mineralogy and Geology, University of Debrecen, Debrecen, Hungary
[2]Laboratory for Heritage Science, Institute for Nuclear Research, Debrecen, Hungary
[3]Mining and Geological Survey of Hungary, Budapest, Hungary
E-mail: laszlo.tim@citromail.hu

Introduction

The hydrothermal ore deposit of Rózsabánya near Nagybörzsöny village is located at the central part of the Börzsöny Mountains in Northern Hungary. The surrounding volcanic area is made up Miocene calc-alkaline intermediate rocks, predominantly andesites with minor amounts of dacites. The ore mineralization occurs as stockwork impregnation in propylitic dacite breccia pipe (PANTÓ & MIKÓ, 1964; NAGY, 1983). The age of the hydrothermal activity is 15.2–14.8 Ma (KORPÁS & LANG, 1993). The ore formation took place in two major phases. The ores of the first phase include mainly pyrrhotite with Fe-rich sphalerite and chalcopyrite. The minerals of the second phase were formed partly by the replacement of the earlier precipitated ores. The ore paragenesis of the second phase is characterized by arsenopyrite, galena, Bi-minerals, Pb-Bi sulphosalts (lillianite-gustavite) and native gold.

Though detailed electron microprobe study has been carried out on the ore minerals of Rózsabánya, trace elements cannot be determined using electron beam methods. We aimed to analyze the trace element contents of the most important ore minerals using the much more sensitive proton-induced X-ray emission (PIXE) technique.

Samples and methods

Samples used in present study were collected from the Rózsa shaft by G. Pantó and L. Mikó during the exploration of the Börzsöny Mts. in the fifties of the last century.

Micro-Particle Induced X-ray Emission (micro-PIXE) analysis was performed using the scanning nuclear microprobe at the Institute for Nuclear Research, Debrecen, Hungary (KERTÉSZ et al., 2015). The nuclear microprobe is installed at the 0° beamline of the 5MV Van de Graaff accelerator. The minerals were irradiated with a focused H^+ beam with 2.5 MeV energy and of 200–300 pA. The beam size was 1.5 μm × 1.5 μm.

Results

Trace element contents of pyrrhotite, sphalerite, chalcopyrite, arsenopyrite, pyrite and galena were determined. Of the minerals, the iron-rich sphalerite contains the widest range of trace elements. The Cd and Mn contents of the sphalerite have already been known from the earlier electron microprobe measurements, but the relatively high concentrations of Co (790 ppm), Cu (950 ppm), and high Ga (2540 ppm) and In (1130 ppm) contents haven't been detected earlier, though traces of In have previously been found by optical emission spectrography in the ores of Rózsabánya. In chalcopyrite, significant amounts of Sn (1010 ppm), In (650 ppm) and Co (1950 ppm) could be analyzed. The only trace element of pyrrhotite is Co (4670 ppm), Cu and Ni could not be detected. Pyrrhotite is one of the oldest and most abundant minerals in the Rózsabánya ore, and later minerals as pyrite, arsenopyrite were partly formed by the alteration and re-arrangement of the high temperature primordial pyrrhotitic material. Therefore, the high concentration of Co in pyrite (3870 ppm) is the result of pyrrhotite alteration and replacement, where the newly formed pyrite "inherited" the Co content of the original pyrrhotite. Arsenopyrite contains more than 1 wt% Co, which is in good agreement with the existing electron microprobe data. The source of the Co in arsenopyrite can either be the altered pyrrhotite, or the hydrothermal solutions of the second mineralization phase. The importance of cobalt in Rózsabánya is shown by the fact that it was detected in almost all major ore minerals. The other significant trace element in arsenopyrite is Se (2430 ppm). Galena crystallized during the late stages of the ore formation. Its trace elements are Ag (950 ppm) and Se (1930 ppm).

These are our first trace element results for the sulphides of the Rózsabánya mineralization. According to our experience, micro-PIXE is a suitable non-destructive method for quantitative analysis of trace elements in ore minerals.

References

KERTÉSZ, ZS., FURU, E., ANGYAL, A., FREILER, Á., TÖRÖK, K. & HORVÁTH, Á. (2015): Journal of Radioanalytical and Nuclear Chemistry, 306: 283–288.

KORPÁS, L. & LANG, B. (1993): Ore Geology Reviews, 8: 477–501.

NAGY, B. (1983): Acta Geologica Hungarica, 26: 149–165.

PANTÓ, G. & MIKÓ, L. (1964): Annals of the Hungarian Geological Institute, 50/1: 1–153.

CRITICAL MINERALS IN BLACK SCHISTS FROM SZENDRŐLÁD (SZENDRŐ MTS., NE HUNGARY)

LESKÓNÉ MAJOROS, L.[1], KARACS, G.[2], KOÓS, T. L.[3], SZAKÁLL, S.[1] & KRISTÁLY, F.[1]
[1]Institute of Mineralogy and Geology, University of Miskolc, Miskolc, Hungary
[2]MTA-ME Materials Science Research Group, ELKH, Miskolc, Hungary
[3]Institute of Energy and Quality, University of Miskolc, Miskolc, Hungary
E-mail: asklivia@uni-miskolc.hu

The EUROPEAN COMMISSION (2020) has recently published the new Study on the EU's list of Critical Raw Materials, in which 30 critical raw materials are included beyond graphite. Natural graphite is associated with several other critical elements, due to their geochemical affinity to organic matter (HOLLAND, 1979; BRUMSACK & LEW, 1982). In our study, we focus on these critical elements and raw materials, namely natural graphite and related elements of graphitization: titanium, niobium, phosphorus, light and heavy rare earth elements (REE).

Rock samples were collected from outcrops along the valley of Helle Creek (NE part of Szendrőlád village, Szendrő Mts., NE Hungary), exposing the Szendrőlád Limestone Formation (Middle to Late Devonian, basin facies) (FÜLÖP, 1994). The collected samples are dark-grey or black coloured, intensely deformed and schistose fine-grained phyllites.

The samples were investigated with polarizing petrographic and ore microscopy (OM), scanning electron microscopy (SEM-EDX), X-ray powder diffraction (XRD), transmission electron microscopy (TEM) and differential thermal analysis (DTA). In addition, experiments on graphite extraction were also performed by froth flotation (CROZIER, 1990) in 5% ethanol solution following the disaggregation by ultrasonic shaking (Hielscher UIP1000hdT).

According to the optical microscopy and scanning electron microscopy (SEM-EDX) results, the samples have metamorphic texture. The matrix consists of oriented and often polysynthetic twinned calcite crystals (usually with low Mg and Fe content). The 50–100 μm sized mica plates (muscovite, Na-bearing muscovite and phengite) and 50–200 μm sized quartz grains can be found mainly in the deformed zones.

Many accessory minerals are also observed by SEM-EDX. As main Ti mineral, 10–50 μm sized TiO_2 minerals (anatase and rutile based on optical observations) are often found in the deformed zones with traces of Nb. As HREE-bearing mineral, 10–30 μm sized xenotime grains occur, while LREE-containing minerals are allanite, 10–20 μm sized bastnäsite-(Ce) needles and 20–80 μm sized monazite-(Ce) grains. Zircon, as Zr-bearing mineral, is also frequent, linked to the deformed zones. Furthermore, as P-bearing mineral, 20–100 μm sized apatite grains are also detected in the samples.

Graphite cannot be detected directly by OM and SEM-EDX, as its thin and μm sized flakes are lost during sample preparation. Only 50–300 μm sized graphitic-illitic mixtures are preserved, which are located in the deformed zones and parallel to the foliation, having high C content, with low S and As content.

Graphite separation experiments were performed to be able to detect graphite directly. The graphitic material recovered by froth flotation was investigated with XRD and TEM. Calcite was removed by acetic acid treatment (5%) and the residue was investigated again with XRD and DTA methods.

According to our results, graphite cannot be detected directly on the XRD curves due to its heavy peak overlapping with quartz peaks. However, its direct quantification is possible by Rietveld refinement. By TEM, 80–200 nm sized, hexagonal-dihexagonal shaped, C-containing grains can be detected with ordered crystal structure. As the thermogravimetric analyzes are performed in air, the thermal reaction of graphite and partially graphitized material can be observed on all simultaneous TG-DTA curves.

Acknowledgement

Supported by the TEKH College of Advanced Studies about Natural Resources, University of Miskolc.

References

BRUMSACK, H. J. & LEW, M. (1982): In: von Rad, U., Hinz, K., Sarnthein, M. & Seibold, E. (Eds.): Geology of the Northwest African Continental Margin. Springer-Verlag, New York, N.Y., 661–685.

CROZIER, R. D. (1990): Flotation – Theory, Reagents and Ore Testing. Course handbook, Camborne School of Mines, UK.

EUROPEAN COMMISSION (2020): Study on the EU's list of Critical Raw Materials – Final Report.

FÜLÖP, J. (1994): Geology of Hungary, Paleozoic II. (In Hungarian). Akadémiai Kiadó, Budapest.

HOLLAND, H. D. (1979): Economic Geology, 74: 1676–1679.

BIO-MINERALIZED MAGNETITE IN BOTTOM SLUDGE OF A CLOGGED GEOTHERMAL WELL

MÁDAI, F., LESKÓ, M. Zs., MÓRICZ F. & KRISTÁLY, F.
Institute of Mineralogy and Geology, University of Miskolc, Miskolc, Hungary
E-mail: askmf@uni-miskolc.hu

The investigated sample was taken from the bottom sludge of a clogged geothermal reinjection well as part of DESTRESS project. Characterization of the solid part of the sample was done by XRF, XRPD and optical + SEM-EDS methods. Black colour of the sludge and sampling conditions point to a reducing environment.

Mineral phases were identified by XRPD pattern was interpreted using Rietveld refinement method. The sample are primarily composed of main rock forming phases of clastic sediments, i.e. quartz, clay minerals (illite, illite-smectite, subordinately kaolinite and chlorite), feldspars, carbonates. The i/sm 11A is the disordered mix-layer of illite-smectite clay mineral phase with low swelling capacity. Sulphur content is very low (0.27%) and sulphide phases were not detected by XRPD. Remarkable feature is the high amount (10.7%) of magnetite which is in line with the significant Fe2O3 content measured by XRF (27.9%) and very low sulphur content.

Crystallite size of the magnetite is very fine, 21 ± 5 nm. The nano-particle size (d: 21 nm) of the magnetite indicates the activity of $Fe^{(III)}$-reducing bacteria in the sludge. The share of mineral phases with volatile components is low, which shows that the predominant part of the LOI (7.5%) is from the decomposition of organic matter. The main chemical components based on WDX-XRF are SiO_2 (43.8%), Al_2O_3 (11.16%) and Fe_2O_3 (27.9%).

Two grams of the sample was washed in acetone to release the fines and obtain the coarser-grained (> 125 μm) fraction. The dried coarser-grained fraction was separated to magnetic and non-magnetic subfractions. Non-magnetic subfraction was composed of sub-angular to rounded quartz grains and well-rounded, light-brown grains of clay-rich concretions with maximum grain size of 1 mm. The magnetic grains comprise the other ca. 40% of the sample and reach maximum 1 mm size. Contrary to the clay concretions, the magnetic grains are always angular and usually platy. Surface is dull and usually black, some grains have reddish or reddish-brown discolouration on the surface.

SEM-EDS observation of selected magnetic grains showed that the surface is covered by globular, botryoidal aggregates. Using high magnification, desiccation cracks are seen on the surface along the globule boundaries. Based on these observations, the magnetic grains have an iron oxide rim on the surface of the grains. The iron oxide rim has a few micrometres thickness only and forms globular, botryoidal aggregates, which have been desiccated under vacuum. The cores of the magnetic grains are composed of ankerite or SiO_2-rich silicates/concretions. The globular, botryoidal form of the iron oxide rim and its desiccation indicates the intensive bacterial activity which produces the nanocrystalline magnetite. One grain composed of globular aggregates of ankerite crystals was also selected to the SEM-EDS analysis. This aggregate is composed of 3-5 micrometres siderite rhombohedrons. This siderite has a 10-11% Ca replacing $Fe^{(II)}$. Rhombohedral crystals are perfect, or slightly resorbed. This aggregate is probably the result of in situ bacterial activity.

Activity of $Fe^{(III)}$-reducing bacteria, such as Geobacter sulfurreducens or Shewanella oneidensis combines the oxidation of organic compounds or hydrogen with reduction of minerals with short-range order (e.g. ferrihydrite), leading to release of Fe^{2+}_{aq} and precipitation of siderite and magnetite (Byrne et al. 2011). Precipitation of magnetite and siderite is expected at reducing, alkaline environments which might take place in the bottom of the reinjection well under presence of bacterial activity.

References

BYRNE, J. M., TELLING, N. D., COKER V. S., PATTRICK, R. A. D., VAN DER LAAN, G., ARENHOLZ, E., TUNA F., LLOYD J. R. (2011): Nanotechnology 22, 455709

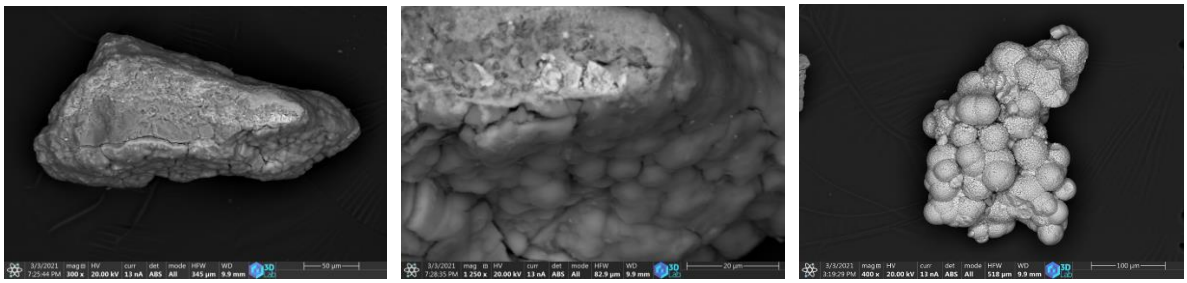

Fig 1.: SEM-BSE images of the bio-mineralized magnetite

TRIASSIC AND CRETACEOUS Ni-Co ORE MINERALIZATIONS WITH SIMILAR MINERALOGY IN DIFFERENT SUPERUNITS OF THE WESTERN CARPATHIANS

MAJZLAN, J.[1], KIEFER, S.[1], MIKUŠ, T.[2] & CREASER, R. A.[3]
[1]University of Jena, Jena, Germany
[2]Slovak Academy of Sciences, Bratislava, Slovakia
[3]University of Alberta, Edmonton, Canada
E-mail: juraj.majzlan@uni-jena.de

Introduction

Hydrothermal mineralizations in the Western Carpathians span a wide range of ages from Variscan to late Alpine, in parallel with the tectonothermal evolution of the Variscan and Alpine orogens. The main superunits (Tatric, Veporic, Gemeric) underwent different degree of Alpine metamorphic overprint but contain texturally and chemically similar ore mineralizations. One simple explanation would be the formation of these mineralizations after the Alpine metamorphic peak that attained the amphibolite-facies conditions in some parts, especially in the southern Veporic Superunit. Hence, we performed mineralogical and geochemical study and radiometric determination of selected ore bodies from each superunit. Parts of the results were already published by KIEFER *et al*. (2020), parts are being prepared for publication at the moment. In this work, Ni-Co minerals gersdorffite, skutterudite and pararammelsbergite were dated by the $^{187}Re/^{187}Os$ method. In some samples, the concentration of the initial Os was negligible and an age from extracted from a single sample. At Čierna Lehota, an isochron was constructed to determine the age of the ores.

The studied ore bodies are located near Dobšiná (Gemeric Superunit), Ľubietová-Kolba (Veporic Superunit), and Čierna Lehota (Tatric Superunit). All these occurrences are dominated by Ni-Co-Fe arsenides and sulfarsenides.

Results and discussion

At Dobšiná and Kolba, the main mineral is gersdorffite, with subordinate amount of nickeline and arsenopyrite. The mineralization commenced with small amount of $NiAs_2$, probably krutovite. The mineralization is hosted in discordant veins with dominant carbonate (siderite-magnesite), albite, and quartz. At Čierna Lehota, the strata-bound mineralization in black shales contains mostly skutterudite and pararammelsbergite, with lesser amounts of other ores; sulfide-richer minerals appear only at the end of the mineralization process.

The principal ore mineralization at Dobšiná occupies structures that can be assigned to the Cretaceous large-scale fan, generated by the northward progression of the Alpine orogenic activity. In agreement with this observation, gersdorffite was dated to 93 Ma, time coincident with the partial exhumation of the Gemeric Superunit after the Alpine metamorphic peak. Additional radiometric (U/Pb, K/Ar) data support these conclusions and agree with the textural evidence at this site.

The mineralizations at Kolba and Čierna Lehota yielded Triassic ages between 230 and 240 Ma. These ages are interesting inasmuch that this time is considered to be a period of quiescence between the fading Variscan orogeny and the later Alpine orogeny. Earlier Pb/Pb model ages (e.g., KOHÚT, 2002) gave similar ages for further small localities Nižné Matejkovo and Čavoj, indicating that such ages are no outliers or results from isotopically disturbed systems. We propose that these hydrothermal systems were fueled by the latest pulses of Variscan magmatic activity (POLLER *et al*., 2005). Ongoing determination of $\delta^{34}S$ values of these ores should pinpoint the source of sulfur and possibly metals.

This work documents regional ore-forming Triassic activity in the Western Carpathians. It formed numerous ore bodies, even though only with small volumes. In the Gemeric Superunit, such mineralizations seem to be missing, likely because these rocks experienced Alpine greenschist-facies that was able to destroy them, even if they existed. Here, the ore mineralizations are of Alpine (Cretaceous) age.

References

KIEFER, S., ŠTEVKO, M., VOJTKO, R., OZDÍN, D., GERDES, A., CREASER, R. A., SZCZERBA, M. & MAJZLAN, J. (2020): Journal of Geosciences, 65: 229–247.

KOHÚT, M. (2002): Mineralia Slovaca, 34: 1–18.

POLLER, U., KOHÚT, M., ANDERS, B. & TODT, W. (2005): Lithos, 82: 113–124.

GEOCHEMISTRY OF TETRAHEDRITE GROUP MINERALS FROM THE JANJEVO Cu-Bi-Ag(Pb,W) LOCALITY, KOSOVO: RESULTS OF EPMA AND LA-ICP-MS INVESTIGATIONS

MEDERSKI, S.[1], PRŠEK, J.[1] & DIMITROVA, D.[2]
[1]AGH University of Science and Technology, Krakow, Poland
[2]Geological Institute, Bulgarian Academy of Sciences, Sofia, Bulgaria
E-mail: mederski@agh.edu.pl

Members of the tetrahedrite group are the most widespread sulfosalts of base metal deposits, where they coexist with common base metal sulfides (BMS) such as sphalerite, galena, and chalcopyrite. In recent years, intensive mineralogical research on tetrahedrite group minerals (TGM) has resulted in a new nomenclature and classification (BIAGIONI *et al*., 2020). Besides, studies on minor and trace elements in TGM using LA-ICP-MS have presented the phenomenon of element partitioning among BMS (GEORGE *et al*., 2017). Despite the widespread prevalence of TGM in hydrothermal systems, there is insufficient data in the literature on trace elements in TGM measured by the LA-ICP-MS technique.

EMPA and LA-ICP-MS techniques were used to analyze major and trace element concentrations in TGM from polymetallic ores from Janjevo (Kosovo) located in the southern part of the Hajvalia-Badovc-Kizhnica ore field, Vardar zone. Contact metasomatic-type Cu-Bi-Ag(Pb,W) mineralization occurs on the contact of the Cretaceous flysch series and Neogene andesites. Members of tetrahedrite group minerals are associated with arsenopyrite, chalcopyrite, pyrite, galena, sphalerite, löllingite, native Bi, ferberite, siderite, quartz, and several sulfosalts containing Cu, Bi, Pb, Ag, Sb, and As such as aikinite, bismuthinite, krupkaite, bournonite, gustavite, cosalite, pearceite, and wittichenite.

TGM from Janjevo form massive aggregates up to a few cm with chalcopyrite and aikinite, as well as idiomorphic crystals up to 1 cm, which are characterized by the oscillatory zonation visible in BSE images. The presence of four members of TGM has been confirmed in Janjevo: tetrahedrite-(Fe), tetrahedrite-(Zn), tennantite-(Fe), and tennantite-(Zn). Complete Sb ↔ As substitution is observed, while Zn ↔ Fe substitution is restricted and is more widespread in tetrahedrite series. Ag ↔ Cu substitution is also constrained, Ag enrichment (up to 1.24 apfu) principally relates to tetrahedrite series (the correlation between Sb and Ag is 0.97). Apart from Fe and Zn, Hg and Cd are the two most abundant divalent cations present in the TGM (up to 340 ppm Hg and up to 530 ppm Cd), while Mn content is up to 50 ppm. TGM host up to 7700 ppm Bi, up to 48 ppm Sn, up to 19 ppm Ge, and up to 9 ppm Tl. Tin, germanium, and thallium have a strong positive correlation with As and Cu (tennantite series). Interestingly, TGM from Janjevo are enriched in In (~40 ppm, up to 69 ppm), which preferentially partition into the co-crystallized sphalerite and chalcopyrite, and was rarely noted in TGM worldwide. Other trace element contents (Ga, Mo, Se, and Te) are below detection limits. Fluctuation in the content of the major and trace elements in TGM allowed tracing changes in the character of fluids that led to the formation of hydrothermal mineralization in Janjevo.

References

BIAGIONI, C., GEORGE, L. L., COOK, N. J., MAKOVICKY, E., MOËLO, Y., PASERO, M., SEJKORA, J., STANLEY, C. J., WELCH, M. D. & BOSI, F. (2020): Journal of Earth and Planetary Materials, 105(1): 109–122.

GEORGE, L. L., COOK, N. J. & CIOBANU, C. L. (2017): Minerals, 7(2): 17.

ACID DRAINAGE FROM SULPHIDIC MINE WASTES: COMPARING CONTINENTAL CLIMATE MAINLAND AND TROPICAL CLIMATE SEA DEPOSITION SETTINGS

MEDIANISTA, R.[1], HARMAN-TÓTH, E.[1,2], IRSHAD, I.[1] & WEISZBURG, T. G.[1,3]
[1] Department of Mineralogy, Eötvös Loránd University, Budapest, Hungary
[2] Eötvös Museum of Natural History, Eötvös Loránd University, Budapest, Hungary
[3] Department of Environmental Sciences, Faculty of Science and Arts, Sapientia Hungarian University of Transylvania, Cluj-Napoca, Romania
E-mail: rlmmed31@gmail.com

Acid mine drainage (AMD) generation has always been abreast during mining activities and even after the deposition of the waste products. In general, it occurs upon oxidation of sulphide-rich materials (e.g., rocks, coarse- or fine-grained waste) producing sulphuric acid and dissolved iron along with other heavy metals. The series of chemical reactions in the oxidation process of sulphides are moderately exothermic which are characterized by high concentrations of oxygen, high temperature, low pH and bacterial activity (VILA *et al.*, 2008). Thus, the difference in these factors will directly influence the rate of AMD generation.

Following these theories, the AMD generation can greatly vary in different depositional environments. Examples of such cases are the AMD generation in the Calancan mine tailings causeway (CMC), Marinduque in the Philippines, a tropical monsoon climate sea deposition setting (Am, BECK *et al.*, 2018) and the Bányabérc waste dump in Hungary, a humid continental climate mainland deposition setting (Dfa, BECK *et al.*, 2018). The climate conditions of the two depositional environments greatly differ in such as the amount of average annual precipitation (965–4064 mm and 750 mm), average annual temperature (26.6 ºC and 9.7 ºC), seasonal cycle (2 vs. 4 seasons) and weather disturbances (Philippines are prone to tropical typhoon). Even the method of deposition differs greatly: sea deposition setting tends to maintain a reduced environment more than the mainland dumping.

This study focuses on the comparison of acid mine drainage generation in different depositional environments (tropical monsoon climate sea deposition and humid continental climate mainland settings). The samples collected in CMC were analyzed using mineralogical methods, then compared to the secondary data in the Bányabérc waste dump.

Macroscopic observation of Calancan mine tailings causeway (CMC) identified active oxidation visible only in the redeposited materials (tombolo) from the original 1990 causeway. The yellow precipitate, an oxidation indication is only found in patches ranging from 6 m^2 to 1400 m^2 and exclusive to the upper 1 cm surface of the materials. This is different from the Bányabérc waste dump in Hungary, where there was wide evidence of active oxidation and deposited materials were characterized by a layer of yellow, brown and red precipitates (FARKAS *et al.*, 2009). The level of alteration in CMC differs in depth and location of the materials while at the Bányabérc waste dump it varied only in depth. This indicates that the change in deposition setting of the material in CMC causes the formation of secondary minerals. The range and rate of alteration could be the result of difference in agitation settings and intrusion of sea water in most part of the causeway, inhibiting the formation of weathering products and/or dissolution of already formed precipitates.

Laboratory analysis (stereomicroscopy, XRD, SEM+EDX, Raman spectroscopy) of the samples from the two study areas shows alteration of the original sulphide minerals (e.g., pyrite). Secondary minerals such as jarosite and iron oxyhydroxides are identified in both depositional settings. The jarosite found in both study areas have composition mostly in K-H_3O jarosite solid-solution series. The substitution of H_3O^+ suggests progressive oxidation process (FARKAS *et al.*, 2009), which should be taken into careful account since it is less stable compared to abundant and less soluble K end-member jarosite (the first to precipitate). The absence of Na-substitution in CMC, at least occasionally intruded by the (Na-rich) sea water, could be explained by the significantly lower solubility of the K end member, or alternatively, by the fact that in the Na^+-rich seawater itself, the presence of Cl^- inhibits the precipitation of Na-jarosite (BASCIANO & PETERSON, 2008).

This study will help us to better understand the AMD generation in the two different depositional settings and how the prevailing environmental conditions influence the formation of secondary minerals.

This work was completed in the ELTE Institutional Excellence Program (TKP2020-IKA-05) financed by the Hungarian Ministry of Human Capacities.

References

BASCIANO, L. C. & PETERSON, R. C. (2008): American Mineralogist, 93: 853–862.

BECK, H. E., ZIMMERMANN, N. E., MCVICAR, T. R., VERGOPOLAN, N., BERG, A. & WOOD, E. F. (2018): Scientific data, 5(1): 1–12.

FARKAS, I. M., WEISZBURG, T. G., PEKKER, P. & KUZMANN, E. (2009): *Canadian Mineralogist,* 47: 509–524.

VILA, M. C., DE CARVALHO, J. S., DA SILVA, A. F. & FI, A. (2008): WIT Transactions on Ecology and the Environment, 109: 729–738.

CULTURAL HERITAGE AND PROTECTION OF HAND-WHEELED POTTERY MANUFACTURE IN WESTERN SERBIA: CHARACTERISTICS OF ZLAKUSA POTTERY BASED ON SEM-EDS AND OPTICAL MICROSCOPY

MILOŠEVIĆ, M.[1], ZDRAVKOVIĆ, A.[1], ĐORĐEVIĆ, B.[2] & JELIĆ, I.[3]
[1]Faculty of Mining and Geology, University of Belgrade, Belgrade, Serbia
[2]National Museum in Belgrade, Belgrade, Serbia
[3]Natural History Museum, Belgrade, Serbia
E-mail: alena.zdravkovic@rgf.bg.ac.rs

Introduction

Traditional coiling and hand-wheel manufacture of pottery from the locally sourced raw clay is characteristic for Western Serbia (DJORDJEVIĆ, 2013) and especially well known in Zlakusa. Pottery from Zlakusa is on the UNESCO Representative List of the Intangible Cultural Heritage of Humanity. In technological terms, it is a unique phenomenon that actively coexists with discovery of new techniques and production processes. This brings to a rise in imitations of this pottery manufacture due to its enlarged popularity. The main goal of this work was to show characteristics of the pottery manufacture based on mineralogy [scanning electron microscopy (SEM-EDS) and optical microscopy] and applying the obtained knowledge in the preservation of this type of cultural heritage in Serbia.

Results and discussion

Clay paste is a mixture of raw clays, consisted of kaolinite/halloysite, illite and smectite minerals followed with smaller amounts of quartz, feldspar and iron oxy/hydroxides and large calcite grains, which is consistent with the previously reported data (MILOŠEVIĆ *et al*., 2019). Sample 1 was prepared by the traditional coiling method on a hand rotated wheel, while sample 2 was made with the application of a modern mould technique. A microscopic examination of the thin sections revealed a uniform mineral composition. No significant differences were observed regarding the inner sections of the pots and their outer rims. Observed pores in sample 1 are of random orientation and size, indicating slower rotations of the potter's wheel during the manufacturing process. Sample 2 has a specific fluid-structure that is consistent with the way it was fabricated. By the size and orientation of the pores, it is evident that the pot was manufactured by the application of a mould. SEM-EDS analysis was performed on the inner parts of the walls of the investigated samples and their surface area. When samples are compared slight difference can be observed. Larger, randomly oriented calcite grains are noted in sample 1. Ground mass is a clay mixture uniformly distributed with larger, mostly rounded pores, consistent with microscopical observations. Sample 2 has a fluid-like structure where both groundmass and pores have a directional appearance, consistent with previous observations, and a slightly higher amount of calcite grains. EDS analysis gives clear differences in the chemistry of the samples. Sample 1 has a higher content of most investigated elements when compared to sample 2, except K and Ca. Amount of K and Ca elements could indicate the presence of a higher amount of illite minerals and carbonates in the clay mixture which is not following sample 1.

Conclusion

How to differentiate traditional pottery products from imitations was the real problem because of their close physical resemblance. The analysed samples of Zlakusa pots showed significant differences from the mineral composition, especially in the terms of elemental composition observed by EDS, to the distribution and appearance of pores concerning the manufacturing process. Further investigations are necessity for an establishment of the standards that will guarantee and protect the originality together with the cultural heritage of the Zlakusa pottery.

Acknowledgment

The present study was supported by the Ministry of Education and Science, Republic of Serbia, Project no. 176010.

References

DJORDJEVIĆ, B. (2013): In: Lugli, F., Stoppiello, A. A. & Biagetti, S. (Eds.): Ethnoarchaeology: Current research and field methods. Conference Proceedings, Rome, Italy. BAR International Series 2472, 49–52.

MILOŠEVIĆ, M., DABIĆ, P., KOVAČ, S., KALUĐEROVIĆ, L. & LOGAR, M. (2019): Clay Minerals, 54: 369–377.

DIM ESEE 2 – DUBROVNIK INTERNATIONAL ESEE MINING SCHOOL – 2021 INNOVATION IN EXPLORATION

MÓRICZ, F., MÁDAI, F. & PAPP, R. Z.
Institute of Mineralogy and Geology, University of Miskolc, Miskolc, Hungary
E-mail: askmof@uni-miskolc.hu

Low level of innovativeness in the RM-sector (Raw Material) of the Eastern and South-eastern Europe (ESEE) region is partly related to lack of professional courses. The DIM ESEE-2 project implementing innovations is a lifelong learning (LLL) project focused on rising innovativeness among raw materials professionals in the ESEE region, having impact beyond and above the duration of the project. It is based on positive results and success of previous DIM ESEE school (2016–2020).

During the preparation phase for the project, DIM ESEE v.2 consortium developed extensive questionnaire for raw materials professionals conducted during January-February 2020, as well as in deep analysis of current ESEE higher education system. Results are pointing to continuous lack of lifelong learning courses for raw materials professionals in the ESEE region, with the exception of obligatory, law-regulated educations for professionals related to safety, working in explosive environment, etc. At the same time classical higher education system with outdated curriculum has very little ability to follow development trends and absorb new innovative and advanced tools and methodologies, reflecting in lower innovativeness rate of their students and alumnus – RM professionals.

Project aims to implement four innovation workshops in exploration, orebody characterization, extraction, and ore processing for the ESEE RM-professionals, which innovation workshops are going to be implemented in Interuniversity Centre of Dubrovnik, in Croatia. In this year the three days workshop will be kept from 20th to 22nd October. The aim is to enhance entrepreneurial and innovative capacity of the region's higher education institutions' graduates and alumni by organizing the following topics:

- Innovation in exploration (2021),
- Innovation in process-oriented orebody characterization (2022),
- Innovation in extraction (2023), and
- Innovation in ore processing (2024).

In this year the focus is on the innovation in exploration, as the workshop highlights on innovative solutions for mineral prospecting and exploration via module divided into three days:

1st day: Main challenges and needs in innovative mineral exploration and robotization.

2nd day: Remote-sensing- and sensor-based techniques and their application in the construction of 3D models.

3rd day: Advanced geophysical data processing and geostatistical methods and their innovative applications for mineral exploration.

Professionals working in raw materials sector can apply, who has good command of English language and basic knowledge related to annual school topic:

- Mineralogy and petrography
- Geochemistry
- Petrophysics
- Economic geology
- Geophysical exploration methods
- Data processing.

We particularly encourage applications of professionals from the following countries: Albania, Armenia, Bosnia and Herzegovina, Bulgaria, Croatia, Cyprus, Czech Republic, Estonia, Georgia, Greece, Hungary, Italy, Kosovo, Latvia, Lithuania, Malta, Moldova, Montenegro, Poland, Portugal, Republic of North Macedonia, Romania, Serbia, Slovakia, Slovenia, Spain, Turkey and Ukraine.

Further three spin-off programs will be organized for RM-students at the participating ESEE Universities. Participating RIS Universities will collaborate in preparation of the joint spin-off workshops for RM PhD and MSc students, using prepared materials of the primary Innovation workshops. For the duration of the project three spin-off workshops are going to be implemented: Miskolc (2022): Innovation in exploration; Zagreb (2023): Innovation in process-oriented orebody characterization; Athens (2024): Innovation in extraction. In view of the pandemic, the workshop will be held in a hybrid way, as both the personal and the online presence is possible. You can apply on the project website (www.dim-esee.eu) or request more information by e-mail (info@dim-esee.eu).

The personal participation costs € 400 (+ VAT), while the online version has a fee of € 100 (+ VAT).

References

DIM ESEE-2: DUBROVNIK INTERNATIONAL ESEE MINING SCHOOL – IMPLEMENTING INNOVATIONS (webpage of the project); downloaded: 2021.03.29.; https://eitrawmaterials.eu/project/dimesee-2

DIM ESEE-2: IMPLEMENTING INNOVATIONS – INNOVATION IN EXPLORATION (webpage of the workshop); downloaded: 2021.03.29.; https://dev.dim-esee.eu/

DIM ESEE-2 INNOVATIVE WORKSHOP – INNOVATION IN EXPLORATION (leaflet of the workshop; in process)

DIAGNOSTIC MINERAL ASSEMBLAGES IN DISTINGUISHING GNEISS VARIETIES OF THE GREAT HUNGARIAN PLAIN'S METAMORPHIC BASEMENT

M. TÓTH, T.
Department of Mineralogy, Geochemistry and Petrology, University of Szeged, Szeged, Hungary
E-mail: mtoth@geo.u-szeged.hu

Introduction

The metamorphic basement of the Pannonian Basin is at present covered by several km thick young (Miocene to present) sediments. Consequently, the petrological and structural evolution of the crystalline rocks can be studied essentially using the bore core material. Numerous previous geochronological data prove that the metamorphism in the entire study area is Variscan in age. Nevertheless, seismic interpretations also confirm a complicated Alpine nappe structure inside the metamorphic mass that significantly overwrote the original Variscan structure. During the subsidence of the Pannonian Basin, at places, metamorphic core complexes formed, resulting in a significant vertical disintegration of the basement. Finally, at present, blocks of incompatible metamorphic and post-metamorphic evolutions compose the metamorphic basement.

First, the rock specimens should be classified using their petrographical and microstructural characteristics to define lithostratigraphic units in such a complicated area. These classes should reflect the essential features of the metamorphic rocks; their protolith composition and metamorphic evolution. So, petrographic classification must be based on mineralogical composition and textural information of the rock specimens.

The most typical rock types of the study area are of very simple mineralogy; they are different quartz and feldspar dominated, mica bearing gneiss varieties. To distinguish the major lithological types, essentially, the accessory mineral phases can be used.

Results

Gneiss types with igneous protolith

Gneissose rock specimens at numerous localities contain syn-kinematic amphibole grains besides the common Qz+Pl+Bt assemblage. The consequent lithology is amphibole-biotite gneiss what regularly coincides with massive amphibolite intercalations of Amph+Pl+Ilm±Gt. This assemblage proves a protolith of mafic igneous composition (basalt), while the quartz and biotite rich varieties (amphibole-biotite gneiss) are more of pyroclastic origin. The latter type may also contain small garnet porphyroblasts.

Gneiss varieties without amphibole usually compose of a very simple paragenesis (Qz+Fp+Bt+Ms). The mineralogical indicators of the protolith in these cases are the accessory phases. Zircon and apatite in numerous specimens are of idiomorphic habit suggesting igneous protolith. These samples are classified as orthogneisses. A few feldspar grains in the most orthogneiss samples are myrmekitic and/or exhibit perthitic microtexture.

Two basic types of orthogneiss are common in the study area. One of them occurs only in a well-defined area in the SE part (Algyő metamorphic high). In these samples, epidote and clinozoisite are diagnostic constituents formed along the retrograde pathway substituting the precursor plagioclase. Another orthogneiss type occurs along a SW-NE zone in the middle region of the basement. These samples commonly contain xenocrysts of diverse mineralogy (garnet, amphibole, clinopyroxene). The xenocrysts are always resorbed, showing wavy grain boundaries. Garnet grains of various chemical composition may occur even in a single specimen, some suggesting metapelitic, while others metabasic compositions. Cores of the amphibole xenocrysts are diverse compositions, while their rims are usually in equilibrium with the matrix minerals. This orthogneiss variety regularly contains xenoliths with significantly different compositions. The most common xenoliths are the amphibolite, garnetiferous amphibolite, and numerous eclogite, granulite, serpentinite, and forsterite marble samples occur. Based on all these textural and mineralogical characteristics, the second orthogneiss type samples defines the same lithology.

Gneiss types with sedimentary protolith

Gneiss varieties with the same rock-forming minerals (Qz+Fp+Bt±Ms) above but without idiomorphic accessories are classified as paragneisses. These specimens also lack myrmekitic feldspar grains. Two basic paragneiss types are distinguished based on their mineral compositions.

One of these contains an M1 metamorphic paragenesis with kyanite and garnet overprinted by a second event (M2) with garnet and fibrous sillimanite. This variety is characteristic above the second orthogneiss type following a few tens of metres wide shear zone. Another paragneiss type contains garnet and rutile (±staurolite) in the M1 paragenesis. A second garnet generation and kyanite characterise the M2 assemblage in this case. All M2 grains (including M2 biotite) are tiny in grain size, suggesting intensive nucleation and high heating rate during the second metamorphic event. The increased field gradient during the M2 event possibly coincided with a contact metasomatic overprint proved by post-kinematic tourmaline and apatite grains in this lithology.

Conclusions

Far the most common lithologies of the metamorphic basement of the Pannonian Basin are

gneiss varieties of identical rock-forming mineral compositions. All rock types contain quartz, feldspar (both K-feldspar and plagioclase) and biotite with or without muscovite. For the classification of the gneissic rock types, accessory mineral phases are involved.

If the sample contains syn-kinematic amphibole (± garnet) grains, the rock type is amphibole-biotite gneiss. This variety usually occurs intercalated with massive amphibolite along the central SW-NE zone in the middle part of the study area. In the case of felsic composition, the shape of the accessory phases (zircon, apatite) is diagnostic. Orthogneiss varieties contain accessories of idiomorphic habit. One orthogneiss variety contains epidote and clinozoisite (epidote gneiss), while another is characterised by the presence of different xenocrysts (Amp±Gt±Cpx). The epidote gneiss type occurs in a small sub-area in the SE part of the basement, while xenocryst-bearing orthogneiss is the lowermost structural unit of the central SW-NE zone. Two major paragneiss types can be distinguished. One of them characterised by an M1: Gt+Ky, and an M2 Gt+Sil paragenesis is an essential constituent of the central zone. The main feature of the other paragneiss type is the tiny grain size of the M2 Gt+Ky+Bt paragenesis. This lithology occurs exclusively in the SE part of the basement.

MINERALOGY OF THE TRIASSIC METAVOLCANICS OF THE BÜKK MTS. (NE HUNGARY)

NÉMETH, N. & KRISTÁLY, F.
Institute of Mineralogy and Geology, University of Miskolc, Miskolc, Hungary
E-mail: foldnn@uni-miskolc.hu

Middle-Upper Triassic successions of the Bükk Mts. are characterised by alternating carbonate-dominated platform and basin facies sedimentary formations with intercalated volcanics. The stratigraphy of this period is uncertain. Syngenetic features are overprinted by low grade regional metamorphism and ductile deformation, and additional local alterations in most rock bodies. These bodies were subject of large-scale tectonic displacements, producing contacts of fragmented fault blocks, where stratigraphic continuity cannot be determined. In several cases it is not clear, if certain formations, even if now adjacent at some outcrops, developed subsequently as part of the same succession, or in synchronous successions at different locations. In consequence of this situation, various hypotheses regarding stratigraphic position of metavolcanics were applied, and metavolcanics formations were mapped variably.

Excessive sampling and testing were performed in the past few years to define the geochemical and mineralogical composition of the metavolcanics formations. Based on trace element geochemistry, metavolcanics can be grouped into three genetic units, also representing chronostratigraphic horizons: (1) alkaline Bagolyhegy Metarhyolite (BMR) of uncertain age, (2) Ladinian calc-alkaline Szentistvánhegy Metavolcanics (SMV) and (3) Carnian alkaline Szinva Metabasalt (SMB). Here we present the result of the mineralogical tests of 41 samples representing these formations. Tests included X-ray powder diffraction (XRPD) of bulk samples, optical microscopy of thin sections and electron probe microanalyses (EPMA) with standardless EDX point and area measurements on polished sections. Quantitative evaluation of the XRPD data was made by Rietveld refinement in TOPAS4 software, providing the rock forming minerals and amorphous content. Only matches of mineral species supported by optical and EMPA observations were accepted. Quantitative data were cross-checked using ICP-AES or WDXRF major element compositions of the bulk samples. In the case of accessory minerals, EPMA and optical microscopy observations were used.

Rock forming minerals are shown on Figure 1. Most important common characteristics are that feldspars are albite and potassic feldspars, and dioctahedral micas have phengitic compositions in every sampled rock. Excess potassic feldspars were found in metasomatic, excess calcite in peperitic rocks. BMR has a simple composition of quartz, feldspars, and sericite. SMV is the most voluminous and heterogeneous of the three formation, samples of this are grouped by differentiation and by structural position (North-eastern vs. South-eastern Unit). Beyond quartz, feldspars and sericite, andesitic and basaltic varieties of the NU contain chlorite, epidote group minerals, pumpellyite and titanite as alteration products of mafic minerals. The same rock types of the SU contain phengite or celadonite of 1*M* polytype and anatase instead of titanite, indicating lower metamorphic grade. SMB rocks are composed mainly of feldspars, chlorite, pumpellyite and titanite, in some cases with significant amount of relict augite and actinolite as its alteration product.

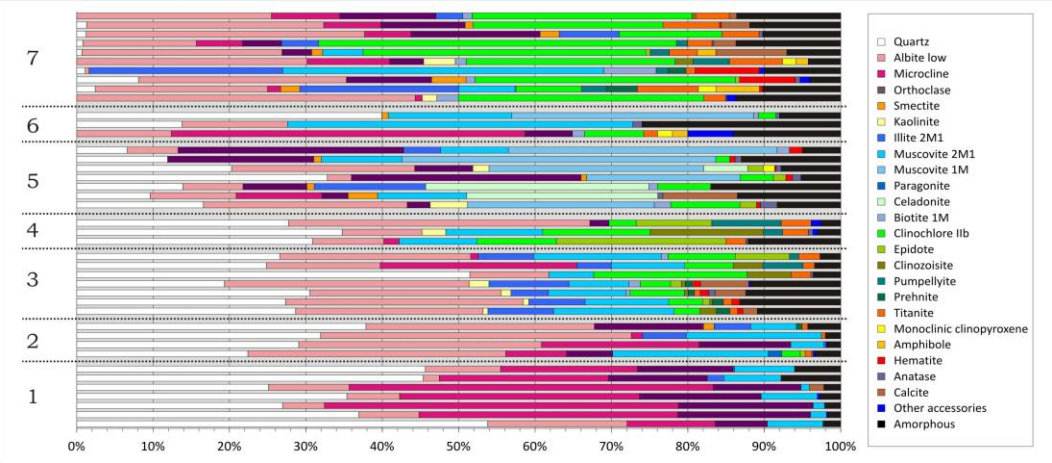

Fig. 1. Quantitative evaluation of the XRPD measurements. Minor phases and varieties occurring in single samples only are merged but identified structural varieties of micas are indicated. Grouping: 1 – BMR metarhyolites, 2 – SMV (NU) rhyolitic/dacitic rocks, 3 – SMV (NU) andesitic rocks, 4 – SMV (NU) basaltic andesitic rocks, 5 – SMV (SU) metavolcanics, 6 – SMV special rocks, 7 – SMB metabasalts.

THE MICROMINERALOGICAL COLLECTION OF THE MINING AND GEOLOGICAL SURVEY OF HUNGARY – AN INTRODUCTION

PÉTERDI, B.[1], SZILÁGYI, V.[2], SZAKMÁNY, Gy.[3], JÓZSA, S.[3], MIKLÓS, D. G.[3] & GYURICZA, Gy.[1]
[1] Mining and Geological Survey of Hungary, Budapest, Hungary
[2] Centre for Energy Research, Budapest, Hungary
[3] Department of Petrology and Geochemistry, Eötvös Loránd University, Budapest, Hungary
E-mail: peterdi.balint@mbfsz.gov.hu

History of the Micromineralogical Collection

The micromineralogical collection of the Mining and Geological Survey of Hungary (MBFSZ) has been established between 1986–1990, in the frame of the project "The study of the recent and fossil river bars of Hungary". This project was stopped abruptly in 1992. The sampling of recent river sediments and Miocene to Holocene age sediments of sand or gravel mines was completed and the shallow drilling program of the alluvial cones of the Danube and Maros rivers was in an advanced state at that time (1992). However, the sampling of sediments from deep drillings was not realized. Sample preparation and most of the planned investigations were finished but due to the sudden stop of the project the results were not gathered and most of them – sedimentological results, spectroscopic results of the grain fraction smaller than 0.063 mm and most of the field reports – were lost.

The samples of the proposed micromineralogical collection "prepared for investigation" remained together and were deposited in the MBFSZ. The results of the composition analyses of almost half of the samples were saved as well. These analyses were based on area estimation of the heavy minerals in the whole mass of the magnetic fractions ("without a sampling of the sample"). In the cases of some selected samples, the analyses were based on polarising microscopy and EPMA. But the documentation of the sampling points was missing – only one representative of the map (1:500.000) showing the sampling points survived. So the collection has become invaluable.

In 2016 the field reports – with the descriptions of all the sampling points and samples, and the field drawings of most of the sampling places – were recovered by a lucky coincidence. Due to these information – and with the remarkable financial and labour expenditure of the Survey – the sample collection was rescued, and it regained its scientific value. Now the samples are professionally stored and inventoried to prevent further deterioration and ensure rapid retrieval.

The content of the Micromineralogical Collection

The micromineralogical collection of the MBFSZ contains the samples of the surficial/near-surface alluvial clastic sediments of the whole territory of the country from 863 sampling points (4326 individually inventoried samples). The samples originate from 754 sites: 510 mines (sand or gravel mines, Miocene to Holocene age sediments), 145 recent river bars and 99 samples from shallow drillings on the Pleistocene age alluvial cones of the Danube and Maros rivers.

From each sampling point, 10–100 kg sediments were collected (according to the average grain size of the sediment), except for the drillings. Due to a sieving – magnetic separation – heavy-media separation method, each sample was separated into 5 or 6 fractions. Ferromagnetic fraction (fr. A): practically magnetite. Three paramagnetic sequences: fr. B: ilmenite, hypersthene, etc.; fr. C: garnets, other pyroxenes, magmatic amphiboles, etc.; fr. D: metamorphic amphiboles, epidote-group minerals, staurolite, etc. Diamagnetic fraction (fr. E): zircon, kyanite, gold, etc. without the residual light minerals. In the cases of the earlier prepared samples the residual light minerals were retained as fr. E and the diamagnetic heavy minerals were named as fr. F.

The inventory records contain data about the sampling site and the sampling point within the site (e.g. sampled layer), grain category (e.g. sandy silt) of the original sample and the original mass of the separated fractions (A-E/F, see above).

Utilization proposals of the Collection

The original project (establishing the collection) aimed at the understanding of the sedimentation history of the filling-up Pannonian Basin. However, the Collection as comparative material is well applicable for several other purposes e.g., ablation area studies; genetic studies of sandstones; archaeometric studies (provenance investigations of sandstone artefacts or ceramics etc., e.g., SZILÁGYI *et al.*, 2021, in this volume); explorations for precious metals and rare elements; geochemical mapping projects (JÓZSA *et al.*, 2020).

References

JÓZSA, S., SZAKMÁNY, Gy., MIKLÓS, D. G. & VARGA, A. (2020): Földtani Közlöny, 150: 291–314.

SZILÁGYI, V., PÉTERDI, B., SZAKMÁNY, Gy., JÓZSA, S., MIKLÓS, D. G. & GYURICZA, Gy. (2021): Acta Mineralogica-Petrographica, Abstract Series, 11, 44

Ni-Co MINERALIZATION FROM DZIEĆMOROWICE U MINE, SUDETY MOUNTAINS, POLAND: MINERALOGY AND CHEMICAL COMPOSITION OF Ni-Co-Fe ARSENIDES AND SULFARSENIDES

PRSEK, J. MEDERSKI, S. & KOZIOL, M.
AGH-UST, University of Science and Technology, Faculty of Geology, Geophysics and Environmental Protection, Kraków, Poland
E-mail: prsek@agh.edu.pl

Uranium deposit, Dziećmorowice-Stary Julianów, is located in the Góry Sowie Mts – part of the Sudety Mountains, Poland. The area is build up by various types of gneisses (cordierite, biotite, mica) with bodies of migmatites and amphibolites. In the broad area of the deposit also Carboniferous rock of the Middle Sudety depression could be found. Whole area is cut by system of faults which were used like channels for the intrusions of acid porphyres. Barite-sulphide (Pb-Zn-Ag) mineralization is connected with that intrusions. Some of that acid intrusions are located directly in the studied U deposit. Two main mineralization type were identified in the deposit – quartz-barite and quartz-calcite mineralization. The quartz barite veins hosted base-metal mineralization (galena, sphalerite and copper minerals) whereas in quartz-calcite veins Ni-Co-Bi-U mineralization occurs.

Minerals from the Ni-Co group are part of the hydrothermal veins. Mineralization is mainly formed by Ni-Co-Fe diarsenides and triarsenides which form massive aggregates in white or pinkish calcite. Size of that aggregates is up to few cm in size. Ni-Co mineralization (stage) is oldest one in the veins. The main minerals in the Ni-Co stage are diarsenides (löllingite-safflorite-rammelsbergite solid solution), triarsenides (mainly skutterudite and Ni-skutterudite, less Fe-skutterudite) and less sulfarsenides (members of cobaltite-gersdorffite solid solution and pure arsenopyrite). Oldest arsenide phases are minerals of the skutterudite group. They occur in form of isometric crystals, often crushed and cataclased. They are partly replaced and overgrown by diarsenides I. Size of the skutterudite aggregates is few mm – up to 1cm. All members of the skutterudite series are presented. Content of As in all phases is similar and mean value is 2.87 apfu. Content of S is up to 0.07 apfu. Fe dominant member is rare and usually it occur in form of veinlet in Ni or Co dominant members. The chemical composition is close to the triple point and average contents of Fe, Ni and Co are 0.36, 0.31 and 0.32 respectively. Co dominant phase – skutterudite is common and generally it forms aggregates with Ni-skutterudite. Average content of Co is 0.52 apfu and it contains 0.2 apfu of Fe and 0.28 apfu of Ni. Ni-skutterudite is the main part of the skutterudite aggregates. Average chemical composition of Ni-skutterudite is characterised by Ni content of 0.53 apfu, 0.21 apfu of Fe and 0.26 apfu of Co. Main phases of the Ni-Co paragenesis are diarsenides I. Its chemical composition is very variable. Diarsenides I are characteristic by intermediate chemical composition with broad Ni-Co-Fe variability. Later chemical composition of the diarsenides II is shifted to the Fe rich members (lollingite II) and Ni rich members (rammelsbergite II) which are younger. Aggregates of the diarsenides are often zonal, where zonality is following bands or crystal shapes or could be completely independent from crystal boudaries. Younger diarsenides II are practically unzonal. The size of the diarsenides I+diarsenides II aggregates is few cm in size. All diarsenides have variable S content which could vary from 0.06 up to 0.2 apfu. Content of Fe in rammelsbergite II is up to 0.2 apfu but generally it is less than 0.1 apfu. Similarly content of Co is up to 0.2 apfu. Löllingite II is generally close to the end composition with content of Ni up to 0.1 upfu and Co 0.09 apfu. Sulfarsenides of the cobaltite-gersdorffite series usually form small thin rims (up to 100 microns) overgrowing triarsenides, diarsenides I and diarsenides II. Sometimes they forms central part of the zonal crystals where younger zones are formed by löllingite III. Similarly arsenopyrite occurs. It forms usually rims or small unzonal crystals growing on the diarsenides I and II or it forms small crystals disseminated in calcite – always in the central part of the veins. Sometimes arsenopyrite form idiomorphic, crushed crystals with weak zonality. Rarely, arsenopyrite form zonal crystals where central part if form by cobaltite and outhermost part by pure löllingite III. Arsenopyrite is close to the ideal composition and content of Ni and Co occasionally reach max. 0.4 apfu and 0.24 apfu respectively, but generally it is lower than 0.03 apfu. Content of As vary from 0.86 up to 1.07 apfu. Minerals of the gersdorffite-cobaltite are more variable. Content of Fe in Co-rich phases is up to 0.2 apfu whereas in Ni-rich phases could reach up to 0.4. apfu. Generally content of Fe in both phases is below 0.06 apfu. Content of Ni in Co-rich phases is dominantly between 0.2 up to 0.46 pfu only in cobaltite in association with löllingite III is up to 0.06 apfu whereas Co content in gersdorffite is between 0.2 and 0.47 apfu. Both members are slightly enriched in As and content of As could be up to 1.3 apfu with mean value 1.15 apfu. It could be caused by replacement of di- and triarsenides by minerals of the cobaltite-gersdorffite series.

General succession of crystallization for Ni minerals is as follows: calcite-triarsenides-diarsenides I – diarsenides II-sulfoarsenides+arsenopyrite I, arsenopyrite II-diarsenides III

MINERALOGY AND CHEMISTRY OF CASSITERITE FROM BUGARURA-KULUTI DEPOSIT, KARAGWE-ANKOLE BELT, RWANDA

RYZNAR, J.
AGH-UST University of Science and Technology, Faculty of Geology, Geophysics and Environmental Protection, Kraków, Poland
E-mail: ryznar@agh.edu.pl

Geological background

Bugarura-Kuluti area belongs to the Central African Mezoproterozoic Karagwe-Ankole Belt (KAB) which together with Kibara Belt (KIB) forms one of the world's largest Ta-Nb-Sn-W province (HULSBOSCH, 2019). This metallogenic province stretches for over 1300 km from southern Uganda through north-western Tanzania, Rwanda, Burundi to the eastern part of Democratic Republic of Congo. The KAB consists mainly with siliciclastic pelite and arenite turbidite sequences which underwent a regional low-grade, greenschist to low-grade amphibolite facies metamorphism (BAUDET *et al*., 1988). The sediments of the KAB were intruded by bimodal magmatism resulting emplacement of the older granites called G1-G3 (1375 Ma; TACK *et al*., 2010) and the younger granites called G4 (986 ± 10 Ma; TACK *et al*., 2010). Granites "G4" are considered as the source of Sn, Ta-Nb and W mineralization and they have been described as F-poor, B-rich, non-deformed equigranular, peraluminous leucogranites (HULSBOSCH, 2019). The younger magmatic event was followed by emplacement of LCT pegmatites with Ta-Nb-Sn mineralization and hydrothermal quartz, quartz-muscovite veins with Sn and/or W mineralization (HULSBOSCH, 2019).

Results and discussion

The cassiterite from all of the type of deposits has common features like twinning, moderate to intense pleochroism, intense colourful anisotropy and mineral inclusions. However, chemistry of cassiterite, quantities and chemistry of mineral inclusions varies in different style of deposits. Moreover, macroscopically, cassiterite shows variations in its size and distribution. The cassiterite from pegmatites doesn't occur in much quantities. Usually, it is very fine-grained and occurs with Ta-Nb mineralization in kaolinized albite, muscovite and quartz zones. The size of crystals rarely exceeds 1 mm. Single crystals contain numerous mineral inclusions of columbite-group minerals. Chemically, cassiterite has elevated ZrO_2 (av. 0.1%), Ta_2O_5 (av. 1.1%), Nb_2O_5 (av. 0,.4%) and decreased TiO_2 (av. 0.1%) content compared to greisen and vein types. The cassiterite from greisen is chaotically distributed in the ore body and size of single crystals is around 1 cm. Mineral inclusions are composed of columbite-group minerals which locate in brighter zones of mineral. Cassiterite has also similar to pegmatite chemical composition with elevated ZrO_2 (av. 0.1%), Ta_2O_5 (av. 0.6%), Nb_2O_5 (av. 0.3%) and decreased TiO_2 (av. 0.05%) content. It is noteworthy that Ta-Nb content in greisen cassiterite is lower than in pegmatite. In both cases Ta > Nb. Hydrothermal quartz veins are the richest in Sn mineralization. The cassiterite concentrates as discontinuous pockets in muscovite selvages and on the contact with quartz. Mineral inclusions are not so numerous like in greisen and pegmatite. They are composed of rutile, ilmenite and rare columbite-group minerals. Contrary to greisen and pegmatite, the vein type cassiterite has elevated TiO_2 (av. 0.5%) and decreased ZrO_2 (av. 0.03%), Ta_2O_5 (av. 0.1%) and Nb_2O_5 (av. 0.1%) content. Fe + Mn of all cassiterite minerals show positive correlation with Nb + Ta which indicate magmatic evolutionary path. This confirms field observations and radial position of deposits around parental granite.

The chemical composition of cassiterite and its mineral inclusions can be considered as a valuable exploration tool when prospecting for primary cassiterite mineralization. During heavy mineral concentrate survey which is largely applied to rare metal mineralization, the chemical composition indicates the nature of primary mineralization (i.e., hydrothermal quartz vein, greisen or pegmatite).

References

BAUDET, D., HANON, M., LEMONNE, E., THEUNISSEN, K., BUYAGU, S., DEHANDSCHUTTER, J., NGIZIMANA, W., NSENGIYUMVA, P., RUSANGANWA, J. B. & TAHON, A. (1988): Annales de la Société Géologique de Belgique, 112: 225–246.

HULSBOSCH, N., (2019): In: Decrée, S. & Robb, L. (Eds.): Ore deposits: Origin, exploration, and exploitation. Geophysical Monograph, 242: 75–107.

TACK, L., WINGATE, M. T. D., DE WAELE, B., MEERT, J., BELOUSOVA, E., GRIFFIN, B., TAHON, A. & FERNANDEZ-ALONSO, M. (2010): Precambrian Research, 180(1–2): 63–84.

RELATIONSHIPS BETWEEN THE COMPOSITION OF VINEYARDS' ROCK, SOIL AND GRAPEVINE PARTS REGARDING CHEMICAL ELEMENTS, ON TWO EXAMPLES FROM MÁD, TOKAJ REGION, HUNGARY

SIPEKI, L.[1], KRISTÁLY, F.[1], SZAKÁLL, S.[1] & DEMETER, E.[2]
[1]Institute of Mineralogy and Geology, University of Miskolc, Miskolc, Hungary
[2]Demetervin Kft., Mád, Hungary
E-mail: sipeki.lilla@gmail.com

Mád is located on the western border of the historical Tokaj wine region, with its more than 900-hectare vineyard territory this makes it suitable for our research. We specifically studied two braes, the Király Hill and the Úrágya Hill. The goal was to examine the chemical elements in different parts of the grape, and to find connections between them and the composition of the vineyard and its soil. We assumed that the elements accumulated by the grapevine may be characteristic to the composition of the local soil. Some elements are expected to crystalize in the form of minerals, depending on their abundance and the plant physiology. In research related to vine and grape mineralization mostly the total or partial chemical composition is reported as "mineral part" thus we take the mineralogical approach to obtain more detailed data on the uptake and distribution of chemical elements which contribute to grape composition.

The choice of the two vineyards is based on their different petrology and geochemistry, while the Király Hill is an area of strong hydrothermal alteration (silicified rhyolite tuff with abundant quartz, kaolinite and alunite), the Úrágya Hill has mainly weathered rhyolite breccia with lesser extent of hydrothermal alteration (quartz, K-feldspars and minor alunite).

Sampling strategy was set up to allow the study of local chemical processes, thus a 2 m deep pit was excavated next to a vine-plant. Soil samples were taken from two depths of the profile, according to the two horizon-like strata of the soil. Rock fragments from the deeper horizon were also collected, assuming that they are important source for soil minerals, even if complex soil colloid transfer processes are considered. Root fragments were cut off from the pit bottom, and samples of leaves, stem and grapes were also collected after grape harvesting.

The rock and soil samples were examined for mineralogical and chemical composition (X-ray powder diffraction, XRD and X-ray fluorescence spectrometry, XRF), identification of soil clay minerals was done by diagnostic XRD investigation. The chemical composition and texture of grapevines parts (root, seed, leaf and peduncle) was investigated by scanning electron microscopy and energy-dispersive X-ray spectrometry (SEM+EDX). Plant parts were also subjected to XRD, to observe minerals in the main crystallized material, the cellulose matrix. Ash content and ash chemical composition was also investigated for some samples by inductively coupled plasma optical emission spectrometry (ICP-OES).

The mineralogy of the rock samples was found to be simple, featuring alunite and quartz on both sites, kaolinite on Király Hill and calcite and abundant sanidine on Úrágya Hill. SEM+EDS investigation of rock samples confirms XRD results and additionally reveals accessory minerals which are important micronutrients, like apatite for P. Other than these minerals the soils contained illite (mixed di- and trioctahedral), albite and smectites.

Chemical elements found in the rock could be found in the soils too, the only exception was sulphur, which was absent from the Úrágya samples. The elements from the soils were also found in the organic parts too, but in varying ratios between the two vineyards and the different plant parts. The Úrágya Hill grape was more enriched in K – related to sanidine, while S and Al beyond K was higher in the Király Hill grape, as defined by elevated alunite content of the rock and soil. Ca and Mg are usually more elevated than Si and Al, and their distribution in the organic tissue is related to specific parts. The highest Si accumulation is observed in the leaves, in organic-crystalline form.

What we also discovered, were idiomorphic calcite, quartz and oxalate mineralizations formed in the plant tissues. The oxalates have been identified as whewellite and weddellite with XRD. Less mineralized micrometric globules can be observed in most of the grapevine samples, which after contacting with iodine gave no reaction for starch, so by elimination we refer to them as yeast.

These results suggest that the enrichment of certain elements in grapevines is site-specific. However, the role of soil fluid migration and airborne soil forming mineral transport should be always considered in such studies. With further studies we can gain information on how the composition of a vineyard's rock and soil affects the grape, the wine made from it – and its „minerality".

FLUID INCLUSION STUDIES FROM THE WESTERN PART OF POLISH TATRA MOUNTAINS, TATRIC UNIT

SITARZ, M.[1,2], NEJBERT, K.[2] & GOŁĘBIOWSKA, B.[3]
[1]Tatra National Park, ul. Kuźnice 1, 34-500 Zakopane, Poland
[2]Institute of Geochemistry, Mineralogy and Petrology, University of Warsaw, Warszawa, Poland
[3]Department of Mineralogy, Petrography and Geochemistry, AGH University of Science and Technology, Kraków, Poland
E-mail: msitarz@tpn.pl

The Tatra Mountains located in the Central Western Carpathians are the highest part of the Carpathian Mountains. Together with 7 other massifs from Slovakia their crystalline core is built with Tatric Unit (ANDRÁŠ & CHOVAN, 2005). In all of them the hydrothermal ore mineralization with similar origin occurs.

In the western Polish part of the Tatra Mountains hydrothermal ore mineralization was an object of interest for mining industry during 16th to 18th centuries. It is connected with crystalline rocks (magmatic and metamorphic) and occurs as a copper and silver mineralization of the abundant polyphase carbonate-quartz and carbonate-quartz-sulphide-barite veins. The hydrothermal ore mineralization was formed at the last stage of granitic magma crystallization from hydrothermal solutions circulating in shear zones and connected to tectonic deformation (GAWĘDA *et al*., 2007). The most common sulphosalt is tetrahedrite, which usually forms massive impregnation, even up to 1–2 cm. Analysis made by WDS showed antimony varieties with substituted As for Sb. Trace elements detected by LA-ICP-MS showed the highest partly substitution for bismuth (up to 1500 ppm), mercury (up to 1845 ppm), cobalt (up to 500 ppm) and cadmium (up to 150 ppm). Concentrations of other trace elements were not significant. Content of Ge, Ga, Mo and Sn are less than 10 ppm and content of Au, In are less than 1 ppm.

In order to determine the origin and composition of hydrothermal mineralization the fluid inclusion studies from quartz were conducted. Research focused in the Polish part of the Western Tatra Mountains in three main locations: Pyszniańska Valley, Pod Banie Gully and Baniste Gully. Phase transitions have been measured using Linkam HFS 91 freezing-heating stage mounted on Nikon Optiphot-2 microscope. Composition of fluids was examined by Raman spectroscopy, which was carried out using Witec Alpha 300 M+ spectrometer with 488 nm diode laser, 600 gratting and 100x Zeiss objective. The size of the observed inclusions closed in the range of 2–6 micrometres. Optical studies of collected quartz samples indicated dominant presence of secondary fluid inclusions, the same as in the High Tatras (JUREWICZ & KOZŁOWSKI, 2003). Measured homogenization temperatures allowed to determine two generations of fluid inclusions: primary with the temperature in the range of 120–170 °C and secondary inclusions in the range of 97–110 °C. The salinity was calculated from the melting temperatures by means of AqSo5e programme. The results showed that the salinity varies between 4.9 and 17.81 wt.% NaCl eq. Due to the small size of the inclusions it was difficult to determine eutectic temperature and estimate the composition of the solutions. However, recent microthermometric studies from similar quartz veins from High Tatra Mountains shows that inclusions are filled with aqueous solutions of salts, mainly NaCl, KCl and $CaCl_2$, and gas or liquid CO_2 (e.g., JUREWICZ & KOZŁOWSKI, 2003).

Results obtained from fluid inclusions present in hydrothermal ore veins from Western Tatra Mountains are similar to data from fluid inclusions occurring in post-mylonitic quartz veins from High Tatra Mts. (JUREWICZ & KOZŁOWSKI, 2003). Mineralizations mentioned above formed due to hydrothermal activity which was probably connected with Variscan stage of the granitoid crystallization. Microthermometric data from Western Tatra Mts. are also comparable with results from other massifs with similar mineralization occurring in Tatric Unit (MAJZLAN *et al*., 2020). Parental fluids are interpreted as basinal brines with a contribution of seawater and/or meteoric water components.

The work was financially supported by AGH University of Science and Technology Grant No 11.11.140.158.

References

ANDRÁŠ, P. & CHOVAN, M. (2005): Journal of the Czech Geological Society, 50/3–4: 143–156.

GAWĘDA, A., JĘDRYSEK, O. M. & ZIELIŃSKI, G. (2007): In: Kozłowski, A. & Wiszniewska, J. (Eds.): Granitoids in Poland. Archiwum Mineralogiczne Monograph No. 1, 341–353.

JUREWICZ, E. & KOZŁOWSKI, A. (2003): Archiwum Mineralogiczne, 54: 65–76.

MAJZLAN, J., CHOVAN, M., HURAI, V. & LUPTÁKOVÁ, J. (2020): Geologica Carpathica, 71: 85–112.

NEW MINERALOGICAL AND GEOCHEMICAL INFORMATIONS ABOUT THE UKRAINIAN CHROMITE ORE DEPOSIT "KAPITANKA"

SOSNAL, A. & PIECZONKA, J.
AGH University of Science and Technology, Kraków, Poland
E-mail: sosnal@agh.edu.pl

Geological background

The purpose of the research of a small Ukrainian chromite ore deposit called "Kapitanka" was to gather new information about the genesis of this deposit through mineralogical and geochemical analysis of chromite samples.

"Kapitanka" deposit is located in Central Ukraine, in the western part of the Kirovograd Region. Geologically, the deposit is settled in crystalline massif in the southern part of the Ukrainian Shield, one of the major units of the East European Platform. The host rocks consist mainly of paleoarchaic enderbite and granulite rock facies, one of the oldest in Europe at 3.6 billion years old (PIECZONKA & PIESTRZYŃSKI, 2009). Chromite ores are located within ultramafic rocks that are partly serpentinized (KULISH *et al.*, 2002). Almost 100 ultrabasic massifs in that region, forming Pervomaisk–Holovanivsk structure, have been identified. Chromite occurrences are already confirmed within 11 of them (KANEWSKY, 1996). "Kapitanka" deposit is the largest one of them, and the only one which was briefly exploited. Even though it is the best-described body in that formation, its genesis is still uncertain. Some structural elements, such as lenticular shapes of bodies, as well as serpentinization, indicate podiform type deposit, however, the geotectonic position is still discussed. Chemical analysis of nearby Lipovenskie massif strongly indicates stratiform type deposit by Cr_2O_3 to Fe_2O_3 ratio of 1.73 and low content of SiO_2 = 0.27%. For comparison, chromites from another nearby massif have Cr_2O_3 to Fe_2O_3 ratio above 2, indicating the podiform type of the deposit (DUKE, 1995).

Methods

Rock samples were gathered in 2018 at one of the abandoned outcrops. Eleven of them were selected to further research after macroscopic description. These samples were prepared for microscopic study in both reflected and transmitted light under the Nikon Optiphot polarizing microscope. Microscopic observation enabled the selection of samples for the microprobe EDS (FEI Quanta 200FEG) and WDS (Jeol JXA-8230 Super Probe) chemical analyses. All microscopic observations and analyses were carried on at the Faculty of Geology, Geophysics and Environmental Protection of AGH University of Science and Technology. Electron microscopic analyses were conducted with the help of Prof. A. Piestrzyński and PhD G. Kozub-Budzyń.

Results and conclusions

Examined rock samples show various properties. Chromite mineralization occurs in both massive and disseminated forms. Host rocks of disseminated ores consist of unaltered olivine and clinopyroxenes. One specimen was a part of quartz vein, with frequent fuchsite instances. Two heavily weathered samples consisted of goethite and muscovite; these samples were taken from "mysterious" puppets found in overburden oxidized layers.

Besides chromite, as expected, the most common ore mineral in samples are magnetite, hematite and ilmenite. XRD analyses confirmed the occurrence of various chromite types, magnetite and ilmenite; and indicated the presence of galaxite. Other minerals confirmed by this method were quartz, jadeite, goethite and kaolinite.

The spinel crystals have maintained idiomorphic shapes and are very rarely fractured, which indicates small tectonic activity in the local massif. Exsolution of solid solution occurs in the spinel crystals in half of the samples. EDS analysis of samples shows that chromium spinel separated into two phases. One phase contains 20% of chromium and 30% of iron; and the other, reduced content of chromium and enriched in iron (8% and 55%, respectively).

Results of WDS analyses of homogeneous chromite crystals have been plotted on the classification diagrams. Most of them indicate podiform type deposit. All samples had Cr_2O_3 to Fe_2O_3 ratio higher than 2 (5.08 minimum), which also confirms this theory (DUKE, 1995). Known deposit type, small tectonic activity of the area and small depth make "Kapitanka" deposit attractive for future exploitation, although, further analyses are required to define accurate resources and average content of chromium, which determines the economic value of this deposit.

References

DUKE, J. M. (1995): In: Ekstrand, O. R. (Ed.): Geology of Canadian mineral deposits. Publisher GSC, 615–624.

KANEWSKY, A. Y. (1996): Chromite ores of Ukraine. Mineral resources of Ukraine, 3: 12–13.

KULISH, E. O., VOINOVSKY, A. S., KOMOV, I. L. & LEBID, M. I. (2002): Mineralogichesky Zhurnal, 24/2–3: 16–25.

PIECZONKA, J. & PIESTRZYŃSKI, A. (2009): Geologia, 35, 2/1: 183–195.

CASSITERITE IN QUARTZ-FELDSPAR VEINLETS OF IGNIMBRITE (SOUTHERN BÜKK MTS., HUNGARY)

SZAKÁLL, S. & KRISTÁLY, F.
Institute of Mineralogy and Geology, University of Miskolc, Miskolc, Hungary
E-mail: askszs@uni-miskolc.hu

An unusual vitreous rock type was found exposed in an experimental quarry in the vicinity of Kács locality. The territory is characterised by various volcanic products, displaying the effects of different alteration processes. The aforementioned rock type is dominantly reddish to light brown with dense network of centimetre-wide veinlets, filled with bright white coarsely crystallized feldspars and quartz. These veinlets are the product of hydrothermal activity affecting a consolidated tuffaceous product undergoing mechanical deformations. A late-stage percolation of fluids is indicated by Mn-oxide rich layers and films covering the feldspar veinlets and thin cracks. The groundmass is built up by fine-grained quartz with phenocrystals of biotite and feldspars in a fluidal-vitrophyric texture, built up by layers of different volcanic stages as indicated by the presence of coarse, highly oriented obsidian windles. The petrography of the formation is characteristic for welded ingnimbrites, tectonized and affected by hydrothermal fluids. The stratigraphic position of the formation corresponds to the Middle Pyroclastic Complex, as the Tibolddaróc unit.

Samples were collected from the different textural-petrographic varieties of the host rock, alteration products and the veinlets. Investigations by X-ray powder diffraction and scanning electron microscopy with energy-dispersive spectrometry was applied to identify and characterize minerals in different textural positions. The hydrothermal veinlets consist of sanidine and quartz (like), mostly subhedral and anhedral crystals. The host rock is built up by subhedral, resorbed quartz and Na-rich plagioclase in a mixed glassy and feldspar groundmass. Millimetre-sized or even larger rounded euhedral ilmenite crystals and biotite phenocrysts can be distinguished macroscopically.

Cassiterite was found related to the sanidine-rich veinlets, as intragranular anhedral aggregates up to 50–100 μm, mostly deposited on the surface on SiO_2 grains (Fig. 1). EDS measurements show that minimal amount of Ti, Mn and Fe is always present, however it was not possible to decide if submicrometric ilmenite inclusions or elemental substitution is the reason. The sanidine in the veinlets has K:Na = 2:1 ratio. The Mn-oxide layers have a widely varying composition including Ca, Fe, Ba and Mg in significant amount, but the presence of Na, S, Cl, K and trace amounts of Co, Ni and Ce are also constant. The high Al and Si content suggest a mixture of clay minerals and Mn-oxides, a few barite crystals were also observed. The biotite phenocrysts are Ti-rich and Cl-bearing annites, showing alteration and loss of Ti-content in the vicinity of the hydrothermal veins. The primary ilmenites are Mg-bearing and show marks of dissolution, while a generation of smaller ilmenite-like crystals in the hydrothermal assemblage tend to have Mn content instead.

XRD measurements were performed on selected materials from host rock and veins. In the hydrothermal assemblage mostly Na-rich plagioclase and sanidine were found. The most important feature is the lack of quartz and dominance of tetragonal cristobalite, meaning that SiO_2 associated to sanidine and cassiterite is signalling a more special environment. The Mn-oxide crusts could not be identified as any crystalline phase, but the presence of 14 Å phyllosilicates was observed.

The textural arrangement and paragenesis of cassiterite is characteristic for the “tin wood” genetical type of Sn-mineralization. The temperature range of mineralising fluids had a wide range, from mesothermal to low epithermal. Cassiterite was deposited in the lower stage, following the sequence of sanidine > cristobalite > cassiterite > Mn-oxides.

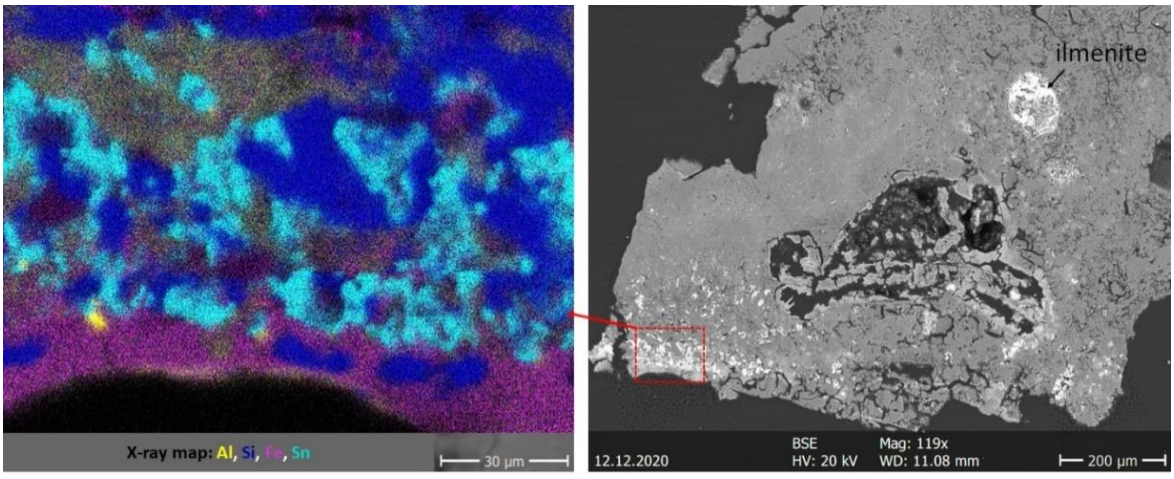

Fig. 1. Textural position of cassiterite precipitation and X-ray map showing its relation to the SiO_2 phase (cristobalite).

ZIRCON U–Pb DATINGS TO UNRAVEL LATE PALAEOZOIC MAGMATIC EPISODES IN THE TISZA MEGA-UNIT: A REVIEW

SZEMERÉDI, M.[1,2], LUKÁCS, R.[2], DUNKL, I.[3], VARGA, A.[1], SEGHEDI, I.[4], KOVÁCS, Z.[2] & PÁL-MOLNÁR, E.[1]
[1] Department of Mineralogy, Geochemistry and Petrology, 'Vulcano' Petrology and Geochemistry Research Group, University of Szeged, Szeged, Hungary
[2] MTA-ELTE Volcanology Research Group, Budapest, Hungary
[3] Geoscience Center, Department of Sedimentology & Environmental Geology, University of Göttingen, Göttingen, Germany
[4] Institute of Geodynamics, Romanian Academy, Bucharest, Romania
E-mail: szemeredi.mate@gmail.com

Introduction

During Late Palaeozoic times several magmatic events occurred in the Central European Variscides associated with a collisional to extensional tectonic environment. The Tisza Mega-unit is not an exception in the broader region, where various Permo-Carboniferous plutonic and volcanic formations are known, cropping out in the Apuseni and the Mecsek Mts. or drilled by exploration wells in the basement. Despite the rapidly spreading method of zircon U–Pb geochronology, quite a few of these rocks were dated so far; however, precise and reliable age results (besides whole-rock trace element and isotope geochemical data) have a key role in the local to regional correlations. In our recent and ongoing studies, a wide range of felsic volcanic and plutonic rocks were dated, representing southern Transdanubia, the basement of the eastern Pannonian Basin (Hungary) and the Apuseni Mts. (Romania) to place Variscan igneous processes in time and to correlate among Late Palaeozoic formations at local (Tisza Mega-unit) to (sub)regional scale (Carpathian–Pannonian region or the broader area of the Central European Variscides). The aims of this abstract are to highlight the new age results and their regional geological significance as well as to provide an insight into ongoing investigations.

Materials and methods

Studied samples included the following formations: Permian felsic volcanic rocks in southern Transdanubia and the basement of the eastern Pannonian Basin (the so-called Gyűrűfű Rhyolite Formation) as well as in the Apuseni Mts.; Permian A-type granitoids, felsic dykes, and diorites in the SW Apuseni Mts. (Highiș massif); and Variscan S-type granitoids (the so-called Battonya granites) in the basement of the eastern Pannonian Basin. In-situ U–Pb zircon age determinations were performed at the GÖochron Laboratories, University of Göttingen by LA–SF–ICP–MS. To gain eruption ages for volcanic rocks, we applied the TuffZirc Age algorithm of ISOPLOT software (LUDWIG, 2002) on $^{206}Pb/^{238}U$ ages, selecting the youngest coherent age group of zircon crystals. In case of plutonic rocks, the same calculation method was used as well, that referred to the main period of zircon crystallization in the magma system.

A summary of the results

Zircon U–Pb datings of Permian felsic volcanic rocks in the Tisza Mega-unit revealed a Guadalupian (~270–259 Ma) voluminous volcanism, the products of which occur from southern Transdanubia to the Apuseni Mts. (SZEMERÉDI *et al*., 2020). So far, these formations were considered to form a Lower Permian marker horizon (representing a single event) in the local to subregional lithostratigraphy, therefore such former interpretations should be revised. Besides connecting Permian felsic volcanic rocks to each other from various parts of the Tisza Mega-unit, zircon U–Pb geochronology (supported by whole-rock geochemistry) helped to reveal plutonic–volcanic connections between them and the A-type granitoids in the Highiș massif (~268–263 Ma; SZEMERÉDI *et al*., 2021). The possibility of similar connections between the Permian volcanic rocks and the underlying S-type granitoids in the basement of the eastern Pannonian Basin was rejected, as the latter showed Tournaisian (~356 Ma) age. As Variscan S-type granites (the so-called Codru granitoids) occur in the Apuseni Mts. too, exploring their connection with basement formations is in the focus of ongoing studies. Our aim is to incorporate all these geochronological results in the local to regional correlation of the Tisza Mega-unit.

This study was financed by NRDIF (K131690 and K108375 projects) and New National Excellence Program (ÚNKP-20-4-SZTE-596 project).

References

LUDWIG, K. R. (2002): User's manual for Isoplot 3.75: A geochronological Toolkit for Microsoft Excel. Berkeley Geochronology Center Special Publication No. 4

SZEMERÉDI, M., LUKÁCS, R., VARGA, A., DUNKL, I., JÓZSA, S., TATU, M., PÁL-MOLNÁR, E., SZEPESI, J., GUILLONG, M., SZAKMÁNY, GY. & HARANGI, SZ. (2020): International Journal of Earth Sciences, 109: 101–125.

SZEMERÉDI, M., DUNKL, I., LUKÁCS, R., SEGHEDI, I., KOVÁCS, Z. & PÁL-MOLNÁR, E. (2021): Geologica Carpathica (under revision).

PROVENANCE STUDY OF ARCHAEOLOGICAL CERAMICS BY HEAVY MINERAL INVESTIGATIONS USING A MICROMINERALOGICAL COLLECTION: A CASE STUDY FROM NE HUNGARY

SZILÁGYI, V.[1], PÉTERDI, B.[2], SZAKMÁNY, Gy.[3], JÓZSA, S.[3], MIKLÓS, D. G.[3] & GYURICZA, Gy.[2]
[1] Centre for Energy Research, Budapest, Hungary
[2] Mining and Geological Survey of Hungary, Budapest, Hungary
[3] Department of Petrology and Geochemistry, Eötvös Loránd University, Budapest, Hungary
E-mail: szilagyi.veronika@ek-cer.hu

Provenance of pottery

Provenance of archaeological pottery means the sources of ceramic raw materials, and this approach helps to determine local, regional or long-distance material supply of pottery handicraft of a given ethnic group or culture. Characterization of a ceramic matrix, i.e., the clastic (clay-silt-sand) raw material type may require detailed (beyond instrumental chemical/ mineralogical methods or conventional petrography, SEM-EDS) investigations in case of common mineralogical composition or fine-grained texture. In such cases, the exact determination of heavy mineral (HM) components of the ceramic matrix provides possibility to connect it directly to the clastic raw material type (region of source) applied (MANGE & BEZECZKY, 2007; BONG *et al*., 2010; SAUER, 2013).

The knowledge on the HM assemblages of potential raw material territories is the key to the successful provenance determination. The micromineralogical collection of the Mining and Geological Survey of Hungary (MBFSZ) provides a useful database for a direct comparison of mineral species detected in archaeological pottery to phases preserved in sediments by conventional petrography or SEM-EDS. As introduced by PÉTERDI *et al*. (2021), the MBFSZ micromineralogical collection covers the surficial/near surface alluvial clastic sediments of Hungary with more than 700 localities. As a result of the continuous evaluation, qualitative-quantitative information on the overall mineralogy is being accumulated. These data are appropriate for a more exact determination of potential raw material territories, and for the localization of paste or tempering material sources.

Case study from NE Hungary (10th c. pottery from Edelény-Borsod)

Heavy mineral composition of pottery from the 10th century settlement of Edelény-Borsod is compared with geological localities of the surrounding Bódva and Sajó river sediments (20 sampling localities from the MBFSZ micromineralogical collection). The observed pottery assemblage could be characterized by a predominant petrographic group containing an opaque minerals-tourmaline-garnet-zircon-brown and green amphibole-(epidote) HM assemblage. As a result of the comparison, it can be concluded that the Edelény ceramics and the Sajó sediments [garnet-(green, brown)amphibole-orthopyroxene-ilmenite-epidote-zoisite-hematite-tourmaline] are more similar than that of the Bódva [iron oxides/hydroxides-hematite-limonite-ilmenite(-magnetite); different appearance of tourmaline and orthopyroxene, presence of blue amphibole]. Representative information on HM species ratios from the pottery material is not possible to gain due to the small sample amount (thin section size), the accidental sampling (plane of the thin section), and the limitations of thin section petrography of ceramics in determination of mineralogy (e.g., opaques). So, much more attention has to be dedicated to the qualitative comparison by the determination of major and minor-trace element composition of HM mineral species (e.g., garnet, zircon, pyroxene and amphibole) by SEM-EDS and LA-ICP-MS (JÓZSA *et al*., 2016; KÜRTHY *et al*., 2018), which data – by determining the origin of minerals – help to better characterize the source region of the ceramic raw materials.

To conclude, the existence of micromineralogical collections (e.g., at the MBFSZ) is a great opportunity for ceramics provenance studies. Although, adequate HM study of archaeological pottery requires as much amount of sample as possible, but it results in comparable and informative data on the raw material provenance. The comparison with the HM assemblages of sediment samples is not quantitative but qualitative. In addition, it requires the deliberate synchronization of determination and categorization of HM species.

References

BONG, W. S. K., MATSUMURA, K., YOKOYAMA, K. & NAKAI, I. (2010): Journal of Archaeological Science, 37: 2165–2178.

JÓZSA, S., SZAKMÁNY, Gy., OBBÁGY, G. & KÜRTHY, D. (2016): Archeometriai Műhely, 13/3: 173–190.

KÜRTHY, D., SZAKMÁNY, Gy., JÓZSA, S., FEKETE, M. & SZABÓ, G. (2018): Archeometriai Műhely, 15/1: 1–12.

MANGE, M. A. & BEZECZKY, T. (2007): In: Mange, M. A. & Wright, D. T. (Eds.): Heavy minerals in use. Developments in Sedimentology, 58: 1007–1033.

PÉTERDI, B., SZILÁGYI, V., SZAKMÁNY, Gy., JÓZSA, S., MIKLÓS, D. G. & GYURICZA, Gy (2021): Acta Mineralogica-Petrographica, Abstract Series, 11, 36

SAUER, R. (2013): In: Bezeczky, T. (Ed.): The amphorae of Roman Ephesus. Forschungen in Ephesos, 15/1: 197–212.

LUMINESCENCE CHARACTERISTICS OF QUARTZ SEPARATES OF DIFFERENT ROCKS AND SEDIMENTS IN HUNGARY

THAMÓ-BOZSÓ, E., FÜRI, J. & BÁTORI, M.-né
Mining and Geological Survey of Hungary, Budapest, Hungary
E-mail: bozso.edit@mbfsz.gov.hu

Introduction

During the OSL (Optically Stimulated Luminescence) dating of Late Pleistocene and Holocene sediments it is observed that the OSL luminescence sensitivity and other luminescence characteristics of quartz show local differences. One cause of these differences may be the different source rocks of the quartz grains. Therefore the luminescence properties of quartz separates from some metamorphic, plutonic, volcanic, and sedimentary rocks and sediments in Hungary were studied in detail to gather complementary data to our previous investigation (THAMÓNÉ BOZSÓ *et al.*, 2020).

Samples, sample preparation and study methods

Quartz fractions were separated from Paleozoic metamorphic rocks: Tolvajárok Leucophyllite, Sopronbánfalva Gneiss and Vöröshíd Mica schist Formations; Carboniferous plutonic rocks: Velence Granite and Mórágy Granite Formations; Miocene volcanics: Gyulakeszi Rhyolite Tuff and Tar Dacite Tuff Formations; Permian, Oligocene and Miocene sedimentary rocks: Balatonfelvidék Sandstone, Hárshegy Sandstone, Törökbálint Sandstone and Kazár Sandstone Formations; and different sands from Eocene to Late Miocene–Pliocene.

First, rock samples were crushed and sieved, sand samples were only sieved, then the quartz was separated from the 0.1–0.16 mm grain size fraction using hydrogen peroxide, hydrogen chloride, heavy liquid prepared from sodium polytungstate (SPT), and then hydrogen fluoride in the same way as for OSL dating, but not in dark conditions. Finally, the quartz grains were mounted on stainless steel disks in 5 mm diameter using silicon oil.

OSL measurements were made according to WINTLE & MURRAY (2006) on RISØ TL/OSL DA–20 reader. The same or very similar luminescence measurement protocols were applied as during the OSL dating of the sediment samples.

Results

Most of the quartz separates were pure enough in terms of luminescence. A part of the quartz separates characterised by a fast decaying OSL signal dominated by the fast component, which is preferable for OSL dating. But the quartz separates from metamorphic and plutonic rocks were mainly dominated by non-fast components. OSL sensitivity measurements indicated that the quartz separates of sediments, sedimentary rocks and some volcanic tuffs are more sensitive than the quartz of the studied metamorphic and plutonic rocks. Due to growing radioactive radiation, most of the samples showed gradually increasing growth curves. But a few separates displayed first quickly increasing, then very slightly changing growth curves with the saturation of the OSL signal at relatively low radioactive doses (e.g. Sopronbánfalva Gneiss, Hárshegy Sandstone and Csatka Formations). Quartz of the Mórágy Granite behaved very differently from the quartz of the other rocks and sediments because its OSL signal was very dim and almost unchanged due to growing radioactive radiation.

Sensitivity change, which was measured after many repeated cycles of illumination, radioactive irradiation and thermal treatment of a few quartz separates, was very small. The thermoluminescence signals of the separates showed very different peaks.

The results of the OSL test measurements (dose recovery ratio, thermal transfer test, recycling ratio, recuperation) showed large scattering. This suggests that in the Late Pleistocene and Holocene sediments the quartz grains that are originated directly from metamorphic and plutonic rocks by erosion show unfavourable OSL properties. Only the quartz of a few formations has appropriate properties from the aspect of OSL dating. They are solely sands and sandstones, first of all sands from the Upper Miocene Kálla Gravel and Upper-Miocene–Pliocene Zagyva Formations.

References

THAMÓNÉ BOZSÓ, E., FÜRI, J., KOVÁCS, I. J., BIRÓ, T., KIRÁLY, E., NAGY, A., TÖRÖKNÉ SINKA, M., KÓNYA, P., MÉSZÁROSNÉ TURI, J. & VÍGH, CS. (2020): Földtani Közlöny, 150: 61–80.

WINTLE, A. & MURRAY, A. S. (2006): Radiation Measurements, 41: 369–391.

SUBMICROMETER-SCALE TEXTURAL RELATIONS OF MANGANESE-BEARING MINERALS IN THE ÚRKÚT MANGANESE ORE DEPOSIT, HUNGARY

TOPA, B. A.[1,2], LESKÓ, M. Zs.[3] & WEISZBURG, T. G.[1]
[1]Department of Mineralogy, Eötvös Loránd University, Budapest, Hungary
[2]Department of Mineralogy and Petrology, Hungarian Natural History Museum, Budapest, Hungary
[3]Institute of Mineralogy and Geology, University of Miskolc, Miskolc, Hungary
E-mail: topabogi@gmail.com

The Toarcian Oceanic Anoxic Event (T-OAE) related geological and biogeochemical processes led to the deposition of manganese ores at Úrkút (Hungary), where both carbonatic and oxidic ore types occur. Both types have been intensively studied in the last decades and fundamental discoveries of POLGÁRI *et al*. (1991, 2012) changed our views on the genesis of the carbonatic ore. The characterisation of the oxidic ore was hindered because of the complex textural relations and the large variety of the micro- and nanometer sized manganese oxide and oxide hydroxide minerals, leaving open questions about some mineralogical processes. Thanks to the intense scientific interest and the mining activities – despite the closing of the mine in 2016 – well documented samples are still available for further research. In this study we focused on the fine micro- and submicro-scale textural relations of ore minerals with the help of samples collected from a geological profile representing an alternating sequence of both oxidic and carbonatic ore layers.

To identify the mineral species and reveal the textural features we combined X-ray powder diffraction (XRD), scanning electron microscopy (SEM), electron beam microanalysis (SEM+EDX) and Raman spectroscopy. Few hundred nanometer thin slices were cut with plasma focused ion beam technique (PFIB-SEM). EDS elemental mapping and line scans were performed for tracing the chemical (thus mineralogical) changes of resolution of a few micrometers, while SEM-BSE images allowed textural resolution even in the submicrometer range. The dominant manganese-bearing mineral phases of the deposit are manganite: $Mn^{3+}O(OH)$, cryptomelane: $K(Mn^{4+}, Mn^{3+})_8O_{16}$ and rhodochrosite: $MnCO_3$, but other manganese-oxides and carbonates with different manganese and calcium content are also important part of the system. The three main mineral phases represent different oxidation states of manganese, so the diversity of their presence indicates geochemical changes in the environment. Tracking the various textural positions of these minerals could help the better understanding of the pre-, sin- and/or post-diagenetic mineral formation processes.

One of these key characteristic features is the bioclast-related textural position of the manganese-bearing minerals. Remnants of these – originally manganese-free – shells can be classified as follows: #1 manganese-free calcite shells surrounded and filled by oxidic manganese matrix and/or veins, #2 manganese-free calcite shells partly replaced by manganite and/or manganese oxides, #3 originally calcite shells fully replaced by manganite and/or manganese oxides. In all cases the shape of the bioclasts is well preserved, indicating substitution processes gentle enough for resulting perfect pseudomorphs. Different degrees of replacement (#1 and #3) may occur even within the same fossil with sharp boundary. The replacement process usually starts with the formation of 1–3 micrometer thin potassium-bearing manganese oxide filling ("veinlets") in the fissures and/or along the borders of the original shell building calcite crystals. The next step of the shell replacement is the complete exchange of calcite for manganite.

Another typical textural feature of the layers occurring through the whole profile is the presence of non-bioclast-replacing veinlets varying from a few to a few hundreds of micrometers in width. The veinlets may be monomineralic or may show a complex, submicrometer range, intimate intergrowth pattern of minimum two manganese oxides and/or oxide hydroxides of different manganese valance states (Mn^{3+}, Mn^{4+}), hindering the direct genetic interpretation.

Detailed analysis of the features of these mineral assemblages could help the understanding of essential mineralogical processes and the environmental conditions during accumulation and crystallization.

Acknowledgements

The research was carried out at the Eötvös Loránd University and at the University of Miskolc both as part of the project implemented in the framework of the Thematic Excellence Program funded by the Ministry of Innovation and Technology of Hungary (Grant Contract reg. nr.: NKFIH-846-8/2019) and the project supported by the Ministry of Innovation and Technology of Hungary from the National Research, Development and Innovation Fund in line with the Grant Contract issued by the National Research, Development and Innovation Office (Grant Contract reg. nr.: TKP-17-1/PALY-2020).

This work was completed in the ELTE Institutional Excellence Program (TKP2020-IKA-05) financed by the Hungarian Ministry of Human Capacities.

References

POLGÁRI, M., OKITA, P. M. & HEIN, J. R. (1991): Journal of Sedimentary Petrology, 61(3): 384–393.

POLGÁRI, M., HEIN, J. R., VIGH, T., SZABÓ-DRUBINA, M., FÓRIZS, I., BÍRÓ, L., MÜLLER, A. & TÓTH, A. L. (2012): Ore Geology Reviews, 47: 87–109.

THE BERAUNITE PROBLEM

TVRDÝ, J.[1], VRTIŠKA, L.[1,2], PLÁŠIL, J.[3], SEJKORA, J.[2], ŠKODA, R.[1], MASSANEK, A.[4], FILIP, J.[5], DOLNÍČEK, Z.[2] & VESELOVSKÝ, F.[6]

[1] Department of Geological Sciences, Masaryk University, Brno, Czech Republic
[2] Department of Mineralogy and Petrology, National Museum, Praha, Czech Republic
[3] Institute of Physics AS CR, Praha, Czech Republic
[4] Geoscientific Collections, Technische Universität Bergakademie Freiberg, Freiberg, Germany
[5] Regional Centre of Advanced Technologies and Materials, Czech Advanced Technology and Research Institute, Palacký University, Olomouc, Czech Republic
[6] Czech Geological Survey, Praha, Czech Republic
E-mail: jt.geologie@gmail.com

Basic iron phosphates of transition metals belong to the most perplexing mineral phases (MOORE, 1969, 1970). Although they are known for a long time and have a relatively simple chemical composition, their detailed study brings a number of surprises. A typical example is beraunite, known for science for almost two centuries. This mineral was first described by BREITHAUPT (1840, 1841) on a sample from the Hrbek mine near Svatá Dobrotivá in Central Bohemia, where it occurs in dark red, semi-transparent tabular to prismatic crystals. Chemical analysis performed at that time showed that it is a hydrated basic iron phosphate, in which trivalent iron is present exclusively.

Structural analysis based on X-ray diffraction has been applied in mineralogy from the first half of the 20th century. During the systematic study of phosphates it was found that some green acicular phases considered to be dufrénite have the pattern identical with beraunite (FRONDEL, 1949). The "green" and "red" beraunites were considered to be varieties of the same mineral species. Subsequent solution of the role of ferrous iron in the structure and its effect on colour was followed by nomenclatural proposals (MOORE & KAMPF, 1992). Current valid names for these minerals are eleonorite for the "red" trivalent iron phase, and beraunite for the "green" mixed-valence compound (CHUKANOV *et al.*, 2017).

As this state does not correspond to the original description of beraunite, new analyses of the original Breithaupt's specimen stored in the Mining Academy in Freiberg and of analogous historical samples from National Museum Prague were performed. The results show the identity of beraunite with the mineral eleonorite described by CHUKANOV *et al.* (2017).

The currently confused nomenclature of iron dominant members of the beraunite series is an example of the situation where the description of new minerals is not supported by the thorough study of type samples and an original literature. A possible solution of this "beraunite problem" is discreditation of eleonorite, preservation the original name beraunite for the "red" trivalent phase, and giving a new mineral name to the "green" mixed-valence member of the series.

Fig. 1. Beraunite from the Hrbek mine, Svatá Dobrotivá (St. Benigna), Beroun, Bohemia, Czech Republic. A sample from the 19th century, National Museum Prague. FOV 0.5 mm. Photo L. Vrtiška.

References

BREITHAUPT, A. (1840): Journal für Praktische Chemie, 20: 66–67.

BREITHAUPT, A. (1841): Vollständiges Handbuch der Mineralogie, Vol. 2: 156.

CHUKANOV, N. V., AKSENOV, S. M., RASTSVETAEVA, R. K., SCHÄFER, C., PEKOV, I. V., BELAKOVSKIY, D. I., SCHOLZ, R., DE OLIVEIRA, L. C. A. & BRITVIN, S. N. (2017): Mineralogical Magazine, 81: 61–76.

FRONDEL, C. (1949): American Mineralogist, 34: 513–540.

MOORE, P. B. (1969): Science, 164, 1063–1064

MOORE, P. B. (1970): American Mineralogist, 55, 135–169.

MOORE, P. B. & KAMPF, A. R. (1992): Zeitschrift für Kristallographie, 201: 263–281.

SLOVAK INDUSTRIAL MINERALS RELATED TO NEOGENE VOLCANIC ACTIVITY - GEOLOGY, MINERALOGY AND APPLICATIONS (BENTONITES, PERLITES, ZEOLITES)

UHLÍK, P.[1], LEXA, J.[2], OSACKÝ, M.[1], KODĚRA, P.[1], VARGA, P.[1], BAI, Y.[1], MILOVSKÝ, R[3], BIROŇ, A.[3], FALLICK, A.E.[4] & PALKOVÁ, H.[5]

[1]Department of Mineralogy, Petrology and Economic Geology, Faculty of Natural Sciences, Comenius University, Bratislava, Slovakia

[2]Earth Science Institute, Slovak Academy of Sciences, Bratislava, Slovakia

[3]Earth Science Institute, Slovak Academy of Sciences, Banská Bystrica, Slovakia

[4]Scottish Universities Environmental Research Centre, East Kilbride, Glasgow, United Kingdom

[5]Institute of Inorganic Chemistry, Slovak Academy of Sciences, Bratislava, Slovakia

E-mail: peter.uhlik@uniba.sk

Introduction

Industrial minerals generate about 43 % from total exploitation of mineral deposits in Slovakia. Total mining output has reached 30.5 Mt in 2018. Carbonates (limestone, dolomite, magnesite, marl) have a dominant position (87 %) in the industrial mineral exploitation (ŠOLTÉS *et al*., 2020). Bentonite, perlite and zeolite also have a long-term tradition in production of industrial minerals in Slovakia. They belong to the most perspective, despite their significantly lower extraction volume compared to carbonates. Especially the production of bentonite and zeolite increases every year and Slovakia belongs to world producers.

The most exploited bentonite and two most significant perlite deposits are located in the Central Slovakia Volcanic Field (CSVF). The most important deposits are related to products of rhyolite volcanic activity of the Jastrabá Fm., which is represented by dykes, extrusive domes, cryptodomes, lava flows and related volcanoclastic rocks. The Jastrabá Fm. rhyolites yield ages ranging from 12.2±0.3 Ma to 11.4±0.4 Ma (CHERNYSHEV *et al*., 2013). The largest zeolite accumulation with the best quality is situated in the East Slovakia Neogene Basin (ESNB). There are also some smaller bentonite deposits and perlite occurrences in the ESNB, which is a volcano-sedimentary basin located on the junction of the Western and Eastern Carpathians in the north-western part of the Trans-Carpathian depression (KOVÁČ *et al*., 1995). The purpose of our paper is to provide an overview of recent results on geology, mineralogy, and the use of Slovak deposits of bentonite, perlite and zeolite.

Perlite

From numerous occurrences of perlite in the Slovakian part of the Western Carpathians only Lehôtka pod Brehmi (LPB) and Jastrabá (JST) represent exploitable deposits. The LPB deposit has been exploited in an open quarry since the year 1963. That led subsequently to the construction of the processing plant for the production of expanded perlite that was modernized two times. The LPB deposit is represented by a pile of extruded hyaloclastite breccia composed of grey porous and dark dense fragments. The JST deposit was discovered during a prospection campaign in the years 1974–1980. It represents the biggest deposit of perlite in the Western Carpathians (HRONCOVÁ, 1989). Currently, the deposit is ready for exploitation. Recent exploration and exploitation at both perlite deposits are operated by the company LBK PERLIT s. r. o. Production ranged from about 16 kt in 2013 to about 48 kt in 2017 (ŠOLTÉS *et al*., 2020). Due to its quantity and quality perlite from these deposits still belongs to perspective raw materials of Slovakia.

The JST deposit is represented by glassy rhyolite breccia composed of porous grey fragments associated with an extrusive dome/coulée. Perlite at both deposits are peraluminous, calc-alkaline of high-K type, poor in phenocrysts (around 5 %) of plagioclase, biotite and minor amphibole (LPB) or sanidine/anorthoclase (JST). Glass at both deposits is silica rich (75.4–79.5 wt.% dry) with Al_2O_3, K_2O and Na_2O as other major constituents. Glass water content (3.0–6.0 wt.%) shows a weak positive correlation with its silica content and a negative correlation with its Na_2O content. Perlites show porosities 5–16 % (dark dense), 16–30 % (grey porous) and 30–44 % (pale grey pumiceous). Narrow stretched pores represent remnants after outgassing of ascending magma while open undeformed pores grew at a low pressure before quenching. The transformation of volcanic glass into perlite took place owing to the hydration by a heated mixture of liquid and vapor of meteoric origin. The hydration was supported by a significant porosity with interconnected pores and by a sustainably elevated temperature (LEXA *et al*., 2021). Slovak crude perlites include a higher amount of loosely bound water [45–60% of total water (H_2O_t), released in the temperature range 0–250 °C] and a lower amount of strongly bound water (1–7% of H_2O_t, released at temperatures over 550 °C) compared to Hungarian and other world perlites (18–50%, respectively, 6–23% of H_2O_t). Slovak crude perlites also contain higher ratio of K_2O to Na_2O (2–2.5) when compared to other world perlites (0.7–1.4, ROULIA *et al*., 2006). These can be important factors that cause discrepancies in the expansibility of perlites among Slovak and world perlites. On the other hand, due to the same reason, the Slovak perlites have a better mechanical stability (VARGA *et al*., 2019).

Knowledge of the water content in perlite is crucial for a wide range of volcanological and material processing studies. For that reason a new method based

on normalizing the near-IR spectra to internal standards was proposed based on the assessment of the water content using the $(\nu + \delta)H_2O$ band near 5200 cm^{-1}. The use of hexadecyltrimethylammonium bromide salt as an inner standard resulted in a better correlation with the results gained from TG or LOI than the results obtained for talc as an inner standard. After the initial experimental adjustment of the proper fractions in mixtures of perlite and inner standard the whole procedure is easy and quick to perform, needing only small amounts of samples. The method provides reasonable resolution within the narrow range of water content of perlites (PÁLKOVÁ *et al*., 2020).

Major industrial utilization of perlite is in the form of expanded perlite, which is produced by a quick heating at 800–1000 °C of grinded natural perlite. Expanded perlite has an extremely low density and a high specific surface area. Its physical-chemical properties induce high sound and thermal isolation capacity, heat resistance, chemical inertness, and high filtration ability of the expanded perlite. These properties lead to its application in various branches of economy, mainly in building industry but also in food industry, agriculture, and environmental protection.

A fine particle size (<100 μm), perlite by-product material (PBM) is not suitable for perlite expansion in Lehôtka pod Brehmi processing plant. Consequently, PBM has very limited application, recently, only as a pozzolanic, partial replacement for cement in concrete. Therefore, a conversion of PBM into zeolites was proposed to recover this by-product and to obtain value-added material with attractive sorption properties. Zeolite synthesis was performed in batch experiments in a wide range of experimental conditions and the reaction products were different zeolite species, namely phillipsite (PHI), zeolite X (FAU) and zeolite P (GIS) (OSACKÝ *et al*., 2020; HUDCOVÁ *et al*., 2021).

Bentonite

Bentonite is a raw material composed predominantly of clay minerals from the smectite group, mainly of montmorillonite. There are 30 registered bentonite deposits in Slovakia, 12 of them are exploited. Total bentonite reserves of Slovakia reach 57 Mt (ŠOLTÉS *et al*., 2020). Slovakia is the fifth largest bentonite producer in Europe and 10th in the world. The most important deposits are located in the Kremnica Mountains (e.g., Stará Kremnička – Jelšový potok, Lutila, Kopernica).

The bulk bentonites from all bentonite deposits of the Jastrabá Fm. consist of similar mineral constituents, in particular smectite, feldspars, mica, opal-CT, kaolinite, quartz, sometimes goethite. The main differences were observed in the quantity of these mineral constituents in samples from different deposits and even in samples from a single deposit. The best deposits contain 80–90 wt.% of smectite. Many authors have indicated the predominance of divalent exchangeable cations (Ca^{2+} and Mg^{2+}) in the interlayer space of smectites. Various methods confirmed that smectite from the Jastrabá Fm. is Al-Mg montmorillonite and the layer charge arises mainly from Mg for Al substitutions in the octahedral sheet. A significant positive correlation was established between cation exchange capacity (CEC) values and smectite. The best-grade bulk bentonites have a CEC about 100 meq/100 g. The insufficient fluid flow rate caused the precipitation of high amounts of opal-C or/and opal-CT (up to 45 wt.%) in some locations (e.g., UHLÍK *et al*., 2012; PENTRÁK *et al*., 2018; OSACKÝ *et al*., 2019).

The older studies have reported that bentonite deposits of the Jastrabá Fm. are primarily formed by alteration of acidic vitric volcanoclastics during diagenesis in a freshwater environment in an open or semiclosed hydrological system (e.g., KRAUS *et al*., 1994). The results of recent studies have shown a strong effect of subsurface hydrothermal fluids (mostly steam-heated meteoric water, outflowing from the Kremnica epithermal vein system located northwards) on the bentonitization of rhyolitic rocks of the Jastrabá Fm. (KODĚRA *et al*., 2014). It seems that the best grade bentonites were formed by the alteration of marginal perlitic breccias of extrusive domes and cryptodomes. The isotope geothermometry results indicated that the lateral mineral zonation in the Jastrabá Fm., namely mixed-layered illite-smectite accumulations in the northern part and smectite accumulations in the southern part of the formation, may be related to the gradual decrease in temperature of the hydrothermal fluids percolating through the rhyolitic rocks from north to south (KODĚRA *et al*., 2014). In addition to more than dozen bentonite deposits also the K-bentonite Dolná Ves deposit is located in the Jastrabá Fm. The major minerals are mixed-layered illite-smectite (I-S) and quartz. Economic accumulation of I-S is unique, only a few similar clay deposits are mined in the world. K-bentonite is used as a ceramic clay with annual production of about 6,000 tonnes (ŠOLTÉS *et al*., 2020). The clays from Dolná Ves contain pure I-S in clay fraction (ŠUCHA *et al*., 1996). In the 90-ties, prof. Šucha collected samples and sent them to the Clay Minerals Society (CMS). Since that time, I-S rich clay from Dolná Ves i.e., ISCz-1 (illite-smectite, former Czechoslovakia) is a part of the CMS Source Clays collection. The recent study confirmed that the expandability of studied I-S samples is between 20 and 42%.

Despite, that Slovakia is a significant producer of bentonite and its quality is mostly high, the home processing is falling behind of its potential and Slovak bentonite have a low added value. The most exported bentonite is in the form of raw bentonite and the second exported bentonite product is a cat litter. Consequently, in 2018 the average price of exported bentonite was 54 EUR/t but the average price of imported bentonite was 308 EUR/t (ŠOLTÉS *et al*., 2020). Slovakia as a "bentonite country" cannot be satisfied with such a price imbalance. The current challenge is to find a way how to optimize the application of Slovak bentonites to increase their added value.

Zeolite

The most important Slovak zeolite deposits occur in rhyodacite volcanoclastic rocks (Hrabovec tuff) of the Lower to Middle Badenian age. The Hrabovec tuff

builds a 7 km long and up to 150 m wide belt between the villages of Pusté Čemerné, Nižný Hrabovec, Kučín, Majerovce, and Vranov in the ESNB (VARGA, 1984). Zeolite is a mostly light-green, fine-grained rock, resulting from alteration of a vitreous material. The major mineral is clinoptilolite-K and -Ca and its content is mostly between 60–80 wt.%. The second most frequent phase is opal-CT or opal-C (15–20 wt.%). Less abundant minerals are plagioclase, K-feldspar, micas, kaolinite and traces of pyroxenes, quartz, zircon and apatite (ŠAMAJOVÁ & KRAUS, 1977; TSCHEGG *et al*., 2019, our unpublished data). The Nižný Hrabovec deposit is the largest zeolite quarry in Slovakia, operated by the company Zeocem, a.s., Bystré, with an annual production of ~180 kt of zeolite. This accounts for 87% of the total mine production in Slovakia (ŠOLTÉS *et al*., 2020). Nižný Hrabovec zeolite is used in its natural and various modified forms. It has various uses in agriculture (used as feed additive, soil conditioner and fertilizer), building industry (pozzolan cement, concrete products, concrete additives), wide variety of environmental uses (excellent filtration and sorption properties are used in water and gas cleaning and treatments) and others (see zeocem.com).

The strongest zeolite alteration of the Jastrabá Fm. is hosted by the hanging wall of rhyolitic extrusive domes at the deposit Bartošová Lehôtka - Paseka, where zeolitised tuffs occur in the area of 600 x 400 m and have thickness of X m to 30–40 m (ZUBEREC *et al*., 2005). The raw material is comprised by green, light-green zeolitic tuffs and pyroclastics. Zeolites are represented by clinoptilolite and mordenite. Zeolite content ranges from a few % up to nearly 50 %. Associated microgranitic rhyolites are affected by postmagmatic silicification and adularisation, with network of opal-chalcedony veinlets. Zeolite alteration has a zonal arrangement with mordenite (± clinoptilolite, kaolinite and opal-CT) preferably closer to the contact with rhyolite, and smectite with admixture of clinoptilolite in more distal parts (KRAUS *et al*., 1994). The deposit is mined irregularly. The raw material is applied in agriculture and environmental protection.

Acknowledgement

The authors gratefully acknowledge financial support from the Slovak Grant Agency (VEGA, projects no. 1/0196/19) and to mining companies LBK PERLIT, s.r.o., REGOS, s.r.o., SARMAT, Ing. Peter Majer, Sedlecký kaolin - Slovensko s.r.o., VSK PRO - ZEO s. r. o., ZEOCEM, a.s., for provision of samples.

References

CHERNYSHEV, I. V., KONEČNÝ, V., LEXA, J., KOVALENKER, V. A., JELEŇ, S., LEBEDEV, V. A. & GOLTSMAN, Yu. V. (2013): Geologica Carpathica, 64: 327–351.

HRONCOVÁ, Z. (1989): Mineralia Slovaca, 21: 561–564.

HUDCOVÁ, B., OSACKÝ, M., VÍTKOVÁ, M., MITZIA, A. & KOMÁREK, M. (2021): Microporous and Mesoporous Materials, 317: 111022.

KODĚRA, P., LEXA, J., FALLICK, A. E., WÄLLE, M. & BIROŇ, A. (2014): In: Garofalo, P. S. & Ridley, J. R. (Eds.): Gold-transporting hydrothermal fluids in the Earth's crust. Geological Society London, Special Publication, 402: 177–206.

KOVÁČ, M., KOVÁČ, P., MARKO, F., KAROLI, S. & JANOČKO, J. (1995): Tectonophysics, 252: 453–466.

KRAUS, I., ŠAMAJOVÁ, E., ŠUCHA, V., LEXA, J. & HRONCOVÁ, Z. (1994): Geologica Carpathica, 45: 151–158.

LEXA, J., VARGA, P., UHLÍK, P., KODĚRA, P., BIROŇ, A. & RAJNOHA, M. (2021): Geologica Carpathica, in press.

OSACKÝ, M., BINČÍK, T., PAĽO, T., UHLÍK, P., MADEJOVÁ, J. & CZÍMEROVÁ, A. (2019): Geologica Carpathica, 70: 433–445.

OSACKÝ, M., PÁLKOVÁ, H., HUDEC, P., CZÍMEROVÁ, A., GALUSKOVÁ, D. & VÍTKOVÁ, M. (2020): Microporous and Mesoporous Materials, 294/1: 109852.

PÁLKOVÁ, H., KUREKOVÁ, V., MADEJOVÁ, J., NETRIOVÁ, Z., UHLÍK, P., VARGA, P., HRONSKÝ, V. & LEXA, J. (2020): Spectrochimica Acta Part A: Molecular and Biomolecular Spectroscopy, 240: 118517.

PENTRÁK, M., HRONSKÝ, V., PÁLKOVÁ, H., UHLÍK, P., KOMADEL, P. & MADEJOVÁ, J. (2018): Applied Clay Science, 163: 204–213.

ROULIA, M., CHASSAPIS, K., KAPOUTSIS, J. A., KAMITSOS, E. I. & SAVVIDIS, T. (2006): Journal of Materials Science, 41: 5870–5881.

ŠAMAJOVÁ, E. & KRAUS, I. (1977): The 7th Conference on Clay Mineralogy and Petrology, Karlovy Vary, 1976, 391–399.

ŠOLTÉS, S., KÚŠIK, D. & MIŽÁK, J. (2020): Slovak Minerals Yearbook 2019. The State Geological Institute of Dionýz Štúr, Bratislava.

ŠUCHA, V., ŚRODOŃ, J., ELSASS, F. & McHARDY W. J. (1996): Clays and Clay Minerals, 44 (5): 665-671.

TSCHEGG, C., RICE, A. H. N., GRASEMANN, B., MATIASEK, E., KOBULEJ, P., DZIVÁK, M. & BERGER, T. (2019): Economic Geology, 114: 1177–1194.

UHLÍK, P., JÁNOŠÍK, M., KRAUS, I., PENTRÁK, M. & ČAPLOVIČOVÁ, M. (2012): Acta Geologica Slovaca, 4: 125–137.

VARGA, I. (1984): Mineralia Slovaca, 16: 371–376.

VARGA, P., UHLÍK, P., LEXA, J., ŠURKA, J., BIZOVSKÁ, V., HUDEC, P. & PÁLKOVÁ, H. (2019): Monatshefte für Chemie – Chemical Monthly, 150: 1025–1040.

ZUBEREC, J., TRÉGER M., LEXA J. & BALÁŽ P. (2005): Mineral resources of Slovakia. Štátny geologický ústav D. Štúra, Bratislava.

FISSURE-FILLING CLAY IN DACITE AT TOKAJ, HUNGARY – A HISTORICAL MEDICINE

VICZIÁN, I.
Department of Mineralogy and Geology, Debrecen University, Debrecen, Hungary
E-mail: viczianif@gmail.com

The historical medicine "Tokaj Earth"

A natural clay variety was mined for healing purposes on the Nagy Hill at Tokaj in the 16th to 18th centuries. Similar materials were widely applied since the ancient times, their name was *bolus* or *terra sigillata* (sealed earth), a variety from localities in Silesia was called *terra Silesiaca.* The Tokaj material was called *"terra medicinalis Tokayensis"*, i.e., Tokaj earth. The historical aspects were discussed in detail by VICZIÁN (2017). Mineralogy was described by VICZIÁN & NÉMETH (2021a, b).

Mineralogy

For the present study two historical samples preserved in mineralogical collections were taken. The first one was collected by József Szabó in 1863 from the Patkó Quarry, on northern end of the town Tokaj, on the NE side of Nagy Hill. The sample is now preserved in the Museum of Sárospatak Reformed College. The other one comes from the Mineral Collection of Debrecen University and was collected by Péter Rózsa in 1980. The locality is Tarcal Quarry, on the W flanks of Nagy Hill. The samples are of light brown colour with some reddish shade, homogeneous, relatively hard with conchoidal fracture. They are porous, strongly adhering to the tongue.

XRD and thermal analyses of the samples were carried out in Department of Mineralogy, Eötvös Loránd University, by Tibor Németh. XRD and thermal analyses show that main minerals are disordered kaolinite (about 65–70 %) and goethite (about 15 %). Kaolinite minerals were characterised by X-ray parameters like H_i: Hinckley Index, and Δ001: width of 001 basal reflection in °2θ units and by thermal parameters like T_{corr}: corrected dehydroxilation temperature, T_d: difference of T_{corr} from standard, T_{ex}: temperature of exothermic reaction in °C.

Genesis

Measured parameters were compared with parameters characterising various genetic groups of kaolinites. One example is shown in Fig. 1.

Disordered kaolinites normally occur in nondiagenetic palaeosols and red clays. Kaolinite of Tarcal sample is extremely disordered, while that of the Tokaj, Patkós Quarry sample is transitional toward the ordered, hydrothermal type but is still in the range of the weathered kaolinites. Even low-temperature hydrothermal kaolinites are much more ordered, therefore *in situ* hydrothermal kaolinites near Mád (e.g., Király Hill, Bomboly, etc.) and lacustrine hydrothermal kaolin deposits at Rátka cannot be directly related to the clay occurrences on Nagy Hill, Tokaj. More similar is the genesis of the Szegi and Mezőzombor fire-clay deposits formed by subaerial weathering in the Upper Sarmatian humid and warm climatic period. However, the time of explosion of Nagy Hill volcano at Tokaj is much later, beginning of Lower Pannonian age. Because of its geologic setting, the *bolus* material cannot be derived of later, possibly Middle Pliocene terrestrial kaolinitic weathering crust that may have developed on the surface of the volcano. The most probable genesis is alteration of the underlying rhyolite tuff and of blocks of dacite by the action of very low-temperature, oxidising and acidic hydrothermal waters, and deposition in the fissures.

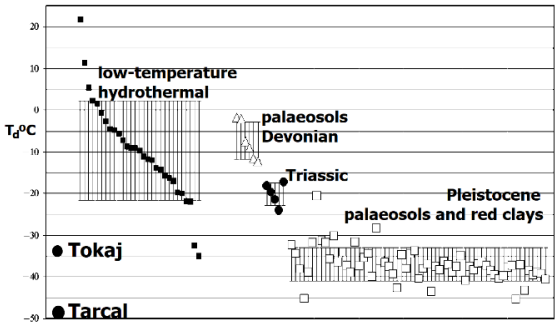

Fig. 1. Measured T_d values in Tokaj, Patkó Quarry and in Tarcal Quarry compared with T_d values of kaolinites formed in various genetic conditions. Figure from FÖLDVÁRI (2008), modified.

References

FÖLDVÁRI, M. (2008): Annual Report of Hungarian Geological Institute, 2006: 169–183.

VICZIÁN, I. (2017): Honismeret, 45/3: 31–38.

VICZIÁN, I. & NÉMETH, T. (2021a): Conference on Mining, Metallurgy and Geology, Cluj-Napoca, 2021, 103–109

VICZIÁN, I. & NÉMETH, T. (2021b): Acta GGM Debrecina, Geology, Geomorphology, Physical Geography Series, in prep.

SN-RICH PHOSPHATES KINTOREITE AND PLUMBOGUMMITE FROM RATIBOŘSKÉ HORY AG-PB-ZN DEPOSIT, CZECH REPUBLIC

VRTIŠKA, L.[1,2], SEJKORA, J.[2], DOLNÍČEK, Z.[2] & MALÍKOVÁ, R.[2]
[1]Department of Geological Sciences, Faculty of Science, Masaryk University, Brno, Czech Republic
[2]Department of Mineralogy and Petrology, National Museum, Prague, Czech Republic
E-mail: lubos.vrtiska@nm.cz

Geological setting

During the revision of the abandoned deposit Ratibořské Hory, phosphates from the plumbogummite group with unusually high contents of Sn were discovered. Historical hydrothermal ore deposit Ratibořské Hory represents a southern part of the Ag-Pb-Zn district Stará Vožice-Ratibořské Hory, situated 8 km northeast of Tábor (Southern Bohemia, Czech Republic). Ag-Pb-Zn district Stará Vožice-Ratibořské Hory is characterized by quartz-carbonate and rarely baryte gangue with abundant galena and sphalerite accompanied by Ag sulphides and with minor Fe-sulphides (ČECH *et al.*, 1952; VRTIŠKA *et al.*, 2019, 2020). Occurrences of supergene minerals there are very sporadic.

Characterization of studied minerals

Plumbogummite and kintoreite are a members of the alunite supergroup with general mineral formula $AB_3(XO_4)_2(OH, H_2O)_6$. Position A is occupied by large mono- (Na^+, K^+, Rb^+, Ag^+, NH_4^+, H_3O^+, Tl^+), di- (Ca^{2+}, Sr^{2+}, Ba^{2+}, Pb^{2+}) or trivalent (Bi^{3+}, REE^{3+}) cations. The octahedrally coordinated position B is usually occupied by trivalent cations such as Fe^{3+}, Al^{3+}, Cr^{3+}, V^{3+} and Ga^{3+}, in some cases it may also contain di- (e.g. Cu^{2+} and Zn^{2+}), or pentavalent (Sb^{5+}) cations. Position X is tetrahedrally coordinated and usually features S^{6+}, P^{5+} and As^5 (KOLITSCH & PRING, 2001; BAYLISS *et al.*, 2010).

Studied phosphates forms yellow, small, finely dispersed aggregates (5–100 μm) in veins with quartz, opal, pyromorphite, acanthite, sphalerite, galena, iodargyrite and undefined Pb-Mn oxide and Sn silicate. **Sn-rich kintoreite** contains in the A-site only Pb (1.01–1.08 *apfu*), B-site is dominated by Fe (2.10–2.85 *apfu*) with contents of Sn (0.16–0.82 *apfu*; up to 15.38 wt.% SnO_2; Fig. 1) and Zn (up to 0.11 *apfu*). Its empirical formula (based on P = 2 *apfu*; mean of the 19 point analysis) corresponds to $Pb_{1.05}(Fe_{2.46}Sn_{0.52}Zn_{0.06})_{\sum 3.04}(PO_{4.00})(PO_{3.00}OH)(OH)_{6.00}$. In much rarer **Sn-rich plumbogummite** the A-site is dominated by Pb (1.06–1.22 *apfu*). The B-site is occupied by Al (2.37–2.68 *apfu*), Sn (0.51–0.55 *apfu*; up to 11.27 wt.% SnO_2) and Fe (up to 0.05 *apfu*). Its empirical formula (based on P = 2 *apfu*; mean of the 6 point analysis) corresponds to $Pb_{1.14}(Al_{2.50}Sn_{0.52}Fe_{0.52})_{\sum 3.06}(PO_{4.00})(PO_{3.00}OH)(OH)_{6.00}$. An intermediate member between Sn-rich plumbogummite and Sn-rich kintoreite was also found. In this **Sn-Al-rich kintoreite** the A-site is occupied by Pb (0.85–1.06 *apfu*) and Ca (up to 0.07 *apfu*), B-site is dominated by Fe (1.30–2.35 *apfu*) with contents of Al (0.33–0.74 *apfu*), Sn (0.47–1.29 *apfu*; up to 24.92 wt.% SnO_2) and Zn (up to 0.09 *apfu*). The X-site contents dominantly P (1.52–1.91 *apfu*) with minor contents of Si (0.06–0.32 *apfu*) and As (0.00–0.24 *apfu*). Sn contents correlate well with Fe+Al contents, which implies that Sn occupies position B. Such high Sn contents in phosphate minerals have not yet been published.

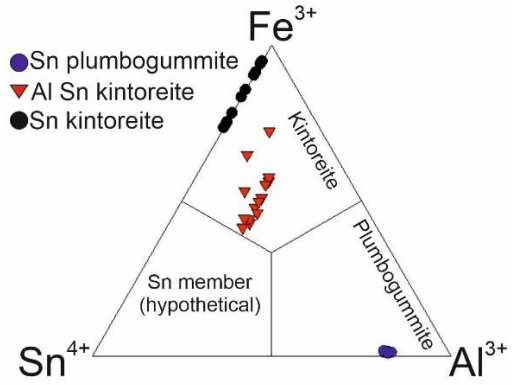

Fig 1.: Ternary diagram of Fe, Al and Sn contents (apfu) in studied phosphates from the Ratibořské Hory

Acknowledgements. This work was financially supported by the Ministry of Culture of the Czech Republic (long-term project DKRVO 2019-2023/1.II.c; National Museum, 00023272).

References

BAYLISS, P., KOLITSCH, U., NICKEL, E. H. & PRING, A. (2010): Mineralogical Magazine, 74: 919–927.

ČECH, V., KOŘAN, J. & KOUTEK, J. (1952): Geotechnica, 13: 1–70.

KOLITSCH, U. & PRING, A. (2001): Journal of Mineralogical and Petrological Sciences, 96: 67–78.

VRTIŠKA, L., MALÍKOVÁ, R., DOLNÍČEK, Z. & SEJKORA, J. (2019): Bulletin Mineralogie Petrologie, 27: 394–410.

VRTIŠKA, L., ŠKÁCHA, P., DOLNÍČEK, Z. & MALÍKOVÁ, R. (2020): Bulletin Mineralogie Petrologie, 28: 69–73.

ESTABLISHING NEW MINERALOGICAL-MONTANISTIC EXHIBITION IN THE HISTORIC TOWN OF SMOLNÍK (SLOVAKIA)

WEIS, K.[1], JELEŇ, S.[1] & NIKOLAJ, M.[2]
[1] Department of Geography and Geology, Matej Bel University, Banská Bystrica, Slovakia
[2] ESPRIT Ltd., Banská Štiavnica, Slovakia
E-mail: karol.weis@umb.sk

The current presentation of history of mining activities in Spiš-Gemer region

Smolník (Schmöllnitz, Szomolnok) used to be an important mining locality and a former administrative center of the Upper Hungary mining, latter Eastern-Slovak mining – former residence of the Upper Hungary Mint Chamber and the Main Chamber of Commerce for the Spiš and Gemer regions. This mining center share similarities with Banská Štiavnica (Schemnitz, Selmecbánya) being relevant for mining localities in Central Slovakia. The end of mining in the region in the early 1990s resulted in a gradual disappearance of employment opportunities in the wider region and also left many important mining facilities to lapse.

The prosperous mining of precious metals, iron and especially copper in the regions of Smolník and Smolnícka Huta was well-documented for 800 years and forms a partial segment in the current museum exhibitions within the wider region – Historical exhibition and Gallery of Mining Museum in Rožňava and Mining museum in Gelnica. The latter is currently integrated within Gelnica municipal administration (WEIS *et al*., 2021). Despite the enormous importance and rich history of Smolník, only the modern history was briefly presented at the small exhibition documenting, more or less, the last 100 years of the town's existence and local industry.

The main purpose and establishment of the mineralogical and montanistic exposition presenting historical mining activities in the area of Lower Spiš

The establishment of the local exhibition presenting mineralogy, deposit conditions and mining activities in Smolník together with immersive elements of the underground of the so-called Elizabeth's house was the result of the joint initiative of civic association Geotour and the Department of Geography and Geology at the Faculty of Natural Sciences (Matej Bel University, Slovakia). The mapping, research in archives and in the field within the territory of Smolník and nearby region resulted in the summary of the collections of ore samples (RYBÁR *et al*., 2017), the most important minerals and various types of artifacts formed the basis for the creation of mineralogical-deposit, alchemical as well as montanistic exposition in the attractive underground (catacombs) of Elizabeth's house. The building currently belongs to the municipality of Smolník and the temporary operator (before handing over the expositions to the municipality) will be Geotour (Civic Association). In addition to the classic exhibits, the history of mining and the importance of Smolník will also be presented through modern audio-visualization technologies, 3D visualizations (Fig. 1) and holographic images (WEIS *et al*., 2016). The exhibition spaces and surroundings will also be used for the activities of educational projects, which will be aimed at schoolchildren and the young generation in general.

Acknowledgment:
The presented contribution is supported by the Research Agency of the Ministry of Education, Science, Research and Sport of the Slovak Republic (project "Summer Mining University", KEGA 041UMB-4/2019).

References

RYBÁR, P., HVIZDÁK, L., HRONČEK, P., JESENSKÝ, M. & ŠIMŮNEK, R. (2017): Acta Montanistica Slovaca, 22: 313–322.

WEIS, K., BEDNÁRIK, P. & MASNÝ, M. (2016): Geographical Information, 20/2: 828–843.

WEIS, K., HRONČEK, P. & JESENSKÝ, M. (2021): Museology and mountain tourism II.: musealization and presentation of collections with mining and montanistic themes in Slovakia./ rec. Molokáč, M. & Neubauerová, J. – Technical University Košice, p. 100.

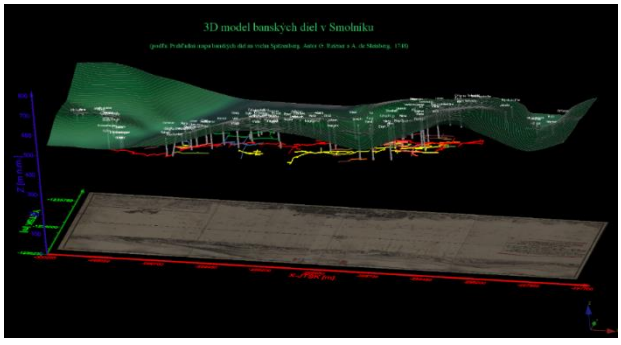

Fig. 1.: 3D virtual reconstruction and visualization of extinct mining works from the historical mining map from 1748

MINERALOGICAL BACKGROUND OF FLUORIDE EMISSION DURING BRICK MANUFACTURING: A HUNGARIAN CASE STUDY

WEISZBURG, T. G.[1,2], KOVÁCS, M.[1], SCHIMEK, É.[1] & HARMAN-TÓTH, E.[1,3]
[1] Department of Mineralogy, Eötvös Loránd University, Budapest, Hungary
[2] Department of Environmental Sciences, Faculty of Science and Arts, Sapientia Hungarian University of Transylvania, Cluj-Napoca, Romania
[3] Eötvös Museum of Natural History, Eötvös Loránd University, Budapest, Hungary
E-mail: glauconite@gmail.com

The essential role of fluoride in the human body is debated, but an excess intake is definitely harmful, causing fluorosis. A natural overdose of fluoride can be related to geological enrichment in the global fluoride belts (CHOWDHURY *et al*., 2019), and is primarily linked to fluid intake. Among the primary hazard sources typically large-scale industrial processes using apatite, fluorite and cryolite are considered. The potential role of clay minerals (ceramics industry) is underestimated, since the (laboratory) dissociation temperature of fluorite, confirmed to form during the firing of clay, is significantly higher (1360 °C) than the industrial temperatures (850–900 °C). However, fluoride emissions are measurable: even in Hungary, far from the global fluoride belts, for one factory, fluoride emissions exceeded the limit for brick production, *i.e.*, 10 mg/m^3 for flue gas (expressed as HF; 4/2011. (I. 14.) VM Decree), therefore, a fluoride-retention equipment had to be installed.

Our study focused first on the raw materials, which has been accompanied by a tunnel kiln experiment to explain the contradiction between worldwide observations (fluoride emission during firing) and the reported (much higher) dissociation temperature of fluorite. The raw material is the Upper Oligocene Kiscell Clay Formation, prevalent in Middle and Northern Hungary, that is applied as a brick raw material at some factories, but contributes to elevated fluoride emission at only one locality. The average fluoride content of the Kiscell Clay is 440±50 ppm, whereas at the problematic locality in Northern Hungary it is 840 ppm for the grey clay and 430 ppm for the yellow variety. The fluoride concentration increases with the decrease of the grain size: from 990±50 ppm in the <10 μm fraction to 1480±50 ppm in the <1 μm fraction indicating that the fluoride content is linked to the clay minerals. The raw material contains chlorite and illite as clay minerals, calcite and dolomite as carbonates with fluoride-fixing potential (through the formation of fluorite) and quartz and feldspar.

The tunnel kiln experiment was done during the triannual maintenance shutdown of the kiln. A systematic set of test bricks went through the cooling tunnel, on subsequent carts, experiencing gradually lower maximum firing temperatures. Temperatures have been recorded throughout the experiment, so that the firing history of the bricks was reconstructed. With the brick set, the change in the fluoride content of the bricks, as a function of maximum firing temperature, was recorded. Brick samples were digested according to the method of INGRAM (1970), and fluoride content was finally analysed by ion-selective fluoride electrode, this way the detection limit went lower than typical for classic analytical procedures.

The experiment revealed that a difference of ~150 ppm exists between the starting material and the final product, that fluoride amount leaves with the flue gas and needs treatment. The fluoride content of the bricks is at the start of firing around 750 ppm and it increases first, until about 510 °C, due to fixing of F^- from flue gas (used for the preheating of the bricks) in the form of fluorite, on the expense of calcite. In the second phase, the first fluoride emission starts at the dehydroxilation of chlorite (at about 550 °C), yielding a decrease in the fluoride content of the bricks. In the third phase, due to fixing of F^- from flue gas by calcite and reactive oxides (dolomite decomposing), the fluoride content of bricks increases again, followed by a decrease due to the dehydroxilation of illite at 720 °C (second fluoride emission). In the fifth phase, brick fluoride content increases again, due to fixing of F^- from the flue gas by reactive oxides (calcite decomposing), up to a maximum brick fluoride content of 1400 ppm. In the last phase, as fluorite starts to decompose, the brick fluoride content decreases (third fluoride emission) to 600 ppm.

Our temperature-controlled experiment has shown that both main clay minerals of the raw clay (chlorite and illite) contribute to the fluoride emission. A volcanic contribution is suspected behind the elevated fluoride content of this specific locality (compared to the other localities using the same raw material). The carbonate content of the raw clay fixes fluoride from both clay minerals and the flue gas (preheating the bricks), causing internal accumulation in longer term. Fluorite decays in the real technological process at around 800 °C, very close to the technological maximum temperature. Evaluating the final fluoride budget, the presence of finely dispersed carbonates in the Kiscell Clay contributes to the final fixing of 80% (600 ppm) of the fluoride content of the brick at 375 °C (750 ppm).

This work was completed in the ELTE Institutional Excellence Program (TKP2020-IKA-05) financed by the Hungarian Ministry of Human Capacities.

References

CHOWDHURY, A., ADAK, M. K., MUKHERJEE, A., DHAK, P., KHATUNA, J. & DHAK, D. (2019): Journal of Hydrology, 574: 333–359.

INGRAM, B. L. (1970): Analytical Chemistry, 42: 1825–1827.

REPLICA OF THE "GREAT TRIANGLE GOLD NUGGET" BELONGING TO BELGRADE UNIVERSITY COLLECTION, GILDED OR NOT?

ZDRAVKOVIĆ, A.[1], MILOŠEVIĆ, M.[1] & JELIĆ, I.[2]
[1] Faculty of Mining and Geology, University of Belgrade, Belgrade, Serbia
[2] Natural History Museum, Belgrade, Serbia
E-mail: alena.zdravkovic@rgf.bg.ac.rs

Introduction

The Collection of Rocks and Minerals, Faculty of Mining and Geology, the University of Belgrade in Serbia, has been holding over a hundred years the gypsum model of triangular shape that represents the replica of one of the world's largest native gold nugget weighing 36.2 kg, known as "The Great Triangle". Nugget model is golden metallic in colour with a shape similar to a rectangular triangle, more or less flat with an average thickness of 8 cm, with a length of about 37 cm and height of about 27.5 cm. In order to enrich the information of gold replica as an exceptional exhibit from the 19th century and to determine its value and significance, it was important to examine the composition of its golden metallic colour surface. Since the gold colour and shine remained the same, did not darken by the time it was assumed that the model is gilded.

Material and method

Chemical composition of the gypsum model surface was carried out in the Laboratory for SEM, Faculty of Mining and Geology, University of Belgrade, using a JEOL JSM-6610LV scanning electron microscope, coupled with an X-Max energy-dispersive spectrometer (Oxford Instruments). The small amount of the skim was gently removed from the surface and glued onto a graphite strip, without covering. Chemical analysis was performed on unpolished pieces, using the EDS detector and the internal standards.

Historic background

The gold nugget was mined in the Southern Ural, in the gold-bearing sands of the Tachkou-Targanka river in 1842. At the time of its invention, the whole area of Zlatoust was the most significant in the world with its gold mines (JONES, 1844). Today, this unique native gold nugget adorns showcases with numerous unique exhibits in the Diamond Fund display in Moscow, Russia, Kremlin. The gold nugget replica, which is kept today in the Collection of Rocks and Minerals, is part of old and numerous mineral collection which numbered 1525 samples donated by the St. Petersburg's State Mining Institute of the empress Catherine II (precursor of Saint Petersburg State University) to the Mineralogical Cabinet of Great School of Belgrade (precursor of Belgrade University) in 1899 (UROŠEVIĆ, 1899). The original accompanying catalogue, written in French and signed by the honoured mining engineer M. Melnikoff, conservator of the Mining Institute Museum in St. Petersburg, contains details of its location of finding, the weight of the natural nugget (Archive of the Collection of Rocks and Minerals), but with no information of the number of the replica made, and the type and manner of material that was used for covering.

Result and conclusion

The data obtained by EDS analysis show that the gypsum model is covered with gold leaf, which was expected according to the macroscopic characteristic of the object. How many such gilded replicas of the original native gold were made in Russia is not yet known. The replica exhibited in the Collection of Minerals and Rocks has not always been treated with care, probably due to a lack of details, which is clearly visible on the surface itself. The acknowledgement that this gypsum model is gilded indicates that the collection donated by the Empress Catherine II State Mining Institute of St. Petersburg had exceptional value, which obliges us to treat it with great care. In this regard, it is planned that its restoration with gold leaves will be done soon so that it can be preserved for generations to come.

References

JONES, T. P. (1844): Journal of the Franklin Institute of the State of Pennsylvania and American Repertory, Third series, 8: 66–67.

UROŠEVIĆ, S. (1899): Comptes Rendus des Séances de la Société Serbe de Géologie, LXXII, Belgrade, pp. 1–6

Index of authors

established in 1922

ACTA MINERALOGICA-PETROGRAPHICA
ABSTRACT SERIES, VOLUME 11, 2021
HU ISSN 0324-6523
HU ISSN 1589-4835